



Universiti Malaysia
KELANTAN

**GEOLOGY AND SLOPE INVESTIGATION USING
RESISTIVITY METHOD IN KG. BUKIT SELAR,
JELI KELANTAN**

by

NUR AZRA BINTI ZAINOL ABIDIN

A report submitted in fulfilment of the requirements for the degree of
Bachelor of Applied Science (Geoscience) with Honours

**FACULTY OF EARTH SCIENCE
UNIVERSITI MALAYSIA KELANTAN**

2019

APPROVAL

“I hereby declare that I have read this thesis in our opinion this thesis is sufficient in terms of scope and quality for the award of the degree of Bachelor of Applied Science (Geoscience) with Honors”.

Signature :

Name of Supervisor : DR. MOHAMMAD MUQTADA ALI KHAN

Date :

UNIVERSITI

MALAYSIA

KELANTAN

DECLARATION

I declare that this thesis entitled “GEOLOGY AND SLOPE INVESTIGATION USING RESISTIVITY METHOD IN KG. BUKIT SELAR, JELI KELANTAN” is the result of my own research except cited in the references. The thesis has not been accepted for any degree and is not concurrently submitted in candidature of any other degree.

Signature :

Name : NUR AZRA BINTI ZAINOL ABIDIN

Date :

UNIVERSITI
MALAYSIA
KELANTAN

ACKNOWLEDGEMENT

First and foremost, I have to thank you my thesis supervisor, Dr. Mohammad Muqtada Ali Khan. Without his assistance and dedicated involvement in every step throughout the process, this paper would have never been accomplished. I would like to thank you very much for the support throughout the process of conducting this paper.

I would also like to dedicate my gratitude to the authority of University Malaysia Kelantan and Faculty of Earth Science for all the facilities and equipment provided throughout this paper.

Moreover, I would like to show my sincere gratitude to Ir. Arham Muchtar Achmad Bahar and Mr. Mohd Syakir bin Sulaiman for their continuous guidance and enthusiasm given throughout this dissertation. Without their guidance and advices, I could not complete my paper by time. Not to forget Mr. Khairul Aizuddin.

Besides that, I would like to acknowledge my parents and siblings for their sincere moral supports. With their unfailing supports and continuous encouragements throughout my years of study, through the process of researching and writing this thesis, this accomplishment would not have been possible without them.

Finally, I must express my very profound gratitude to my mapping team Qamarul, Amir Zakaria, Fatin Idayu, Khalida, Low Kean Hong. For many memorable evenings out and in, I must thank everyone above for listening to and, at times having to tolerate me throughout the mapping session. For my ERI team, Muzzakir, Haikal, Najeebah, Nabihah, Syamimi, Enalina and Zalikha. The ERI field study has been fun with their laughter and jokes. I also place on record, my sense of gratitude to one and all, who directly or indirectly, have lent their hands in this paper.

Thank you.

Azra Zainol

2019

GEOLOGY AND SLOPE INVESTIGATION USING RESISTIVITY METHOD IN KG. BUKIT SELAR, JELI KELANTAN

ABSTRACT

Geological mapping and resistivity survey were carried out in Kuala Balah district mainly covered by Kg. Bukit Selar, Jeli Kelantan. Slope failure phenomenon is a common natural hazard in Malaysia in which due to change in slope angle, weakening of earth materials due to the weathering, increased in water content, heavy rainfall distribution and overloading. The objectives of this study were to produced geological map of study area with the scale of 1:25,000, to analyze the subsurface factors of slope failures by using Electrical Resistivity Imaging (ERI) method, and to determine type and direction of failure by using kinematic analysis method. Geological mapping in the study area has shown that the area is mainly composed of granitic rocks (microgranite and porphyritic granite) overlain by the Quaternary alluvial deposits. The Schlumberger and Pole-Dipole arrays with a maximum electrode spread of 200 m was conducted by placing five resistivity lines on slope failure along the road direct to TNB Pergau Hydroelectric power station. The data were collected by using ABEM Terrameter LS electrode selector system, and processed by using RES2DINV software. The results were presented in the form of two-dimensional (2D) resistivity profiles providing a view of the subsurface distribution of the granitic rock, geological structures, and water content. The results show that the slope failed due to the presence of seepage. Kinematic analysis was conducted as the additional method by analyzed the structural geology of the rock slope using stereonet and the result obtained were type and direction of the slope failure. The findings of this study show that all the methods, geological mapping, resistivity, and kinematic analysis are reliable for slope investigation.

Keywords: geological mapping; electrical resistivity imaging (ERI); kinematic analysis; slope investigation; Kuala Balah district, Kelantan

UNIVERSITI
MALAYSIA
KELANTAN

GEOLOGI DAN KAJIAN CERUN MENGGUNAKAN KAEDAH KERINTANGAN DI KG. BUKIT SELAR, JELI KELANTAN

ABSTRAK

Pemetaan geologi dan penyelidikan kerintangan dijalankan di daerah Kuala Balah terutamanya yang diliputi oleh Kg. Bukit Selar, Jeli Kelantan. Fenomena kegagalan cerun adalah kejadian geobencana semulajadi di Malaysia yang disebabkan oleh perubahan sudut cerun, kelemahan bahan bumi akibat luluhawa, peningkatan kandungan air, taburan hujan lebat dan beban yang terlalu banyak. Objektif kajian ini adalah untuk menghasilkan peta geologi kawasan kajian dengan skala 1: 25,000, untuk menganalisa faktor-faktor bawah permukaan kegagalan cerun dengan menggunakan kaedah Imej Kerintangan Elektrik (ERI), dan menentukan jenis dan arah kegagalan cerun dengan menggunakan kaedah analisa kinematik. Pemetaan geologi di kawasan kajian telah menunjukkan bahawa kawasan tersebut terdiri daripada batuan granit (mikrogranit dan granit porfiri) yang dilapisi oleh deposit aluvial Kuaternari. Susun atur Schlumberger dan Pole-Dipole dengan penyebaran elektrod maksimum 200 m telah dijalankan dengan menjalankan lima profil garis rintangan pada cerun di jalan utama ke stesen janakuasa hidroelektrik TNB Pergau. Data dikumpulkan dengan menggunakan sistem ABEM Terrameter LS, dan diproses dengan menggunakan perisian RES2DINV. Hasilnya dipaparkan dalam bentuk profil rintangan dua dimensi (2D) yang memberikan gambaran penyebaran batuan granit, struktur geologi, dan air bawah permukaan. Keputusan menunjukkan kejadian tanah runtuh adalah kerana kehadiran resapan. Kaedah analisa kinematik telah dijalankan sebagai kaedah tambahan dengan menganalisa geologi struktur cerun batu menggunakan perisian stereonet dan hasil yang diperolehi adalah jenis dan arah kegagalan cerun. Hasil kajian ini menunjukkan bahawa semua kaedah, pemetaan geologi, kerintangan, dan analisa kinematik boleh dipercayai untuk penyasatan cerun.

Kata kunci: pemetaan geologi; imej kerintangan elektrik; analisa kinematik; penyasatan cerun; Daerah Kuala Balah, Kelantan

TABLE OF CONTENTS

APPROVAL	II
DECLARATION	III
ACKNOWLEDGEMENT	IV
ABSTRACT	V
ABSTRAK	VI
TABLE OF CONTENTS	VII
LIST OF TABLES	X
LIST OF FIGURES	XI
LIST OF ABBREVIATIONS	XIV
LIST OF SYMBOLS	XV
CHAPTER 1 INTRODUCTION	
1.1 Background of study	1
1.2 Study Area	3
1.2.1 Location	4
1.2.2 Road	4
1.2.3 Demography	6
1.2.4 Land use	7
1.2.5 Social economic	8
1.2.6 Rainfall	9
1.3 Problem Statement	10
1.4 Objectives	11
1.5 Scope of study	11
1.6 Significance of study	11

CHAPTER 2 LITERATURE REVIEW

2.1	Introduction	13
2.2	Regional Geology and Tectonic Setting	13
2.3	Stratigraphy	16
2.4	Structural Geology	17
2.5	Historical Geology	19
2.6	Landslide	20
	2.6.1 Slope stability analysis	21
	2.6.2 Study about landslide	22
2.7	Geophysical method	24
	2.7.1 Electrical surveys: Resistivity method	24
	2.7.2 Type of resistivity array	26
	2.7.3 Study about slope failure using resistivity array	29

CHAPTER 3 MATERIALS AND METHODS

3.1	Introduction	33
3.2	Materials	35
3.3	Methods	39
	3.3.1 Preliminary Study	39
	3.3.2 Field study	39
	3.3.3 Laboratory Investigation	43
	3.3.4 Data Processing	45
	3.3.5 Data Analysis and Interpretation	47

CHAPTER 4 GEOLOGICAL MAPPING OF STUDY AREA		
4.1	Introduction	49
4.2	Geomorphology	53
4.3	Lithostratigraphy	67
4.4	Structural Geology	79
4.5	Historical Geology	89
CHAPTER 5 SLOPE INVESTIGATION BY USING ELECTRICAL RESISTIVITY SURVEY		
5.1	Introduction	91
5.2	2D electrical resistivity imaging study	92
5.3	Survey lines location	93
5.4	Electrical resistivity imaging of slope investigation	96
5.5	Kinematic analysis of slope failure	112
5.6	Discussion	116
CHAPTER 6 CONCLUSION AND RECOMMENDATION		
6.1	Conclusion	117
6.2	Recommendation	118
REFERENCES		119
APPENDIX I		122
APPENDIX II		124
APPENDIX III		127

LIST OF TABLES

NO.		PAGE
1.1	The population of each sub-district of Jeli, 2000	6
1.2	The breakdown of the population by race in Jeli district	6
1.3	Present landuse by Kelantan state in year 2012 (in hectare)	7
1.4	Current landuse breakdown area Jeli, Kelantan (2017)	8
2.1	Suitability of various geophysical methods for different landslide types and landslide related features	24
3.1	Materials and equipment	36
4.1	Relationship between absolute elevation and morphography (Van Zuidam, 1985)	53
4.2	Scale of weathering of sediment and rocks. (Tucker, 2003)	58
4.3	Petrographic description of microgranite	75
4.4	Petrographic description of porphyritic granite	78

LIST OF FIGURES

NO.		PAGE
1.1	Base map of study area	5
1.2	Monthly average rainfall in Jeli of the year 2017	9
2.1	Tectonic setting of South-east Asia region	14
2.2	Geological map of Peninsular Malaysia	15
2.3	Geological map of Kelantan state	18
2.4	Arrangement of current and potential electrodes for the Dipole-dipole, Wenner and Schlumberger array	28
2.5	Example of resistivity data from the slope at Banding Island	31
3.1	Research flow chart	34
3.2	The approximate range of resistivity values of common rock type.	41
3.3	Arrangement and geometric factor for each array	42
3.4	a) Rock cutting step. b) Polishing step.	44
3.5	a) Rock sample frosted on glass slide. b) Slide ready for petrography analysis.	45
4.1	Traverse map. (a) Paved road in study area. b) Unpaved road in the study area. c) Reserved forests in study area. d) Rubber plantation in the study area.)	52
4.2	Geomorphology Map of study area	55
4.3	3D topography map of study area	56
4.4	a) A cascade in Sungai Suda. b) A cascade in Sungai Terang	60
4.5	A pothole structure on granite body of Sungai Suda	61
4.6	Mid-channel bar in Sungai Pergau tributary	62
4.7	Drainage map of study area	64
4.8	Mass wasting nearby Sungai Suda area	66
4.9	Geological Map of study area	68
4.10	Stratigraphy column of study	70
4.11	Slate outcrop in the study area	72
4.12	Hand specimen of slate	72
4.13	Microgranite outcrop found in Suda river area	74

4.14	Hand specimen of microgranite	74
4.15	Porphyritic granite outcrop found at Sungai Suda	77
4.16	Hand specimen of porphyritic granite	77
4.17	Structure map of study area	80
4.18	Lineament map of study area	82
4.19	Rose diagram of lineaments	82
4.20	Rose Diagram for joint analysis at checkpoint J1	84
4.21	Conjugate joint structure (yellow dashed lines) of granite body at Sungai Suda	84
4.22	Rose Diagram for joint analysis at checkpoint J2	85
4.23	Conjugate joint structure (yellow dashed lines) of granite body at Sungai Terang	85
4.24	A reverse fault of the microgranite unit at Sungai Suda	86
4.25	a) Minor fault on the microgranite unit in Sungai Suda. b) Minor structures on the microgranite unit at Sungai Suda.	87
4.26	a) Quartz vein on porphyritic granite at Sungai Terang. b) Quartz vein on porphyritic granite at Sungai Suda.	88
5.1	ERI survey lines map in study area	94
5.2	Location of survey lines	95
5.3	Slope failure in study area	96
5.4	a) Set-up for an electrode. b) Set-up for spread Survey Line 1.	97
5.5	Set-up for center of spread Survey Line 1	98
5.6	Inverse resistivity and IP pseudosection the topography of Survey Line 1	100
5.7	a) Set-up for an electrode. b) Set-up for spread Survey Line 2 in W-E direction	101
5.8	Set-up for center of spread Survey Line 2	102
5.9	Inverse resistivity and IP pseudosection the topography of Survey Line 2	103
5.10	Inverse resistivity and IP pseudosection the topography of Survey Line 3	105

5.11	a) Set-up for an electrode. b) Set-up for spread Survey Line 4 in SW-NE direction.	106
5.12	a) Set-up for spread Survey Line 4 in SW-NE direction. b) Set-up for center of spread Survey Line 4.	107
5.13	Inverse resistivity pseudosection the topography of Survey Line 4	108
5.14	Inverse resistivity and IP pseudosection the topography of Survey Line 5	111
5.15	Streographic projection of joint in Slope 1	112
5.16	Contour of closely spaced joint data were plotted on the stereonet	113
5.17	Best fit plane for each joint set were plotted on the stereonet	114
5.18	The slope geometry was plotted as a dashed plane in the stereonet	115

LIST OF ABBREVIATIONS

km ²	Kilometre square
km	Kilometre
m	Metre
Kg.	Kampung
Sg.	Sungai
ERI	Electrical Resistivity Imaging
IP	Induced Polarization
FOS	Factor of safety
GIS	Geographic Information System
GPS	Global Positioning System
TNB	Tenaga Nasional Berhad
Opx	Orthopyroxene
Qtz	Quartz
Msv	Muscovite
F	Feldspar
PPL	Plane polarized
XPL	Cross polarized
RMS	Root mean square
msec	Meter second

LIST OF SYMBOLS

$^{\circ}$	Degree
$^{\circ} \prime \prime$	Degree Minute Second
%	Percent
σ	Sigma
Ωm	Ohm meter

UNIVERSITI
MALAYSIA
KELANTAN

CHAPTER 1

INTRODUCTION

1.1 Background of Study

Landslides may be considered as common natural hazards in Malaysia and in many cases leading to significant economic losses and even fatalities. Since recent landslides cases happen in Malaysia often resulted in reactivation of old landslides. Thus, the importance to prevent these landslides is to detect and investigate older landslides in more details in order to gain more insight into land sliding processes characteristics in a particular region. Through this information, the current landslides assessment can be improved (Bell, Kruse, Gracia, Glade, & Hordt, 2006).

All major landslides have natural causes, however, this phenomenon also resulted from human activity. As mentioned by James S. Monroe, Reed Wicander et al. (2007), there are various factors to cause mass wasting or landslides. These include a change in slope angle, weakening of earth materials due to weathering, increased water content and overloading. Besides, the relationship between topography and geology of an area also an important role in determining slope stability.

This proposal entitled Geology and slope investigation using resistivity method in Kg. Bukit Selar, Jeli Kelantan is a research study to be carried out to examine the slopes as they have enough potential gradients to landslides or slope failure to occur by applying electrical resistivity imaging (ERI) methods. Kinematic analysis method was also conducted as an additional method to investigate the type and direction of slope failure. This prospect study is located in Kg. Bukit Selar, Jeli

area. The study area is chosen because it is believed to have a high potential for slope failure to occur.

In Malaysia, this phenomenon is one of the most prominent geohazards that accounts for colossal losses every year. The factors of mass movement in Malaysia can be due to natural causes or human activity. The natural causes of mass movement are gravity, water, earth material and triggering events and human activities include are improper construction, a consequence of flawed design and non-maintenance of slopes. There several types of mass movement; slump, rockslide, rock fall, mudflow, earth-flow, creep and debris flow.

Geophysical methods such as seismic, electrical resistivity, microgravity, self-potential, electromagnetic and self-penetrating radar are more suitable for geological hazards investigation due to their nonintrusive nature and cost-effectiveness. ERI method was used by many researchers because it can help determine the location of geological hazards by analyzing the study area and with data collected. This method can establish a relationship between porosity and resistivity of soil and rock samples through subsurface resistivity distribution via 2D electrical resistivity profiles.

This research investigated the level of risk by conducted kinematic analysis on the joints. The kinematic analysis method is conducted to measure the type and direction of slope failure. As all know, geohazard is dangerous to the community and must be mitigated.

1.2 Study Area

Kelantan is one of the states in Malaysia which positioned at the north-eastern part of the Peninsula Malaysia. This state is bounded with the Pahang to the south, Perak to the west, and Terengganu to the east. Kelantan has 11 districts with the total area of 15,099 km². The districts are Bachok, Gua Musang, Jeli, Kota Bharu, Kuala Krai, Lojing, Machang, Pasir Mas, Pasir Puteh, Tanah Merah, and Tumpat. Jeli has located in the western part Kelantan. Jeli district lies in between latitude 5°42'00" and longitude 101°50'00".

This research is conducted in Kuala Balah sub-district which mainly covered by Kg. Bukit Selar, Jeli. Kg. Bukit Selar is located in Southern part of Jeli district, Kelantan. The total area of the research area is 30 km². Figure 1.1 shows the base map of the study area. The study area mainly composed of granitic rock; microgranite and porphyritic granite, and slate. The area is suitable for this research because it has the potential for high-risk landslide activity area.

Jeli district can be accessed by three main roads; from the west via the Gerik-Jeli highway, from the east via Tanah Merah, and from the south via Mempelam, Jelawang in Kuala Krai. The main land use in Jeli district is forestry which covered almost 70% of the district. There are several numbers of reserved forest located in this region in which are Gunung Basor, Gunung Stong, Sg. Sator reserved forest and Jeli reserved forest. Basically, Jeli is classified as a rural area. Sungai Pergau, Sungai Renyok, Sungai Suda, and Sungai Balah are the main rivers in Jeli region.

1.2.1 Location

Kelantan is one of the states in Peninsular Malaysia. It is part of the Central Belt of Peninsula Malaysia which surrounded by Thailand, Terengganu, Pahang, and Perak. The study area is specifically located in Kuala Balah, Jeli district. Jeli is situated in the western part of Kelantan. The district is approximately 129, 680 hectares and consists of 3 sub-district; Jeli, Batu Melintang, and Kuala Balah. The study area is bounded from latitudes $5^{\circ} 30' 23''$ N to $5^{\circ} 27' 42''$ N and longitudes $101^{\circ} 51' 17''$ E to $101^{\circ} 54' 02''$ E (Figure 1.1).

1.2.2 Road

The study area is served by the main road which heading to Dabong. It is Federal Route 66 which is a federal road in Kelantan linking the town of Jeli to the village of Kg. Bukit Tebok to Manek Urai. The primary location is from Kuala Balah to Dabong and Gua Musang. Along the Federal Route 66, there are many villages of local ethnic Jeli-Dabong which dominated with Malays populations. The study area also has an unnamed road in Kg. Bukit Selar to Sg. Terang power station.

This study area can be easily accessible by vehicles like a car or motorcycle. In Jeli-Dabong area, there is a direct geographic relationship between land use system and road network. Unpaved road also common in the study area. Basically, to access the small villages, rubber plantation, and villagers' farms.

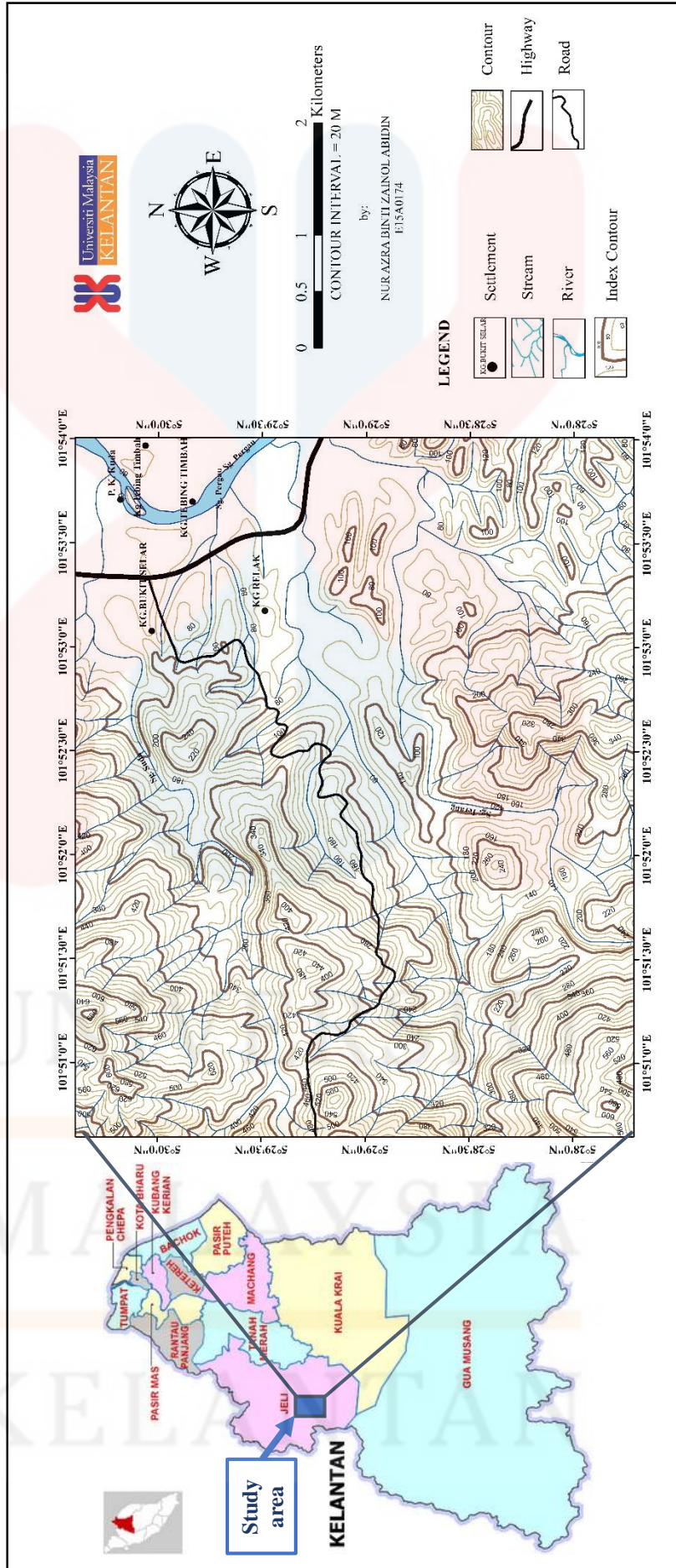


Figure 1.1. Base map of study area

1.2.3 Demography

According to Jeli Land and District Office, the population of Jeli is estimated at 36,512 people which is 2.78% of the total population in Kelantan in 2000. The number of people in Jeli is estimated at 42,872 people which consist of 21,764 men and 21,108 women. The breakdown of the population by each sub-district are shown in Table 1.1.

The area of Jeli district consists of different ethics and group which is dominated by Malays and followed by Orang Asli. The breakdown of the population by race are shown in Table 1.2. Based on data obtained from Department of Orang Asli Development, Jahai Tribe is the highest population in Jeli district of Kelantan. They were gathered in Rual and Jeli River in Hulu Kelantan.

Table 1.1: The population of each sub-district of Jeli, 2000

District	Male	Female	Total
Batu Melintang	4,826	4,864	9,690
Jeli	10,820	10,300	21,120
Kuala Balah	6,118	5,944	12,062
Overall			42,872

(Source: Jeli Land and District Office website)

Table 1.2: The breakdown of the population by race in Jeli district.

Race	Total
Malay	42,400
Orang Asli	472
Overall	42,872

(Source: Jeli Land and District Office website)

1.2.4 Landuse

Based on Table 1.3, there several categories of land use in Kelantan in which are built up, infrastructure and utilities, agriculture, forests, and water body. The highest total area of land use in Kelantan is forest, 962, 496.34 hectares with 63.7%. From the statistic in Table 1.3, it shows most of the Kelantan area had been preserved and unexplored for land use and any mankind purpose in the year 2012. However, the unexplored land is decreasing through as the urban and agriculture activities are increasing from time to time.

Table 1.4 shows the land use statistic of Jeli district for the year 2017 and the highest percentage of Jeli districts land use is a forest. Jeli is mainly covered by reserved forest where the thick forest is under the constitutional protection of legal systems. The percentage of land use for agriculture is also high due to the main social-economic of local residents is agriculture. The settlement areas are scattered distributed.

Table 1.3: Present land use by Kelantan state in the year 2012 (in hectare)

Landuse category	Total area (Hectares)	Percentage (%)
Built up	52, 962.07	3.5
Infrastructure & utilities	17, 970.99	1.2
Agriculture	453. 958.08	30.1
Forest	962, 496.34	63.7
Water body	23, 074.51	1.5
Total	1, 510, 461.99	100.00

(Source: Jabatan Perancangan Bandar dan Desa, Semenanjung Malaysia)

Table 1.4: Current land use breakdown area Jeli, Kelantan (2017)

Landuse category	Area (Hectare)	Percentage (%)
Water body	1,785.033	1.229
Forest	99,058.455	68.200
Industry and Commercial	80.159	0.0489
Infrastructure and Utilities	29.672	0.020
Institution	426.216	0.293
Built-up	6.474	0.004
Transportation	1,739.550	1.198
Agriculture	40,381.765	27.802
Settlement	708.490	0.488
Unexplored land	1,003.839	0.691
Recreational land	27.434	0.019
TOTAL	145,247.086	100.00

(Source: Department of Town and Country Planning)

1.2.5 Social Economic

Jeli district mainly consists of oil palm plantation and forest for agriculture purpose. Hence, the main socioeconomic of local residents is a farmer and rubber tapper. This shows the agriculture sector gave high influence to social-economic for residents in the study area which led to the average developed of this district in the past decade. The agriculture sector has provided job opportunities for local residents. Mostly, settlements in Jeli district are villages which both Malays villages and Orang Asli villages.

1.2.6 Rainfall

The rain distribution of an area may affect the rate of weathering process of rocks. Forecast of geohazards can be predicted from the incensement of rainfall. Typically, during monsoon season, the rainfall distribution will significantly higher than usual. The amount of rain distribution on December is relatively highest and may lead to major flood event especially in lowland areas. Figure 1.2 shows the monthly distribution of average rainfall of Jeli district in the year 2017 and 2018 respectively. In year 2017, Jeli received the lowest rainfall in February and March and highest rainfall in August.

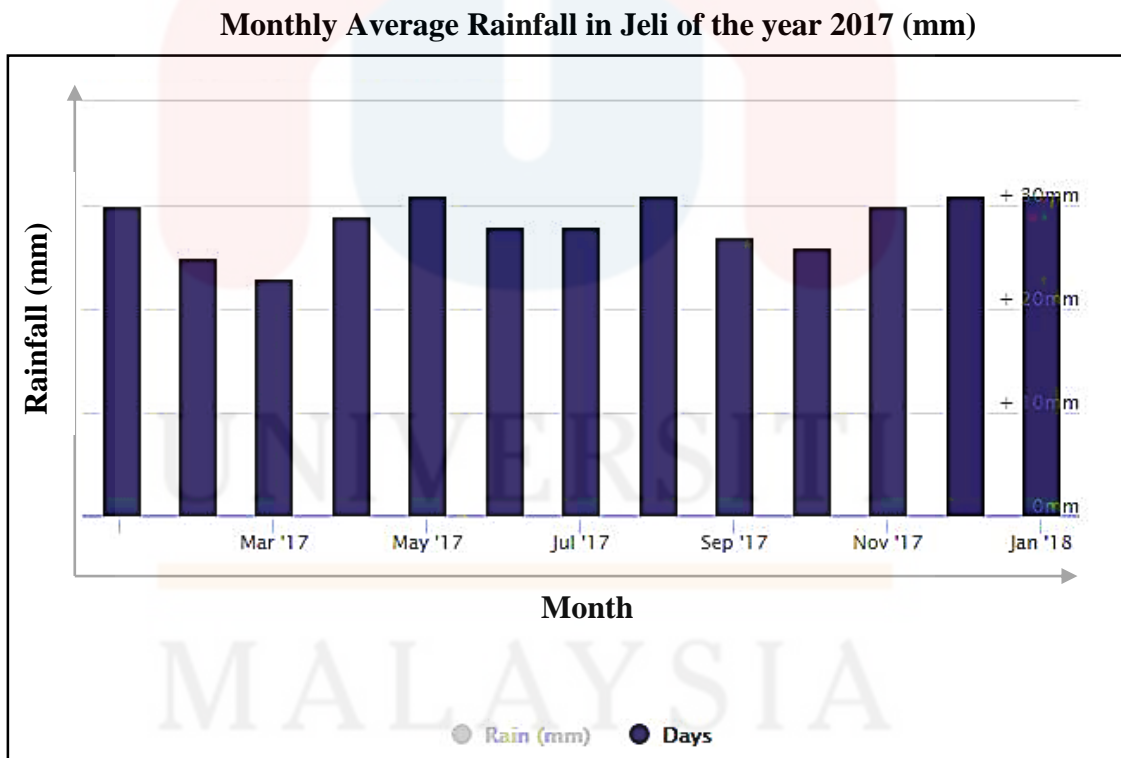


Figure 1.2 Monthly average rainfall in Jeli of the year 2017
 (Source: Department of Irrigation and Drainage Kelantan, Malaysia)

1.3 Problem Statement

Present geological maps of the study area are generally discussed dominantly on lithology of the area. Some changes occur to the lithology in the area which may result from weathering and erosion in which the processes are a naturally occurring process. So, it is necessary to update the new geological map with small-scale (1: 25,000) for research purposes.

A landslide has become a threat to residents because it can cause many kinds of destruction such as loss of lives and properties damaged. There are various factors which resulted due to mass wasting or landslides in which are a change in slope angle, weakening of earth materials due to weathering, increased water content, heavy rainfall distribution, and overloading. The geology and landforms of the prospect area show the area has the potential of slope failure. In this research, the slope occurrences are investigated based on water content, geological structures, and lithologies by using ERI method.

Due to lack of information about previous landslides on the state of the soil or rock that has a high potential of landslides, this may lead to more risk and hazards. Therefore, the present study to be carried out for investigation of slope failure using resistivity method. Electrical Resistivity Imaging (ERI) method is a new approach in site investigation which can minimize the destruction of the soil. Moreover, the resistivity method covers a large area with continuous information about the soil profile.

1.4 Objective of Study

The main objectives of the research project:

1. To produce an updated geological map on the scale 1:25,000 of the study area.
2. To analyze the subsurface factors of slopes by using Electrical Resistivity Imaging (ERI) method.
3. To determine the type and direction of failure by using kinematic analysis method.

1.5 Scope of Study

This research covered a wide scope of studies which includes geological, geophysical study, and kinematic analysis. The study area covered only 30 km² total area. The geological study includes geomorphology, stratigraphy, and structural geology of the study area. ArcMap software was used to make a geological map. The geophysical study covers the internal factors about the slope which are subsurface water content, geological structures, and lithology. Electrical Resistivity Imaging, ERI method is used to conduct the investigation of slope subsurface. In addition, the type and direction of slope failure are measured by using kinematic analysis method.

1.6 Significance of Study

This study is helpful as reference of prospect area through the production of the 1:25,000 scale geological map. Moreover, this research project provides geophysical slope subsurface factors in the prospect area. This research can also

estimate the level of hazard and risk through classification and extent of landslides which measured by using kinematic analysis. Hence, this research is helpful for the infrastructure plan. The most important is this study also beneficial for the academic purpose for students and industrial technical purpose researchers as a reference in the future.



CHAPTER 2

LITERATURE REVIEW

2.1 Introduction

This chapter provides details review about the previous study which related to the research prospect. Through literature review, various elements such as regional geology and tectonic setting, stratigraphy, structural geology, historical geology and landslide investigation in the study area are obtained. On this review, numerous sources providing the definitions related to the term landslides and followed by its classification types and factors of mass wasting. Resistivity study is also reviewed in this chapter.

2.2 Regional Geology and Tectonic Setting

Peninsula Malaysia is lies within of the Eurasian Plate, the South-East Asian part of which is known as Sundaland. The region is underlain by two North-South trending basement terranes juxtaposed during the Permo-Triassic by the closure of Paleo-Tethys along the Raub-Bentong Suture (Hutchison et al., 2009). According to Searle et al., (2012), Bentong-Raub suture is the main Paleo-Tethyan suture in Malaysia (Figure 2.1).

Kelantan is located at the Central Belt of Peninsula Malaysia and part of Bentong-Raub suture. The locality of Kelantan showed that the state consists of a central zone sedimentary and metasedimentary rocks bordered on the west and east by

granites of the Main Range and Boundary Range respectively (Swee Heng et al., 2006).

The Main Range granites range from monzogranite to syeno-granite. Post-collision uplift and late orogenic granitic trends showed the general trend of Main Range granite province (Figure 2.2). It said to be related to the Indosinian collisional orogeny and has S-type characteristics (Hutchison et al., 2009).

Jeli district is situated in the western part of Kelantan. It is located near Kelantan-Perak state border and Malaysia-Thailand international border. Basically, Jeli is divided into three sub-districts; Jeli, Batu Melintang and Kuala Balah (Nazaruddin, 2015). Jeli district is located at the foot of the Main Range of Peninsula Malaysia. Mostly, the main range is composed of granitic rocks with several enclose of sedimentary or metasedimentary rocks. The granitic rocks are stretching along the western part of Kelantan up to the state boundary of Perak and Pahang.

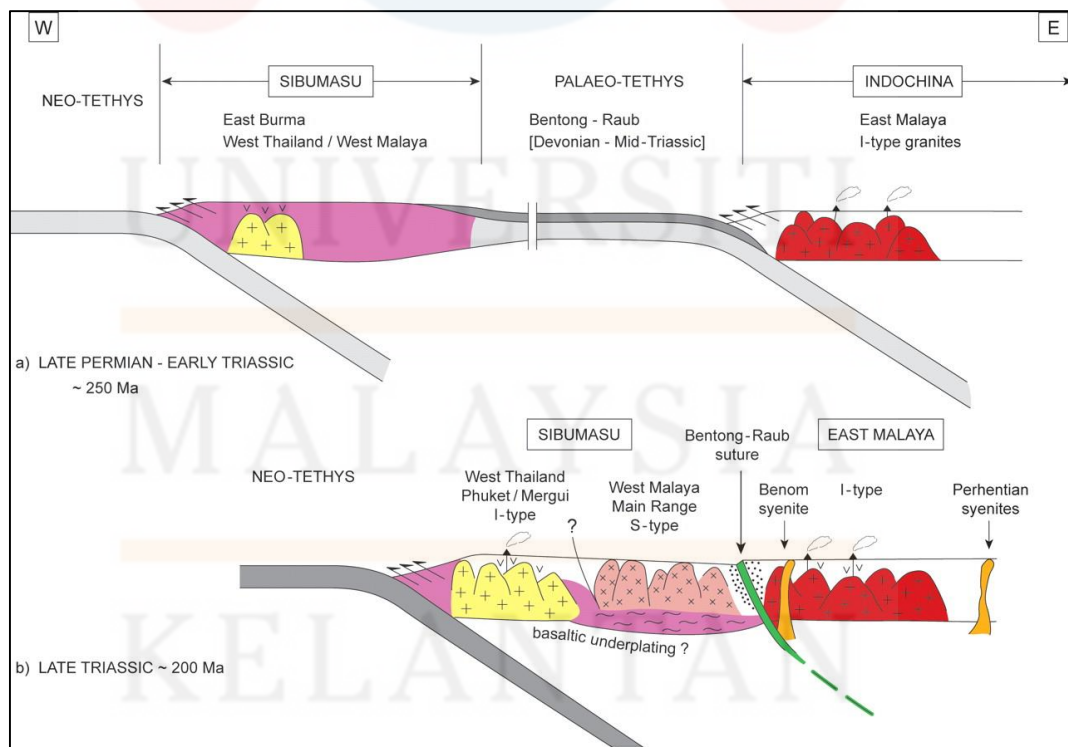


Figure 2.1. Tectonic setting of South-east Asia region. (Source: Searle et al., 2012)

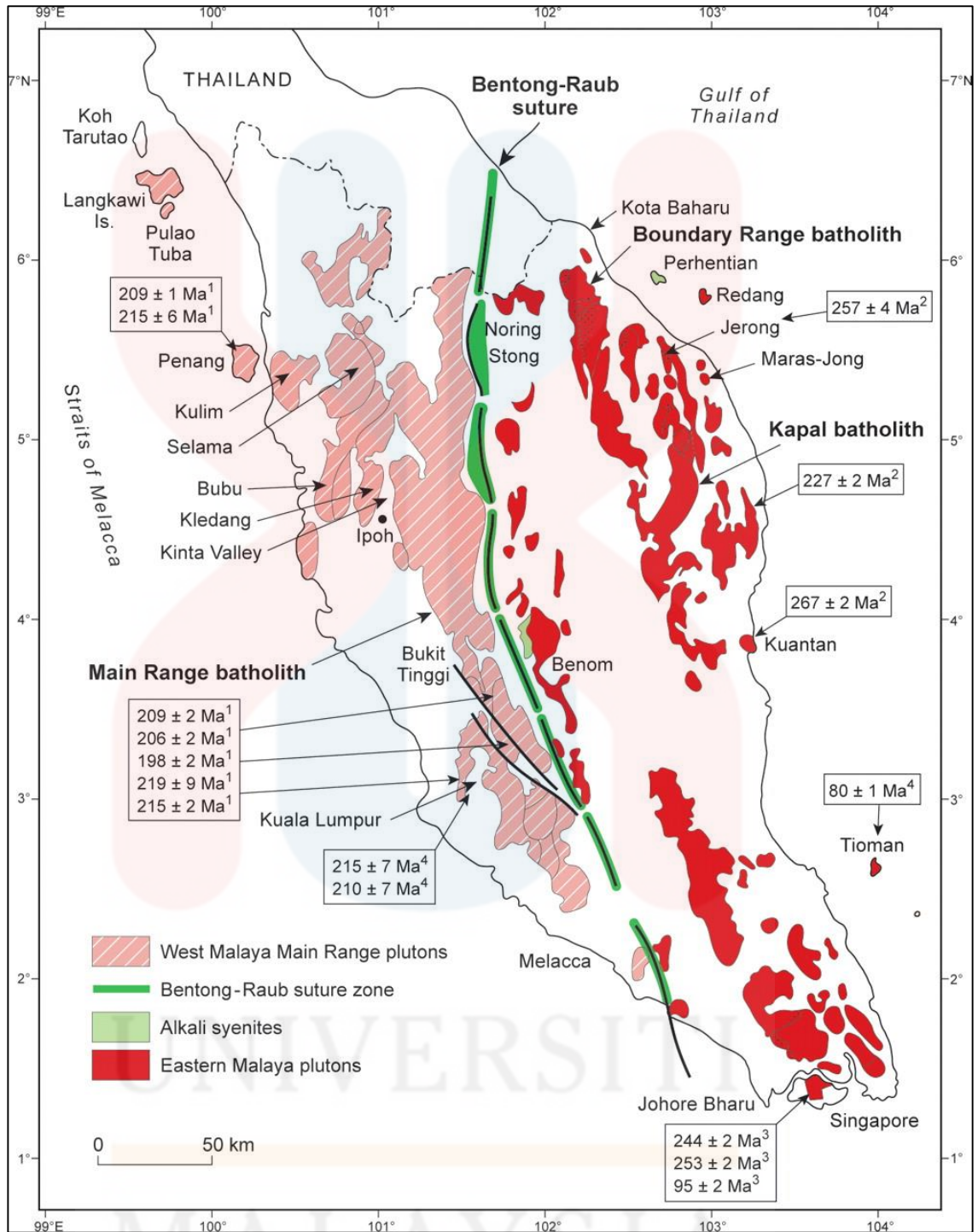


Figure 2.2. Geological map of Peninsular Malaysia. (Source: Searle et al., 2012)

2.3 Stratigraphy

The stratigraphy of Kelantan includes several formations which are Aring Formation, Taku Schist, Gua Musang Formation, Telong Formation, Gunong Rabung Formation, Koh Formation, Badong Formation and Stong Migmatite Complex. During Paleozoic era, Taku Schist and Aring Formation are formed and the others formations are formed during Mesozoic era (Hutchison et al., 2009).

The country rocks of Stong Complex are considered to be Permo-Carboniferous to Early-Triassic age. They mainly consist of carbonaceous shales with minor developments of pure and impure limestone, while the volcanic and volcanoclastic material of andesitic to the rhyolitic composition may be significant within the area. According to Loganathan et al., (1967), the lower age limit of the granites is set by the stratigraphic age of the enveloper of Carboniferous to Triassic while the upper age is not well defined stratigraphically.

Lithologies of Jeli district are split into three rock types; (i) Triassic sedimentary rocks (Gunong Rabong formation), (ii) Permian sediment rocks (Gua Musang formation), and (iii) granitic rocks (acid intrusive). Kg. Bukit Selar is located at the southern part of Jeli district. Typically, Kg. Bukit Selar is composed of Stong Migmatite Complex which includes Noring Granite, Kenerong Leucogranite, and several undifferentiated rock units (Mohd Rozi Umor, 2006).

2.4 Structural Geology

Peninsula Malaysia is a Paleozoic-Mesozoic structure which is part of the Pacific orogeny which experienced complex tectonic activity, orogenic, and post-orogenic. The layering of sedimentary rocks was transformed into a series of gigantic folds during the Mesozoic era. At the same time, a number of granitic intrusions occurred within Peninsula.

During Paleozoic and Mesozoic eras, tectonic activities in Peninsula Malaysia affected the land mass principally in the formation of faulting and folding (Hutchison et al., 2009). Faulting and folding are observed as regional and local structures. Folding, jointing, and faulting in the sedimentary rocks and jointing and faulting in granitic rocks are the local structures. Kelantan has a dominant structural pattern along a north-south to northwest-southeast directions (Figure 2.3). However, Jeli district's dominant local structures are along northwest-southeast and northeast-southwest directions (Umor, Ghani, & Mohamad, 2012).

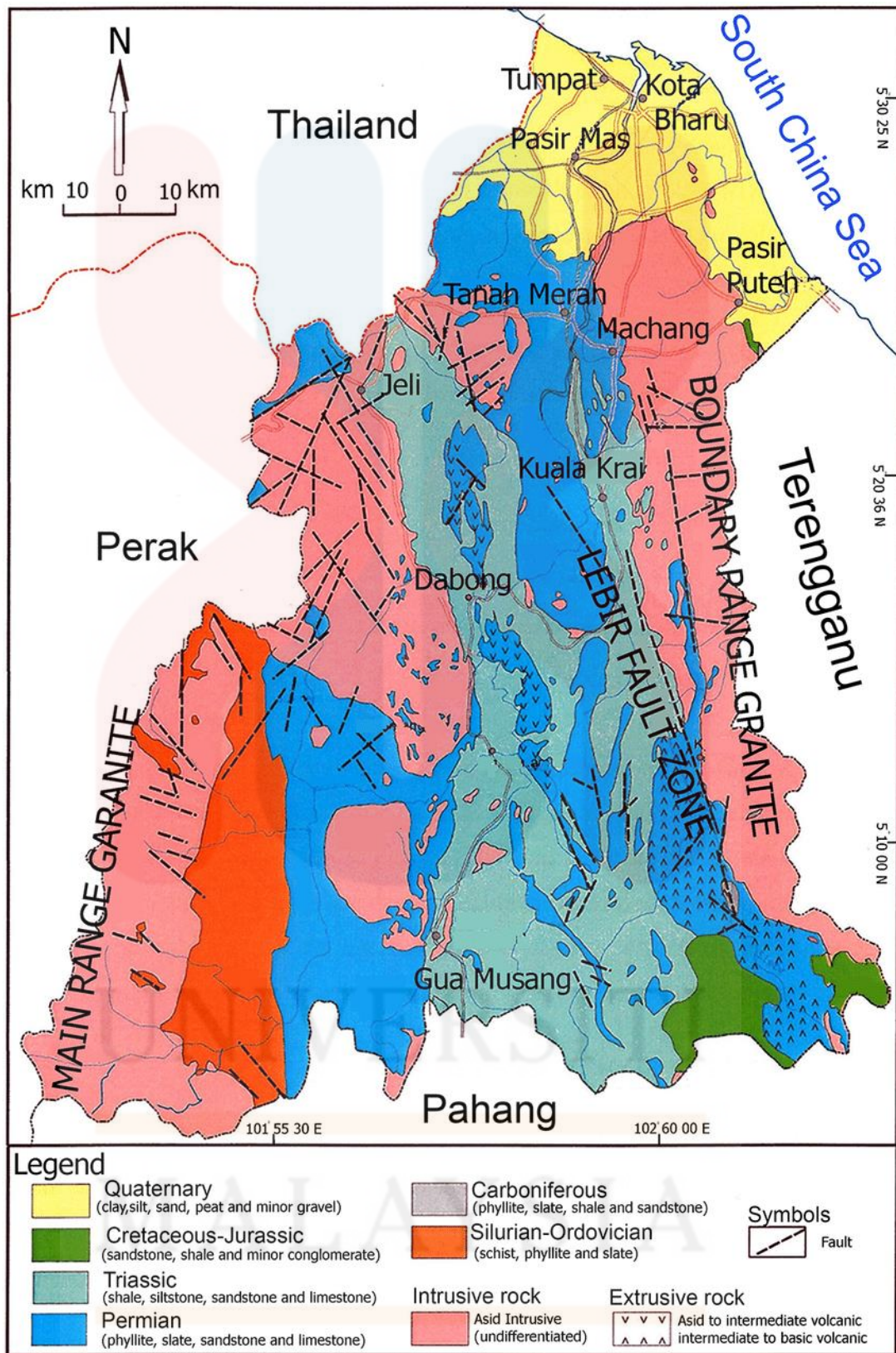


Figure 2.3. Geological map of Kelantan state. (Source: Pour & Hashim, 2017)

2.5 Historical Geology

According to the research by Tanot Unjah et al., (2002), the diversity of geomorphologic features of Stong Migmatite Complex is made up by three rocks unit which are Berangkat Tonalite, Kenerong Leucogranite, and Noring Granite. In Kelantan, the variety mountain landscape is exposed by these rocks. The landforms are interpreted as young stage geomorphology based on the presence of waterfalls and rapids at the steep-sloped drainage areas.

Noring Granite of Stong Migmatite Complex represents five rock types; porphyritic granite, microgranite, phyllite, tuffaceous sandstone, and xenoliths of sedimentary origin. Xenoliths are widespread within Noring Granite. The xenoliths showed similarity with metasediment within the area through petrographic study. Thus, the origin of the xenolith is the similar age with metasediment.

Other two components of Stong Complex in the order of decreasing age are Kenerong Leucogranite and Berangkat Tonalite which originated from the same magma that undergone differentiation. The origin of the magma either it is from Main Range Granite Batholith or Eastern Belt Granite is being determined by X-ray fluorescence (XRF). The Stong Complex is from I-type granites of the Eastern Belt Granite (Hutchison et al., 2009).

MALAYSIA

KELANTAN

2.6 Landslide

The term landslide denotes the movement of the mass of rock, debris or earth down a slope. The phenomenon described as landslides are not limited to land or to sliding. (Cruden & Varnes, 1996). According to Barta et al (2005), movement of landslide typically occurred repeatedly in old landslide region. This is because the old landslide has a tendency to reactivate. Slope stability can be described as the inherent structural integrity of a slope to undergo failure. Failures can occur as slides, cracks and slope movement. Slope failure is a common geological hazard in tropical countries like Malaysia, which is characterized by a humid, a tropical region and thick weathering profile. Slope failure is the main factor of landslide phenomenon.

According to Walker & Shiels (2013), there is three type of movement in a landslide; slide, flow and falls. Sliding can occur through a rotational movement called slump or along a plane. Flows consist of mass movement (influenced by gravity), and they are similar to creeps and spreads, and mass transport (when rock or soil is transported by a moving medium such as water, air, and ice). Landslides also include falls, an outwards and downwards movement of rocks and debris with exposes faces.

The stability of natural and man-made slopes is an essential matter for many types of sites uses and their purpose, whether the development of infrastructure, homes or natural resources. Slope stability is influenced in large part by their geological and geotechnical characteristics of the bedrock and soil that composed the slope. Normally, the strength of these material plays an important part in slope stability. However, for slopes that predominantly made of bedrock, usually, the most important factor is the geological structure of the rock. The geological structure can indicate the orientation, location, and spacing of discontinuity within the bedrock mass and such

discontinuity are comprise those along bedrock bedding, joints, fault and shear (Palaskar, 2016).

2.6.1 Slope Stability Analysis

According to Yilmaz (2011), movement of rock debris or earth down a slope is defined landslides or slope failure phenomena. Slope failures are complex events and the factors that affect slope stability are difficult to measure, particularly shear strength parameter values of the soil and groundwater conditions. Ideally, the stability problems can be discovered and addressed before a slope failure occurs. It is necessary to evaluate the stability of the concerned slopes or to investigate the factor of the slope failures.

This phenomenon can be triggered by a variety factor, either external or subsurface factors such as intense rainfall, earthquake shaking, water level changes, increased water content and increased in slope angle (James S. Monroe Reed Wicander, 2007). Human activities such as excavation of slopes for road cuts are also one of the factors triggering slope failure which caused unstable hill-slope areas. A serious slope movement occurred at 36.2 km of the Gerik-Jeli Highway in 1999, due to the highway construction. (Muhammad Barzzani Gasim et al. , 2015).

One crucial part to identify risk in slopes is to determine the Factor of Safety (FOS) which will indicate the stability of a certain slope. There are few parameters to be obtained before calculating FOS are cohesion, internal friction angle, and unit weight of soils. Since most o landslides occurrence in Malaysia is because of

infiltration, the pore water pressure and moisture content also contribute to FOS value. (Syed B. Syed Osman, 2014).

The essential conditions and factors which contribute to the disruption of stability of slope are topography, loose stratum, active groundwater, intense freeze-thaw erosion and human engineering activities (Hu, Shan, & Jiang, 2014). Due to complex geology and structural characteristic of meta-sedimentary and metamorphic rocks, cut-slopes on them have a stability problem.

The geological structures and lithologic units have a probability in determining the potential landslide area. It is hypothesized that highly faulted and folded are weak rock sequence which has a high probability of slope failure to occur. It is believed due to long exposure, the climatic factors and weathering process have caused the crop out of these rocks and experienced failure and movement.

2.6.2 Study about landslide

In the early 1980s, the Gerik-Jeil Highway was constructed between the northwestern region and the eastern coast of the Malaysian Peninsula. The highway cuts across variable type of rocks in which are variably dipping sedimentary, metamorphic rocks and granitoids. Recent slope failures have occurred in weathered cut-slope of the area due to structurally controlled events (Muhammad Barzzani Gasim et al. , 2015). Some discontinuity surveys and slope failure studies are conducted along the Gerik-Jeli Highway by Rafek and Komoo (1989) and Jamaluddin (1991), they concluded that structurally controlled failures were dominant in this area.

According to Shuib, Taib, & Abdullah, (2006), East-West Highway slope instability is a serious problem due to steep topography and cut-slopes, unfavorable geological condition and adverse climate. Several detailed discontinuity surveys and analysis have conducted along the highway through GIS and geophysical method. Common failure modes of rock slopes along the highway deduced from the studies are mainly composed of planar, wedge, toppling and circular failures typical of cut-slope failures in hilly and mountainous terrains. Engineering geologic analysis and slope stability kinematic analysis are previous field assessment conducted to summarise the characteristics of slope material (K., 2004).

2.7 Geophysical Methods

Surface-based geophysical exploration often provides the quickest and most economical means of obtaining general information of subsurface conditions over relatively large and rugged areas. Through investigation and mapping of the distribution of physical properties of earth materials, indirect information related to landsliding can be achieved. Different surface-based geophysical methods as shown in Table 2.1 provide a different kind of landslide-related features (Bell et al, 2006).

Table 2.1: Suitability of various geophysical methods for different landslide types and landslide related features.

Methods		Rock slides	Soil slides	Quick clay landslides	Rock falls	Property determination for geotechnical purposes	e.g. artefacts, pipes, foundations	Ground water/soil moisture
Seismic methods	Refraction/Reflection	+	+	+	?	+	-/(+)	+/-
	Tomography	+	+	-	-	+	(+)	-
	Passive seismic	+	+	-	+	-		-
	Surface waves	?	?	+	-	+		-
Electro-magnetic methods (EM)	Low frequency	+	+	-	-	-	+	+
	Ground-penetrating radar (GPR)	+	+	-	+	-	+	+
Resistivity measurements		+	+	+	?	-	(+)	+
Self-potential (SP)		+	+	-	-	-	-	+
Induced polarisation (IP)		-	-	+	-	-	-	+
Gravity		?	?	-	+	+	-	-
Magnetism		?	?	-	-	-	-	-

+ = suitable, (+) = partially suitable, - = not suitable, ? = depends on the site or needs further analysis

(Source: Bell et al, 2006).

2.7.1 Electrical surveys: Resistivity method

Surface-based measurement of the electrical resistivity of earth materials involves the introduction of an electrical current into the ground and the measurement of materials' resistance to the current. Gelisli & Ersoy (2017) stated that by making the measurements along the ground surface, a resistivity distribution in subsurface able

to be determined. It is based on the potential difference between two potential electrodes placed within the field created by the current electrodes. The resistivity of a material is a measure of how well the material retards the flow of electric current. Resistivity is often encountered in physics when discussing the resistance of an ideal cylinder of length L and cross-sectional area A of uniform composition. The resistivity can be express in the equation as;

$$R = \rho \frac{L}{A}$$

and the SI unit for resistivity is Ohmmeter (Ωm).

Commonly used electrode configurations include the Wenner array, Schlumberger array, and dipole-dipole array. Basically, the depth of investigation of resistivity survey is proportional to the spacing of the current electrodes. However, the penetration of the electrical current into the ground still depends on the resistance of individual layers and their distribution (John, 2003).

According to Gibson & George (2013), the four standard electrode configuration which commonly employed in electrical surveying, and the electrodes arrays, geometric factors, and apparent resistivity equations are considered below. In the Wenner array, the electrodes are equally spaced with the two potential electrodes between the two current ones. Schlumberger configuration has the potential electrodes between the current electrodes, but the distance ($2l$) between them is considerably less than the distance ($2L$) between the current electrodes (typically, $L \geq 5l$). The potential electrodes are assumed to be in the center of the array. However, the potential also can be in between C1 and C2. Pole-dipole produces asymmetric anomalies that are consequently more difficult to interpret than those symmetric arrays. Peaks are

displaced from the centers of conductive or chargeable bodies and electrode positions have to be recorded with a special case. At the point mid-way between the moving voltage electrodes, the values are plotted. The pseudo-section result shows depth penetration varied by varying n (John, 2003). The dipole-dipole array is said by John (2003), to be popular in induced polarization (IP) work. This is because the complete separation of current and voltage circuits reduced the vulnerability to inductive noise. Basically, the larger the value of n , the deeper the penetration of the current path sampled.

2.7.2 Type of Resistivity Array

According to Reynolds (2011), the value of the apparent resistivity depends on the geometry of electrode array used, as defined by geometric factor, K . There are three main type of electrode configuration in common use, two which are named after their originator, Frank Wenner (Wenner array, 1912), Conrad Schlumberger (Schlumberger array) and another one is Dipole-Dipole array. That there are so many different array types is indicative of the flexibility of the resistivity technique, but it is more to recognize the advantages and disadvantages of each array; familiarity with the array type, availability of cabling and data acquisition software and data processing and inversion software, as well as site-specific factor.

According to Loke (1999), the arrays that are most commonly used for 2-D imaging surveys are Wenner, dipole-dipole, Wenner-Schlumberger, pole-pole, and pole-dipole. There is a certain parameter that should be considered in choosing the array used; first is the sensitivity of the array to vertical and horizontal changes in the subsurface resistivity, secondly the depth of investigation, the horizontal data

coverage, and the signal strength. The sensitivity function basically helps us to measure the degree to which a change in the resistivity of an area of the subsurface will influence the potential measured by the array. The higher the value of the sensitivity function, the greater is the influence of the subsurface region on the measurement.

In geophysics, the three common types of arrays have their own electrode configuration, also known as a geometric factor, K . In Wenner configuration, four electrodes were arranged in a straight line with constant separation, a . For Schlumberger arrangement, the distance between potential electrodes ($2l$) is smaller than the distance between current electrodes ($2L$). In Dipole-Dipole array, potential electrode $P_1 P_2$, located at the outside of current electrode $C_1 C_2$. Both electrodes have same separation, a (Figure 2.4). (Samsudin, 1990)

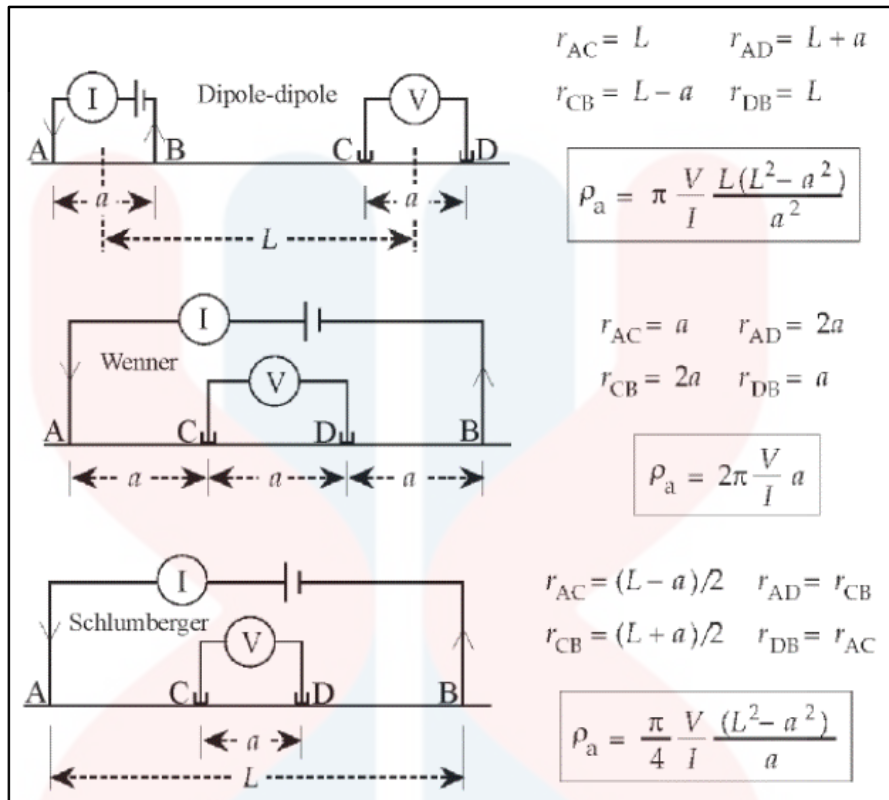


Figure 2.4 Arrangement of current and potential electrodes for the Dipole-dipole, Wenner and Schlumberger array
 Source: (W., 2007)

According to Telford *et al* (1990), although have a simple geometry, Wenner array arrangement is quite inconvenient for fieldwork. For some depth exploration, electrodes in Wenner array are expanded about a fixed center, increasing the spacing in steps. For lateral exploration or mapping, the spacing remains constant and all four electrodes are moved along the line, then on another line and so on.

The Wenner configuration is the simpler in that current and potential electrodes are maintained at an equal spacing a . In surveying with the Wenner configuration all four electrodes need to be moved between successive readings. This labour is partially overcome by the use of the Schlumberger configuration in which the inner, potential electrodes have a spacing $2l$ which is a small proportion of that of the outer, current electrodes ($2L$). (Kearey *et al*, 2002).

According to Aizebeokhai, (2010), the dipole-dipole array is the most sensitive to resistivity variation below the electrode of each dipole pair and very sensitive to horizontal variation. Instead of that, the dipole-dipole array is relatively insensitive to vertical variation in subsurface resistivities. The dipole-dipole array is very poor in mapping horizontal structure such as sills, sedimentary or horizontal layer. However, this array is very suitable to map vertical structure like dikes and cavities. The depth of this array depends on the spacing between current electrode a , and the distance between two dipoles and is generally lower than Wenner array. The major disadvantage of this array is the signal strength decrease with the increasing dipole pair distance.

2.7.3 Study about slope failure using resistivity method

Yilmaz (2011), has carried out an electrical resistivity imaging study over a slope failure in Elmadag district of Ankara-Kirikkale highway. ERI method was chosen as a method due to the ability to explicate complex subsurface structures. The result obtained is a high-resolution image of subsurface patterns of electrical resistivity. Dipole-dipole array with an electrode spacing 5 m for eight resistivity profile extending 275 m was used. Total 58 electrodes separated by 5 m multi-electrode 2D device were used.

The magnitude of electric resistivity particularly depends on a grain size of the rocks, contents of water and its mineralization (Bárta et al, 2005). Increasing contents of water in the rock and with increasing mineralization of water results in decreasing of electric resistivity. However, resistivity increases with an increased grain size of the

rock. Hence, resistivity measurements allow good separation of individual structural elements of the rock massive and to observe changes in time.

A high-resolution image of subsurface electrical resistivity can be obtained using electrical imaging resistivity, ERI method. The 2D ERI technology is a combination of vertical electrical sounding and resistivity profile measurement techniques. Hence, the discontinuity between landslide material and bedrock can be identified. Through 2D ERI method, data is presented in pseudo-section. Pseudo-section is a representation of apparent resistivity variations in the subsurface. Resistivity distribution data is obtained through 2D inversion of apparent resistivity data. Typically, grain size, porosity, contents of water and mineralization of the rocks contribute to varying range electric resistivity values of rocks (Bakhshipour et al, 2013).

The ERI data traditionally presented in the form of pseudosection, which provide the picture of the subsurface resistivity of the slope (Yilmaz, 2011). Inversion of the data through Res2dinv software is required to obtain a 2D true resistivity section. This software is reliable for complicated geoelectrical conditions, without any reservations for the zone between the ground level and bedrock (Bárta et al., 2005).

The application of geoelectrical survey has theoretically stated that the water content in subsurface materials has a close positive correlation with the electrical conductivity. However, this hypothesis can turn negatively in the case of the natural slope that has many uncertainties. When evaluating the structure and function of the natural slope, the slope materials usually shows a variety of resistivity values ranging from low to high values. Normally, high resistivity values indicate a low conductive

zone while a low resistivity value is always assumed to be a high conductive zone which reflects to be a weak zone.

In tropical climate country as Malaysia, weathering process is much progressive thus accelerating the transformation of homogeneous subsurface material into heterogeneous subsurface materials. As a result, water content can be inconsistently present due to the heterogeneous materials derived from the rapid weathering condition from a heavy rainfall phenomenon. The progressive weathering process was believed to be the main reasons that caused the slope materials to be disintegrated by physical weathering and decomposed by chemical weathering thus producing heterogeneous subsurface slope material (Mohd Hazreek *et al*, 2012).

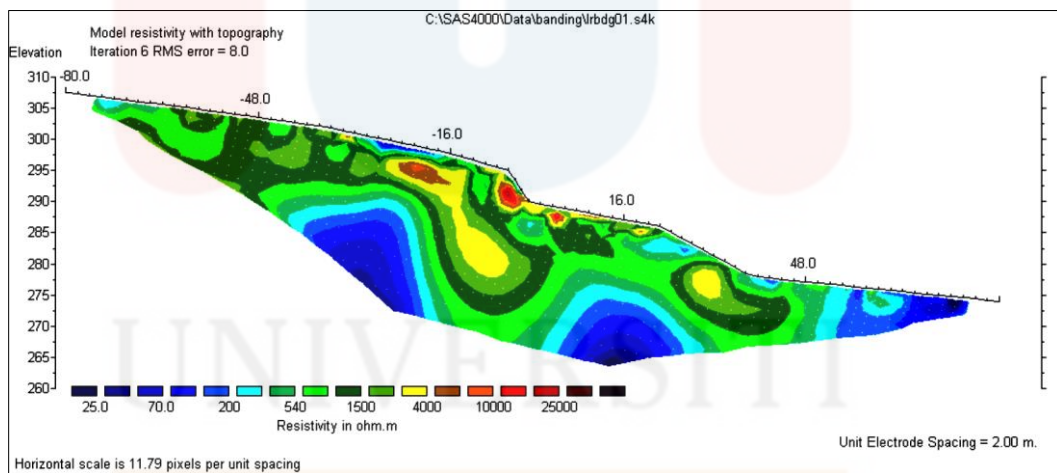


Figure 2.5 Example of resistivity data from the slope at Banding Island (Source: Aishah et al, 2009)

Figure 2.5 illustrates the results along Line 2 which shows the electrical resistivity distribution of the subsurface in the vicinity of the collapsed multi-story building. The area is underlain by weathered Argillaceous Facie. The image shows that most of the subsurface formation has electrical resistivity distribution less than 4,000 ohm-m. Ground very near to the Tasik Temenggor water line has a resistivity less than 200 ohms indicating the Argillaceous Facies are water-saturated. Water saturated zone also be can be found at depths 15 meters below the ground surface. Field observation had indicated that the high resistivity (greater than 4000 ohm-m) zone present near to the earth surface in the image is related to loose weathered meta-argillite found in the area.

CHAPTER 3

MATERIALS AND METHODS

3.1 Introduction

This research project is conducted within Kuala Balah district mainly covered by Kg. Bukit Selar, Jeli, Kelantan. For this research, there are various materials and methods are used in order to conduct geological mapping, geophysical investigation, kinematic analysis, laboratory analysis, data interpretation, and report writing. Basic geological mapping and kinematic analysis materials are such as a hammer, GPS, compass, hand lens, and sample bag are used. ERI method is being applied during slope investigation to classify the bedrocks and structural characteristics.

The method is a series of steps taken to complete a certain task by referring to the objectives. For methodology part, geological mapping method includes data collection on geomorphology, lithology, stratigraphy and structural geology of the study area. While for slope investigation, this research is focused on a geophysical survey of the subsurface factors of slope failure. Kinematic analysis includes measuring of the joints spacing, aperture, trend, and plunge.

The research flow chart is present in Figure 3.1. Research flowchart helped to ensure this research is successfully conducted according to the time limit.

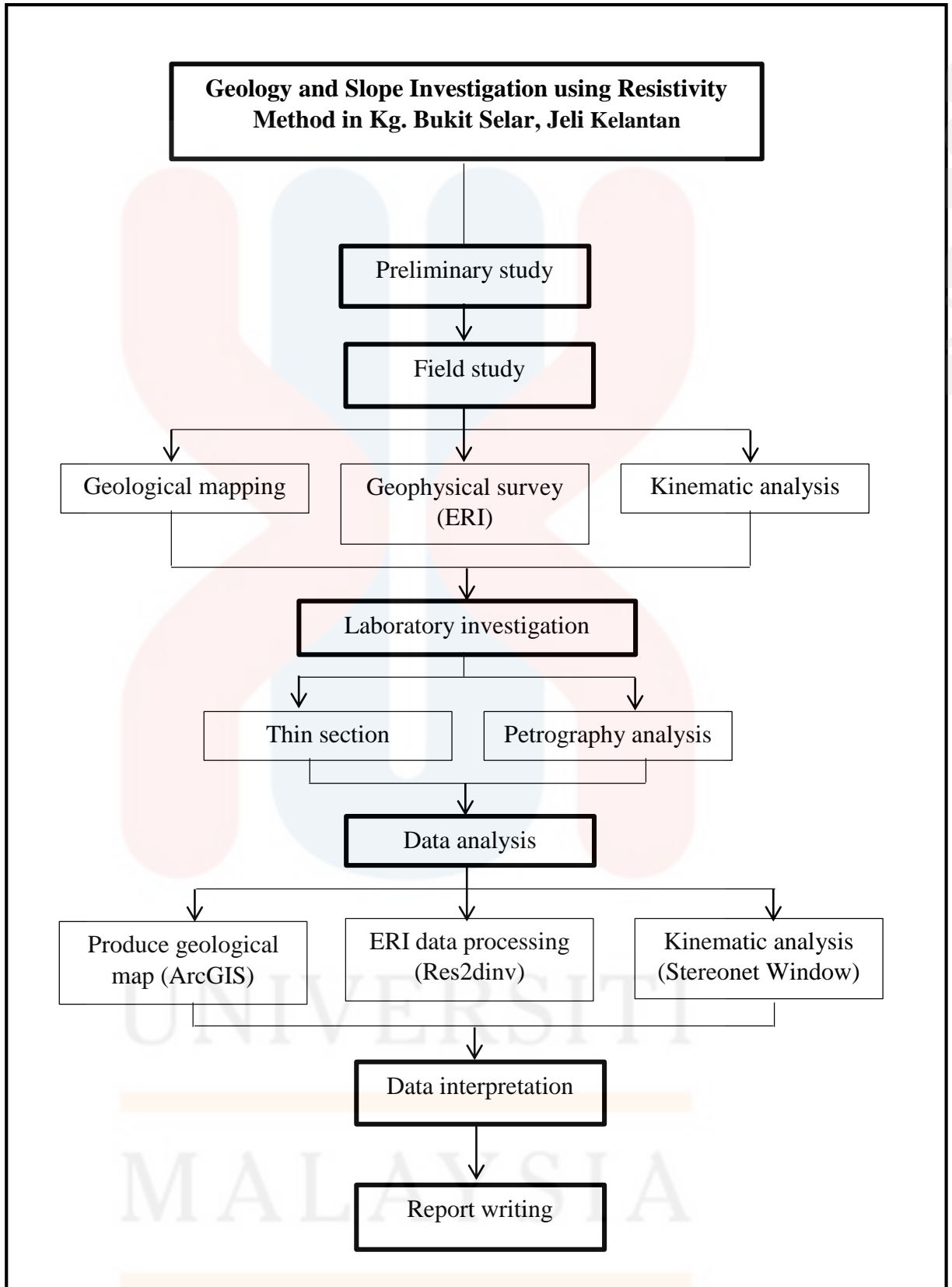


Figure 3.1. Research flow chart.

3.2 Materials


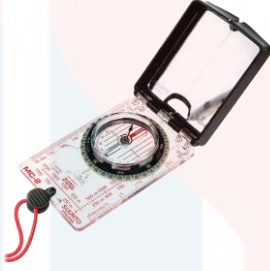


Materials are the equipment or apparatus needed in order to complete the research according to the objectives. For this research, there are several types of equipment being used based on the methodology for both field data collection and data analysis.






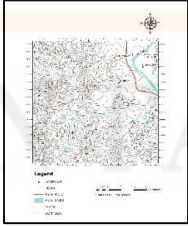
Data collection will involve geological mapping, geophysical investigation, and kinematic analysis of the study area. During geological mapping and kinematic analysis, the materials needed are GPS, compass, tip-point hammer, sample bags, hand-lens, hydrochloric acid (HCl), stationeries and field notebook for rock and soil sampling. An ABEM Terrameter LS is used to perform the electrical resistivity measurements for geophysical study in the field by utilizing the Pole-dipole and Schlumberger Configuration. Vertical changes, horizontal structures and strong signals strength able to be detected by these configurations.



Data analysis includes production of geological map, geophysical analysis, and kinematic analysis. Laboratory analysis will be divided into two parts, thin section process, and petrographic analysis. Microscope, are tools needed in the petrographic analysis. Microscope, are tools needed in the petrographic analysis. ArcMap 10.2 software will be used to do field data analysis. Materials used for data analysis for ERI study and kinematic analysis are Terrameter LS Toolbox, Res2dinv, Stereonet Window and GeoRose softwares.

The materials used throughout this research are shown in Table 3.1.

Table 3.1: Materials and equipment

No.	Name	Tools	Uses
1.	GPS	 <p>Source: Google image</p>	<p>A modern device which can pinpoint the position on the Earth 's surface with the help of satellites that orbiting the Earth.</p>
2.	Compass	 <p>Source: Google image</p>	<p>For navigation and orientation that shows the direction relative to North, South, East, and West</p>
3.	Hammer	 <p>Source: Google image</p>	<p>To break the rocks for sampling purposes.</p>
4.	Hand-lens	 <p>Source: Google image</p>	<p>To identify the hand specimens where the grain size or crystal size that build up the rocks can be observed.</p>
5.	Measuring tape		<p>To measure something from grain size to bed thickness.</p>

		 <p>Source: Google image</p>	
6.	Hydrochloric acid	 <p>Source: Google image</p>	To differentiate different types of rocks or minerals such as limestone, quartz, calcite, and dolomite.
7.	Stationery	 <p>Source: Google image</p>	To write down all the data information
9.	Sample bag	 <p>Source: Google image</p>	To store the rock specimen before its processed into thin sections.
10.	Camera	 <p>Source: Google image</p>	To take a picture with scale for references on doing data analysis.
11.	Base map	 <p>Source: Google image</p>	To allocate the study area and assume the structure that may occur.

12.	<p>ERI method apparatus</p> <ul style="list-style-type: none"> i. ABEM TERRAMETER LS 1000 ii. Connectors iii. 2 potential electrode iv. 2 current electrodes 	 <p>Source: Google image</p>	<p>To measure variations in the electrical resistivity of the ground, by applying small electric currents across arrays of ground electrodes.</p>
	ArcGIS software	 <p>Source: Google image</p>	<p>Used to produce map of study area. The traverse marked using GPS is transferred to the software.</p>
	Terrameter LS Toolbox software		<p>The data from ERI field survey is transferred to PC by using this software.</p>
	Res2dinv software		<p>Inversion of pseudosection. Data from Terrameter LS Toolbox is interpreted using Res2dinv.</p>
	Stereonet Window software		<p>A software in which able to display geological data for kinematic analysis.</p>
	GeoRose software		<p>This software presented the joints reading which used for forces interpretation.</p>

3.3 Methods

3.3.1 Preliminary Study

Preliminary study has been done to collect information from the previous study which related to research objectives and study area. Sources of information in the preliminary study include articles, books, journals, thesis, and map. The information is gathered for literature review process. A literature review is a core to propose and conduct a research. From the sources, there is some research has been carried out on slope investigation but in different work scopes such as GIS and engineering. Google Earth, GIS software, and topographic have been used to locate the exact location of the study area. Discussion with the supervisor also part of the preliminary study especially in choosing suitable title and objectives for this research.

3.3.2 Field study

This research entitled Geology and Slope Investigation using Resistivity Method of Kg. Bukit Selar, Jeli Kelantan is focused on geology and slope investigation using ERI method of the study area. For slope investigation, kinematic analysis is also conducted as an additional method to identify the type and direction of slope failure. There are some criteria such as geological characteristic needed to be assessed to be the most important for slope failure investigation in the study area. For identify the geological characteristics, field sampling and the geophysical survey is conducted during field study.

i. Geological mapping

Geological mapping is a method to study the geology of prospect area which includes geomorphology, lithology, stratigraphy and structural geology aspects of the study area. During geological mapping, the data is collected by traversing, sketching, field observation, and field sampling.

Traversing is a method of making an observation of outcrops along the path across the study area. Traverse plan is made before going to the field. Traverses are pre-determined routes, where the contacts and other geological features are extrapolated between the traverses and the map of the geology of the area is prepared.

At the prospect site, a sketching is important as it provides the site description. For drawing sketch, the geological data such as outcrop dimension, bearing, and environment have been recorded. Other geological data such as vegetation and civil objects are additional.

Field sampling is a necessary task in conducting geological mapping. The samples of soil and rock are collected from the site according to the changes of lithology units. The geological description is recorded at every observation or sampling station. Every details of the geological information are recorded. It is essential to see the rocks distribution to correlate with slope failure potential as the large distributions of some rocks can be indicated as the high potential of slope failure.

ii. Geophysical test (Electrical Resistivity Imaging, ERI)

This ERI method is helpful to obtain subsurface structures in direction of the sliding movement. 2-D resistivity imaging is methods which use electrical current directed into the ground and is able to identify the different subsurface lithology. This method has few abilities which required for slope investigation in the study area such as to provide the data about subsurface structure, water content, and types and thickness of the subsurface lithology layer. Figure 3.1 shows the range of resistivity expected for common rock types. Hence, the subsurface factors of slope failure can be determined.

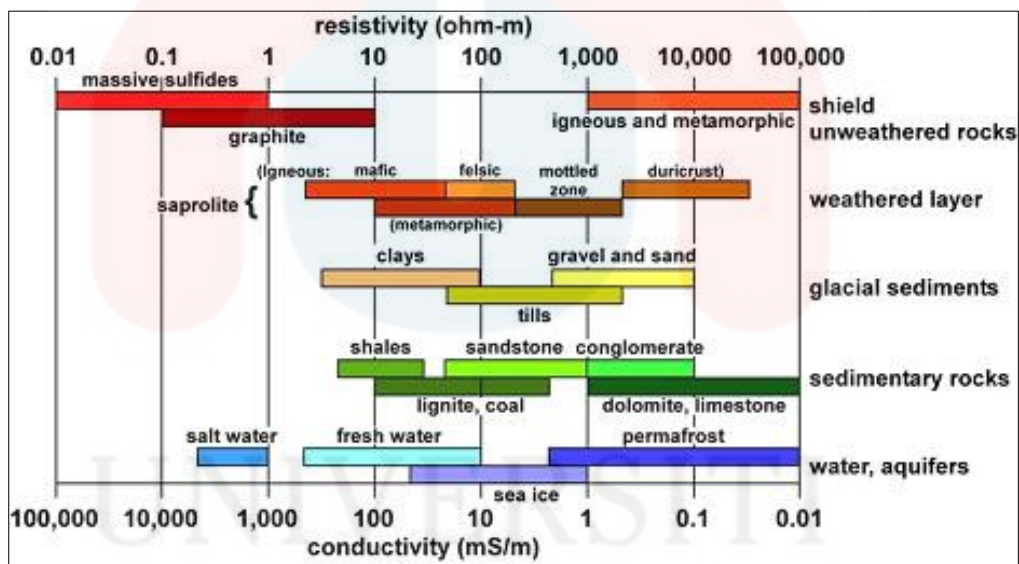


Figure 3.2 The approximate range of resistivity values of common rock types. (Source: Palacky, 1988)

The resistivity method calculates the resistivity and chargeability distribution of the subsurface materials. Different types of materials provide different resistivity and chargeability values. Vertical depth of resistivity measurement is affected by the electrodes arrangement and length of the line.

During slope investigation using ERI method for this research, two array configurations have been used in which are Schlumberger and Pole-Dipole configuration. Each type has a different configuration and geometric factor as shown in Figure 3.2. The Schlumberger configuration in which the inner, potential electrodes have a spacing $2l$ which is a small proportion of that of the outer, current electrodes ($2L$).

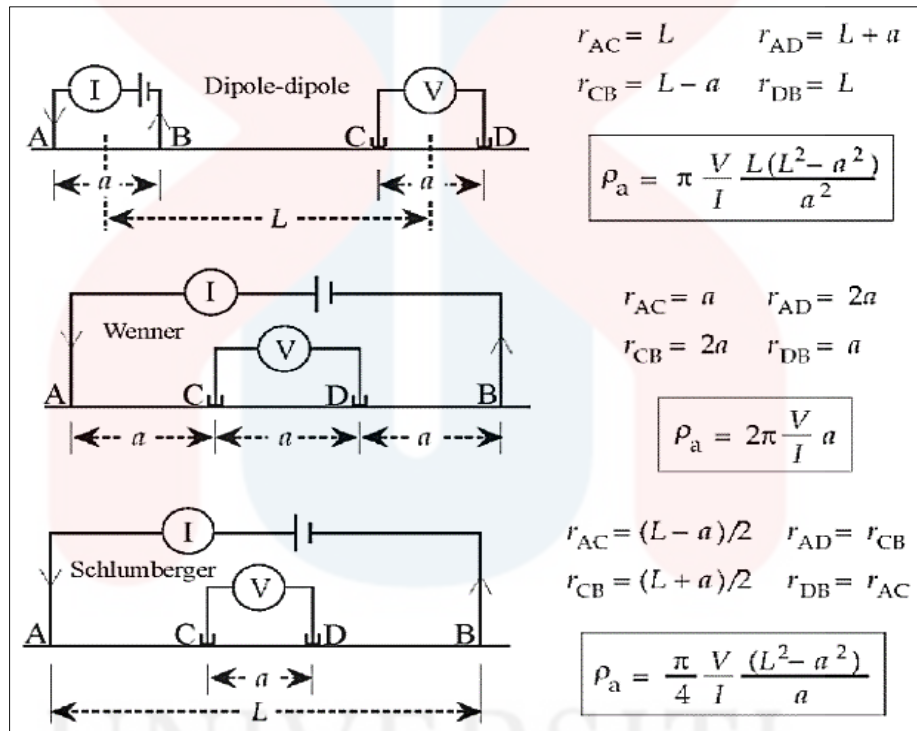


Figure 3.3 Arrangement and geometric factor for each array.

As mention above, ABEM Terrameter SAS 1000 with Pole-Dipole and Schlumberger configuration are being used to study the slope subsurface characteristics in the study area. Two survey lines with electrodes spacing of 5 m and three survey lines spacing of 5 m were used for the study area. Pole-Dipole configuration of two survey lines with total 200 m and Schlumberger configuration of three survey lines with total length of 200m are injected during the slope investigation using ERI method.

Pole-Dipole array is chosen because this protocol covered a greater depth for subsurface materials. As the slope is considered as a big size slope, greater depth for subsurface study is needed. Pole-Dipole array is used for two vertical lines along the slope. This protocol, the current electrode C2 is fixed at remote distance. The spacing is representing by the potential electrodes P1-P2 and P1-C1 is the distance of 'n' factor. A good horizontal coverage and more sensitive to vertical structure is the advantage of this array.

Schlumberger array is chosen because fewer electrodes needed to be moved for each sounding and it has better resolution and greater probing depth and less time-consuming field deployment. The horizontal coverage of Schlumberger is better than Wenner array. However, the signal strength is higher the Pole-Dipole array. Both criteria are important to produce higher signal levels for deeper measurement and sensitive to resistivity variations with depth. Various kinds of data will be acquired from resistivity methods such as subsurface structures, the type and thickness of the bedrocks, sliding plane, and contents of water. Tomographic inversion is achieved from processing using Terrameter LS Toolbox and Res2dinv.

3.3.3 Laboratory Investigation

i. Thin section process and petrography study

Petrography thin section analysis will be used to investigate the process of rock formation and the composition of the mineral. In this method, the rocks and soil samples will be processed through petrography thin section to investigate the geology of the study area. Thin section involved three stages; sectioning, grinding and lapping.

In this research project, one or two samples are processed for each lithology in the study area.

Figure 3.4(a) shows the rock cutting process in which the hand specimen is cut into suitable size. Figure 3.4(b) shows the polishing step. The rock sample is polished in order to reduce the rough surface of the rock due to the rock cutting step. It is important because the rough surface can cause bubble when frost on the glass slide. Figure 3.5(a) shows the sample has been frost on glass slide. Figure 3.5(a) shows the end products of thin section processes.

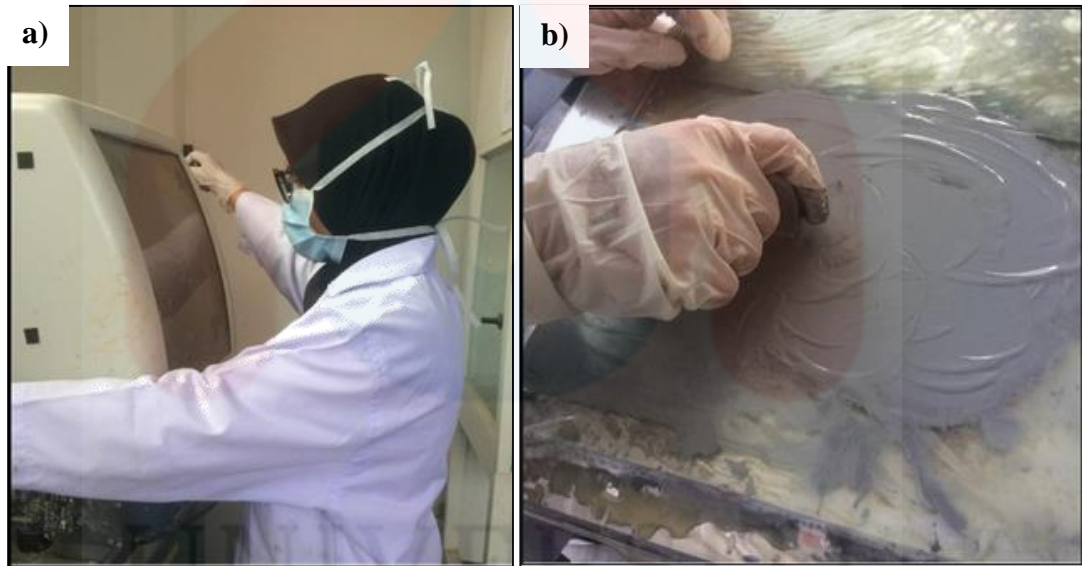


Figure 3.4. a) Rock cutting step. b) Polishing step.

UNIVERSITI
MALAYSIA

KELANTAN

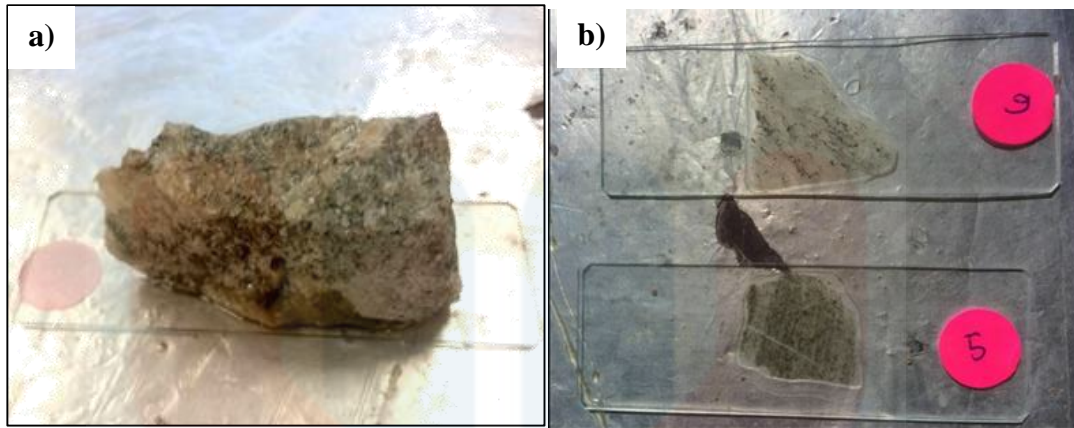


Figure 3.5. a) Rock sample frosted on glass slide. b) Slide ready for petrography analysis.

3.3.4 Data Processing

All the obtained geological data from the field study are processed by using the GeoRose, Streonet, ArcGIS, Terremeter LS Toolbox and Res2dinv software. GeoRose and Streonet window software are used in processing joint, fold and fault data collected. Geological data such as strike and dip are plotted in the software and direction of force acted on the study area is explained. Geological map of the study area is produced by using ArcGIS software. While Terrameter LS Toolbox and Res2dinv software are used to display the pseudosections of the apparent resistivity of the geophysical tests.

ii. Field Data Analysis

Field data analysis is a process to produce a geological map on scale 1:25,000 of the study area. The shapefile data acquire during fieldwork is layered on ArcMap 10.2 software. The data is processed according to type of map need to be produced. Thus, geological map, topography map, drainage pattern map, geomorphology map, structure map, and 3D map.

iii. Geophysical Data Inversion using RES2DINV

The apparent data obtained at field is processes by using Terrameter LS Toolbox before being processed using Res2dinv. The elevation recorded during field study is added in order to produce topography pseudosection. Electrodes spacing and elevation are added in 'Edit electrode coordinates' section for World X and World Z columns.

Pole-Dipole and Schlumberger configuration data obtained is inverted and the process by using Res2dinv software via apparent resistivity to obtain true resistivity and true depth of resistivity image. The inversion of resistivity and IP data is conducted by a least-square method which involving finite-element and finite-difference methods. A good pseudosection to be interpret is a low rms error pseudosection which in range below 15%.

Data from Terrameter LS Toolbox is read in Res2dinv. Bad datum will be exterminated to reduce rms error. However, a valid pseudosection should has at least half of the data according to the configuration used. High damping factor is needed

for high noise data. Cutoff data section is used because the inverted pseudosection is still has high rms error in which more 15%.

3.3.5 Data Analysis and Interpretation

i. Geologic data

The rose diagram produced through data processing step help in the interpretation of forces acted and deformation history of the study area. The data are then reconstructed and discussed the result. The petrographic analysis during laboratory investigation helped in the origin of rocks. Colour variation under the plane polarized light, fracture characteristics of the grains, refractive index, and optical symmetry were observed under a microscope. Hence, structural analysis and lithology analysis are analysed and plotted on a geological map by using ArcGIS.

ii. Resistivity data analysis

Basically, ERI data processing and interpretation involved inversion and forward modeling. Forward modeling is the theoretical inverse of the data inversion process which can be utilized both prior to data collection or after data inversion. While inversion process, the theoretical is compared with the observed pseudosection and the resistivity of each of the model grid elements is adjusted. The whole process is repeated iteratively until the rms difference drops to pre-specified level. The resistivity data will be conduct by using the Res2dinv software. The software will be used to determine a 2D resistivity model for the data obtained from ERI survey.

Inversion pseudo-section will be interpreted to determine the resistivity of the materials.

iii. Kinematic analysis

The data obtained from the field study is plotted on Stereonet Windows software. The data collected from field study are joint spacing, persistence, trend and plunge. All joints trend and plunge readings is plotted as line on the stereonet. Then, each joint set is converged in as one distribution. The contour is added in order to determine the pattern of each joint set. Best lines constructed based on the contours are interpreted by referring the position with the slope face.

CHAPTER 4

GEOLOGICAL MAPPING OF STUDY AREA

4.1 Introduction

Geology in this chapter is discussed based on the data acquired during geological mapping. Geographically the study area is located at the longitude of E 101°50'38" until E 101°54'01" and at the latitude of N 05°27'42" until N 05°30'24". The study area covered approximately 30 km². This chapter is further discussed based on geomorphology, lithostratigraphy, structural geology, and historical geology of the study area in order to understand the geologic character of the study area. Accessibility to the study area, settlement, vegetation and traverse map of the study area is also discussed in this chapter. All recorded data is plotted in the geological map of Kg. Bukit Selar was showed Appendix 1 with scale exact 1:25,000.

4.1.1 Accessibility

Accessibility explained the way in which the study can be reached. Basically, accessibility is the outcomes related to transportation activities. Hence, both socioeconomic activities and accessibility can be interrelated. This study area can be easily accessible by vehicles like a car or motorcycle. In Jeli-Dabong area, there is a direct geographic relationship between land use system and road network.

There are two types of roads which are the main roads that accessed by all vehicles, and also local village pathways which usually used by the villagers' small vehicles. The main road that is used daily by the residents is Jalan Dabong-Gua Musang (Federal Route 66), linking the town of Jeli to the village of Kampung Bukit Tebok to Manek Urai. Another unnamed road which directs to TNB Pergau Hydroelectric power station is rarely used by people (Figure 4.1 (a) and Figure 4.1 (b)).

4.1.2 Land use

The places and areas that are settled by humans are considered as a settlement. Jeli district area is yet still considered as a rural region because the proportion of the households are vulnerable to poverty was observed lowest in Jeli. Within all these areas, there are plenty of villages that settled in here. There are three village capitals located in the northeastern part of the study area, Kg. Bukit Selar, Kampung Tebing Timbah, and Kampung Relak. Most of the residents work as farmers and rubber tappers to live life every day. These agriculture activities have great influence on the socio-economic of the residents.

Vegetation distribution in the study area can be divided into three categories; forest, rubber plantation, and villager farms. Forestry is very common in the study area because Jeli district has a high distribution of reserved forest. The study area includes two reserved forests; Hutan Simpan Gunung Basor (with total area 40,790 hectares) and Hutan Simpan Gunung Stong Utara (with total area 11,044 hectares). This reserved forest covered most part in the study area in the western part (Figure 4.1 (c)). For the rubber plantation, it covered eastern part of the study area at the region with elevations ranging from 100 m to 240 m (Figure 4.1 (d)). Based on observation, rubber plantation is the main socioeconomic activity of villagers and also consider as their

main of income. The villagers also planted various kinds of fruits such as durians, rambutans, langsat and etc, to sell. Fruit farms were planted in the area where near to settlement.

4.1.3 Traversing of the study area

In order to collect geological data, rock sampling and measuring, the geological mapping of Kg. Bukit Selar was covered through traversing and observation methods. Before traversing, the traverse route and target was planned before going to the fieldwork. Approximately, the whole geological fieldwork was done in 10 days to complete.

Traverse and observation map is shown in Figure 4.1. Generally, the study area was traversed along rivers as there are numerous rivers and streams located within the study area. Besides, the fresh outcrops are well exposed along the rivers. Geological structures observation is made by analyzing the lineaments before going to the field. The changes in lithology and structures were marked and recorded during geological mapping. The figure shows the stations where the observation is done respectively. The stations are divided into three parts, observation with sample, observation without sample, and petrography analysis. The station which observation with sample is the checkpoints where the hand specimens are taken for observation. There are seven stations where the petrography analysis is conducted.

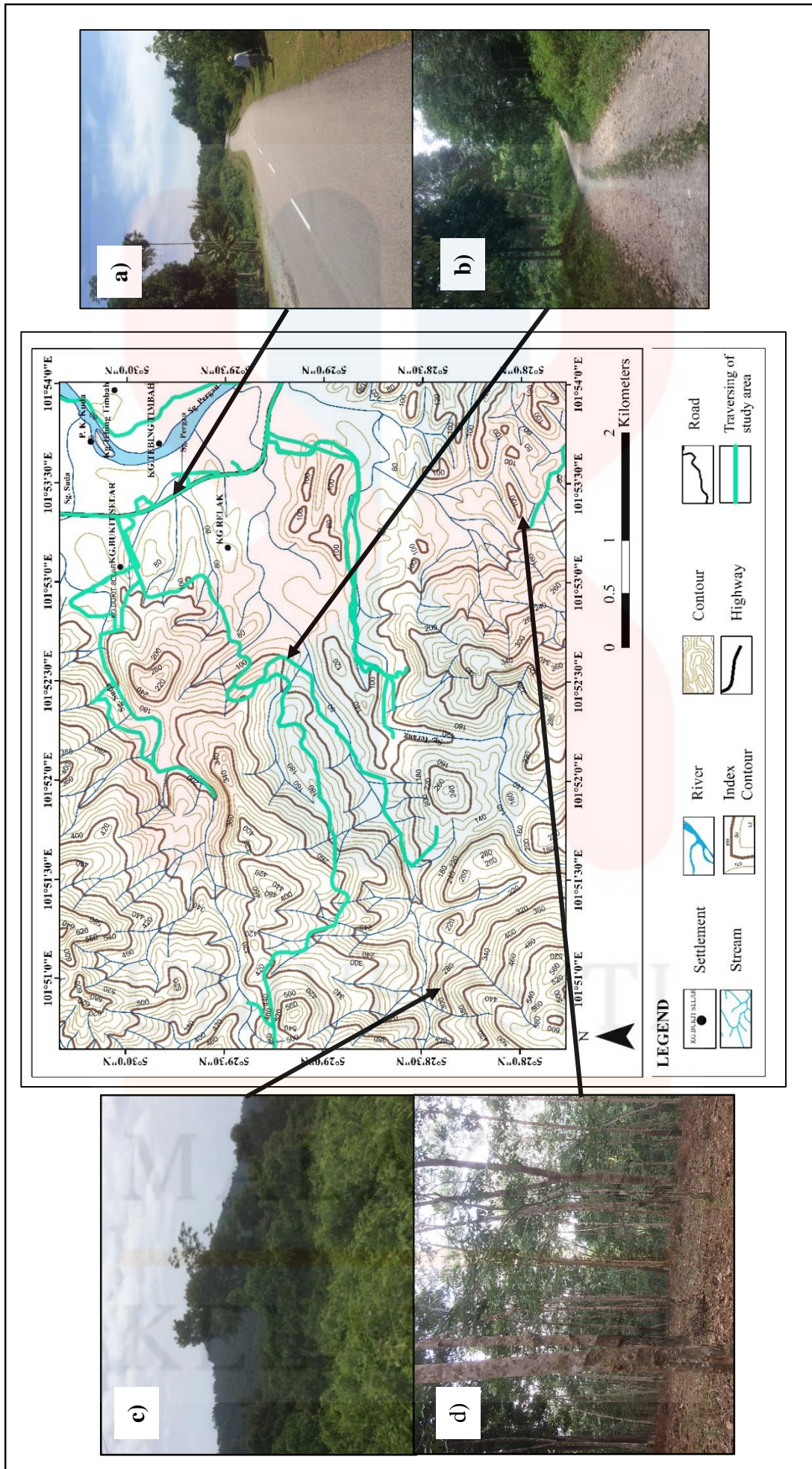


Figure 4.1. Traverse map. (a) Paved road in study area. b) Unpaved road in the study area. c) Reserved forests in study area. d) Rubber plantation in the study area.)

4.2 Geomorphology

Geomorphology refers to a scientific term of study of landform which contributes to their origin, evolution, form, and distribution across the physical landscape. Geomorphology is related to Earth's landforms and the features which influenced its formation. This section often included the topography, weathering, and drainage pattern. Figure 4.2 shows the geomorphology map of the study area which divided according to the landform and elevation.

4.2.1 Topography

Topography is the arrangement of the natural and artificial physical features of landform. This term refers to all physical attributes of earth surface which includes mountains, hills, valleys, plains, and water bodies. This study area consists of varies landform from hills to plains and numerous size of water bodies. Hilly landform has a wide class, comprising units with varies morpho-structures. It is classifying by referring to Van Zuidam (1985) morphology classification (Table 4.1). Plain landform is rather flat, sometimes very gently sloping and the surface lower than the surrounding features.

Table 4.1. Relationship between absolute elevation and morphography (Van Zuidam, 1985)

Absolute Elevation (mean sea level)	Morphography Element
< 50	Lowland
50 – 100	Low-lying plain
100 – 200	Low hill
200 – 500	Hill
500 – 1.500	High hill
1.500 – 3.000	Mountain
>3.000	High mountain

As shown in the 3D topographical map in Figure 4.3 and geomorphology map in Figure 4.2, the elevation increasing towards the western part of the study area. Hilly landforms in the prospect area are ranging from 300 m to 600 m above the mean sea level. The highest elevation in the study area is 620 m which are reserved forest Gunung Basor area. The reserved forest is covered with deep forest. This highest elevation area (more than 600 m) have a series with the rough profile. Slopes are straight with steepness ranging from moderate to steep. In this area, narrow V-shaped valleys and shape crest are frequently found. Areas with elevation ranging from 300 m to 500 m have a large variety of slope steepness, length, and shape. Due to the hill is a plutonic hill, the formation showed sharp crests even at an elevation lower than 600 m.

From the contour pattern, the close-spacing contour lines denote steep slopes and wide-spacing contour lines show gentle slopes. V-shaped contour lines represent the stream beds and narrow valleys that the 'V' pointing towards uphill. The sharper the V-shaped, the steeper the valley. The U-shaped contour lines indicate a ridge and point downstream toward lower elevation. For this study area, the U-shaped contour lines pointed downstream toward the eastern part. The pattern also shows the flow of magma.

Alluvium in the study area located at the north-eastern part. Alluvial sediments are transported downslope by weathering of granite unit and also by Pergau river flow. The sediments are deposited in river valley area which the water flow started to decelerated. In this prospect area, alluvium is deposited in channel fill landform and floodplain area. Observed alluvial sediments in the study area are gravels, sands, and silts.

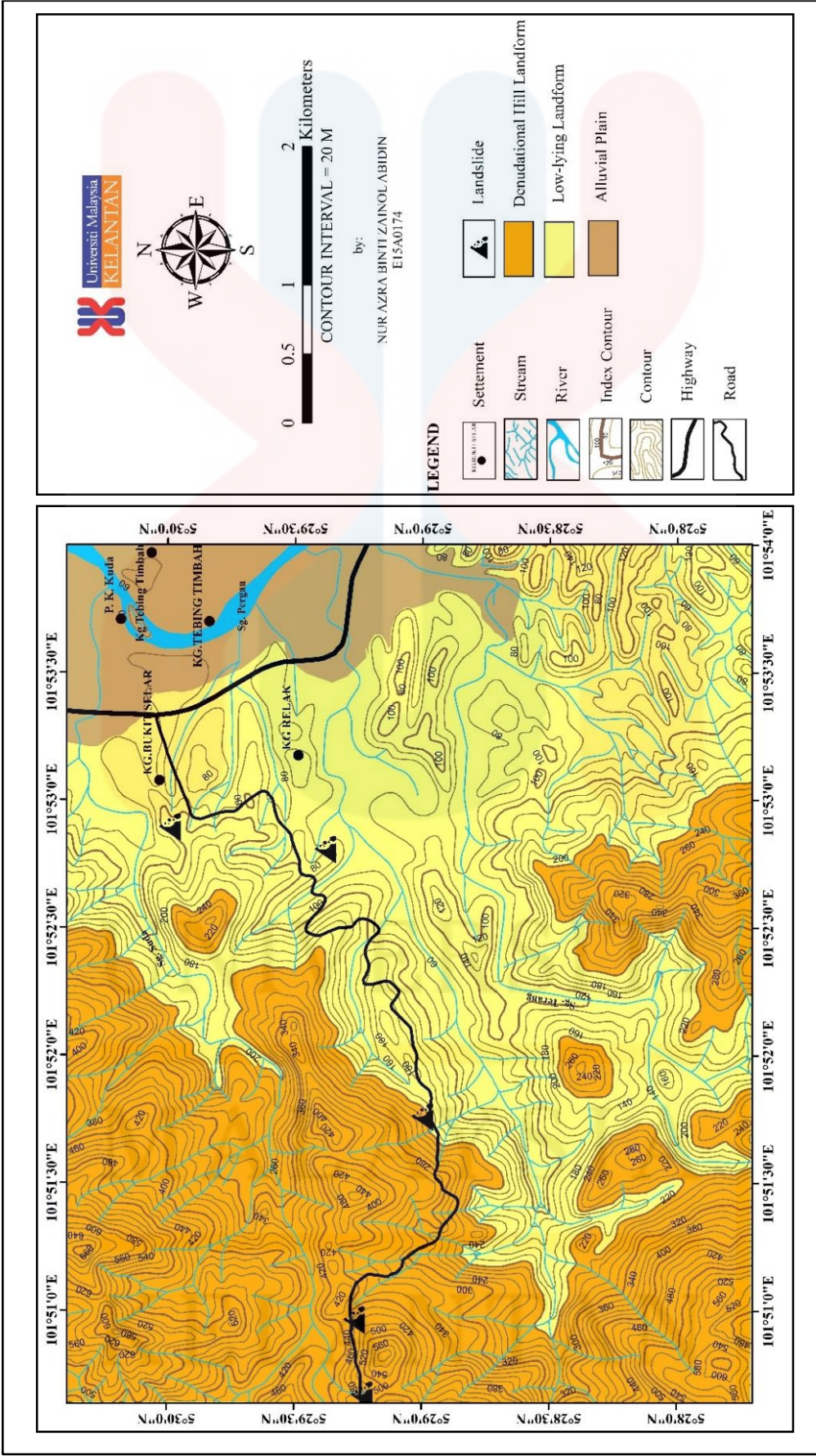


Figure 4.2. Geomorphology Map of study area.

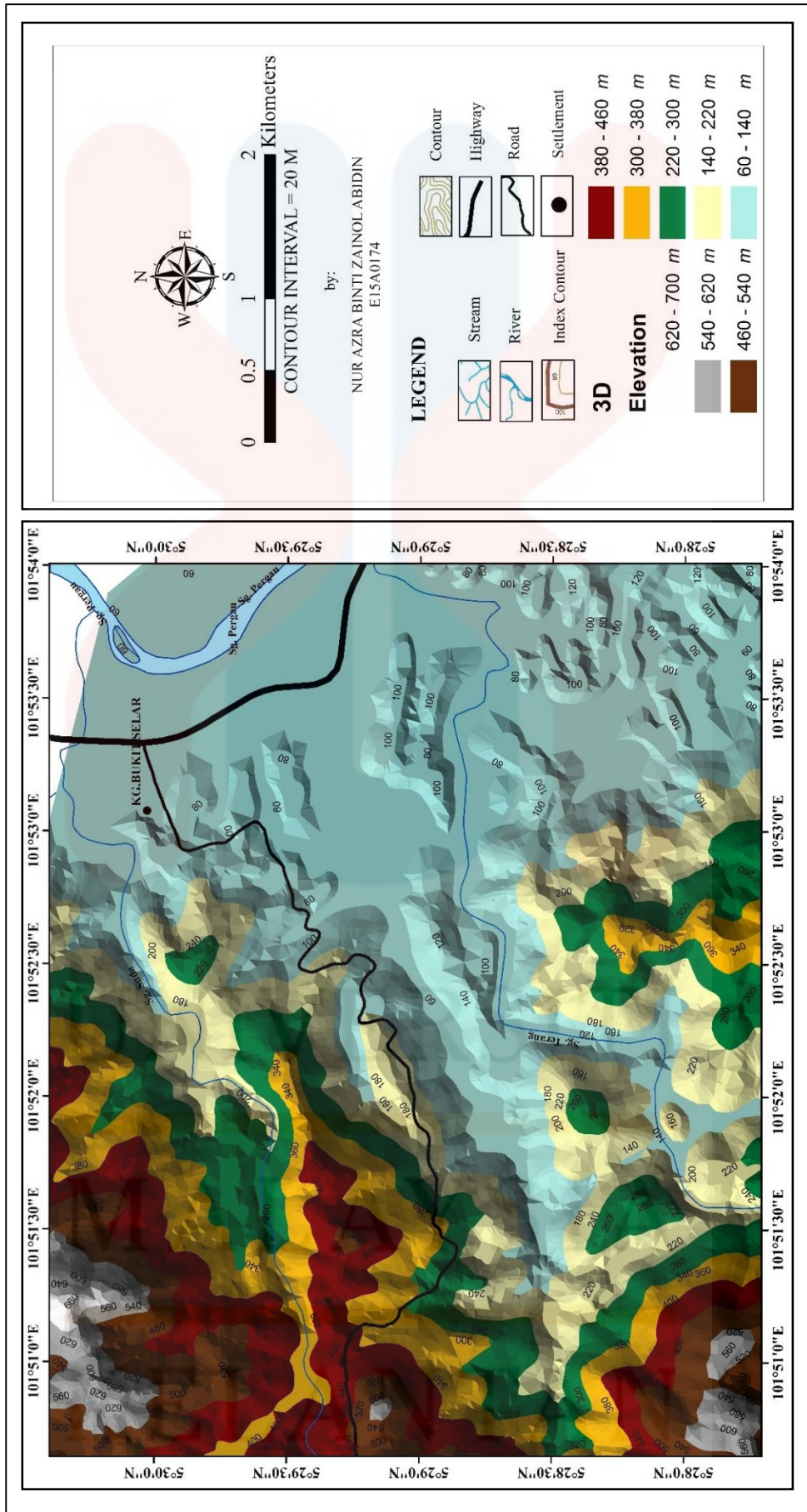


Figure 4.3. 3D topography map of study area

4.2.2 Weathering

Weathering is a process that breaks down rock at the earth's surface into smaller pieces via physical, chemical, and biological mechanism. Weathered rock eventually becomes soils through the weathering process. This process altered the physical and chemical properties of rocks. Generally, there five main factors which control the rate of weathering such as, material's properties, climate, total surface area, chemical reaction and time. For Malaysia, it is well known for its tropical climate which receives heavy rainfall and warm climate most of the time. These hot, warm, and damp weather occurred in turn repeatedly have increased the rate of weathering on the earth surface.

Weathering of rock can be classified into six general grades according to Table 4.2. Generally, from highly, medium to slightly weathered is through the decreases vertically increasing depth (Eldin et al., 2013). These grades are differ based on the changes in the extent of alteration on the surface, its strength, and along the fractures.

This prospect area is located at Sungai Terang cascade area and the surrounding area. Dominant lithology in the study area is granite intrusive rock. The granite intrusive rock area is hilly landform with fresh rock to moderately slightly weathered rock (Class I to III). However, there is a slate unit and alluvium in the eastern part and the area is low-lying plain landform which is the highly weathered area. Typically, all weathering types have caused changes of structure and disintegration of rocks in this study area. A huge mass wasting also found in the western part of the study area. The mass wasting which classified in the study area is rockfall and landslide. These mass wasting are widely found along the road to Gunung

Basor. Denudation occurred due to the relationship between weathering and mass wasting process.

Table 4 2. Scale of weathering of sediment and rocks. (Tucker, 2003)

Term	Description	Grade
Residual soil	All rock material is converted to soil. The rock structure and material fabric are destroyed. There may be a change in volume, but the soil has not been transported significantly	VI
Completely weathered	All rock material is decomposed and/or disintegrated to soil. The original structure is still largely intact	V
Highly weathered	More than half of the rock material is decomposed or disintegrated to a soil. Fresh or discoloured rock is present either as a discontinuous framework or as corestones	IV
Moderately weathered	Less than half of the rock material is decomposed or disintegrated to a soil. Fresh or discoloured rock is present either as a continuous framework or as corestones	III
Slightly weathered	Discoloration indicates weathering of rock material and discontinuity surfaces. All the rock may be discoloured by weathering	II
Fresh	No visible sign of rock weathering; perhaps slight discoloration on major discontinuity surfaces	I

Physical weathering is the dominant weathering type found in the study area. Physical weathering recognized in the study area are exfoliation, hydration and dehydration, and stress release. Exfoliation typically in an upland area where there is exposure of igneous rocks. The fractures formed parallel or sub-parallel to a nearby surface. This process occurs due to the pluton at depth is under high pressure from underlying rocks. It tends to be uniform and lack fractures. The rock mass is subjected to the progressively lower pressure of overlying rocks as the progressive erosion started to occur. This leads to the tension in directions at right angles to the land surface. This tension is relieved by the formation of cracks which follow the land

surface. Formation of new low-density minerals is formed once the cracks are filled with water and caused chemical weathering. Thus, cracks and slabs of rock are detached from the surface.

Due to alternate wet and dry seasons in the climatic zone, hydration and dehydration physical weathering occurred. The fractures on the granite body alternatively expand with water and develop shrinkage cracks as they dehydrate. Increasing permeability along the shrinkage cracks. Aiding chemical weathering from rainwater and waterlogged resulted in landslides. Stress release is a phenomenon in which the granite body crystallize at below the surface, it is uplifted and caused erosion to the underlying rocks. It contained energy is released by outward expansion. These rocks have elastic properties and being compressed by the overburden rocks. Outwards expansion resulted in the formation of sheet joints which is almost parallel the exposed rocks. Opened stress-release fractures are susceptible to enlargement by solution from rainwater and other processes. Stress-release is ubiquitous in brittle rock.

Organic processes are the main mechanism of biological weathering. There are several factors caused biological weathering such as biochemical solution brought by the action of bacteria and humic acids derived from rotting organic matter. Some physical fracturing of rock caused by tree roots. By animals, their burrowing activity contributes to this weathering.

4.2.3 River Morphology

a. Cascade

Sungai Terang is the main cascade in the study area in which is a tributary of Sungai Pergau (Figure 4.4 (a) and (b)). This cascade is located in Kg. Relak. It has numerous rapids and cascade. Lithologically, Sungai Terang cascade is part of Stong Migmatite Complex. Based on observation, this area composed of almost 80% of porphyritic granite. The large body of granitic rocks in this cascade has the existence of many pothole structures of different sizes. Other geological features found are joints, veins and faults. For the river flow, the river flow current is very high at high elevation and start to decreasing at low elevation. The water flows downhill, from high elevation towards area low elevation. The river flow at downstream is wider that uphill river flow.



Figure 4.4. a) A cascade in Sungai Suda. b) A cascade in Sungai Terang.

MALAYSIA
KELANTAN

b. Potholes

Cascade flow at river erosion terrace formed by large granite body can be seen in Sungai Suda. This cascade formed due to the different height between the three terrace erosion. Due to the erosion, crafting effects features are formed on the granite body such as potholes. From the observation, the potholes in the study are crafted in different sizes as shown in Figure 4.5. Potholes are a direct consequence of the abrasion process and vertical erosion. Over time, small depressions within the bedrock develop due to the turbulence forces water downhill. The turbulent flow deepens the depression over time and forms a small circular basin. The debris or gravel abraded the sides of the potholes and caused the increases in diameter.



Figure 4.5. A pothole structure on granite body of Sungai Suda.

KELANTAN

c. Sandbars

A bar in a river is a region which the sediments are deposited by the river flow. There are several types of bars include mid-channel bars, point bars, and mouth bars. Erosion, transportation and deposition are involved in bar formation. There several stages in bar formation. Based on field observation (Figure 4.6), the bars found in the study area are mostly mid-channel bar which formed longitudinally at the centre of the river body. Channel bar formed when the river flow diverted away from the bar, however, the sediments are deposited at the bar. Common bar type found in the study area is sandbar in which the influx of the sands leads to the development of channel bar.



Figure 4.6. Mid-channel bar in Sungai Pergau tributary.

KELANTAN

4.2.4 Drainage Pattern

River systems in geomorphology are known as drainage pattern. Drainage pattern is defined as a system that develops a space for water flows due to rainfalls. The drainage system is one of geomorphology region from which a stream receives runoff, through flow, and groundwater flow then divided from each other by watershed. Based on empirical studies, drainage density and bedrock lithology, and the type of dominant rocks can be responsible for many drainage pattern details. In geologic formation with stronger rock types, erodibility in fractured rock along joints control the network pattern. Development of drainage basin is through the influence of precipitation and temperature upon vegetation cover (Goudie, 2004).

Based on the drainage map in Figure 4.7, there are two types of drainage pattern found in the study area; dendritic pattern and parallel pattern. The dendritic pattern is the most common drainage pattern found in the study area.

Sungai Pergau is the main river present in the study area which connected to two tributaries, Sungai Terang and Sungai Suda. Water current in Sungai Pergau is slow because it is located on low-lying plain landform. Sungai Pergau experienced low erosion rate on its river basin. Most sediments deposited found along the river are gravel to pebble sized sediments. Boulders-sized sediments also found along the river in which this showed the river experienced high flowing water current that enables to transport heavy sediments for long distance. This may occur during heavy flood or monsoon season annually.

From Figure 4.7, there two types of drainage pattern observed in the study area; dendritic and rectangular pattern. The dendritic pattern is a very common drainage

pattern. This is a randomly developed, tree-like pattern composed of branching tributaries and the main stream. They usually formed in an area that the channels follow the slope of the terrain. A dendritic pattern develops in this area because the rock beneath the stream has no particular fabrics or structures and easily eroded in all directions. This pattern is found in granite unit. Due to the granite intrusive rock, the dendritic pattern formed in V-shaped valleys which the rock types must be impervious and non-porous.

Besides dendritic pattern, trellis pattern also observed in the study area. This drainage pattern is characterized by a network of parallel or sub-parallel streams developed along strike and dip directions. Such patterns typically reflect a marked structural control by faults, joints, alternating soft and hard beds. Tributaries are at right angle to the streams. As shown in the geological map (Figure 4.9), the lithology of trellis drainage pattern is metamorphic rock, slate unit.

From Figure 4.7, the northern part of the study area shows that the stream system mainly consists of straight line segments which are observed as sub-parallel drainage pattern. The parallel pattern forms where there is a pronounced slope to the surface. A parallel pattern also develops in regions of parallel, elongate landforms like outcropping resistant rock bands. Tributary streams tend to stretch out in a parallel-like fashion following the slope of the surface. This pattern also may indicate the presence of a major fault that cuts across an area of steeply folded bedrock. The area is the microgranite unit area in which has been experienced several deformations.

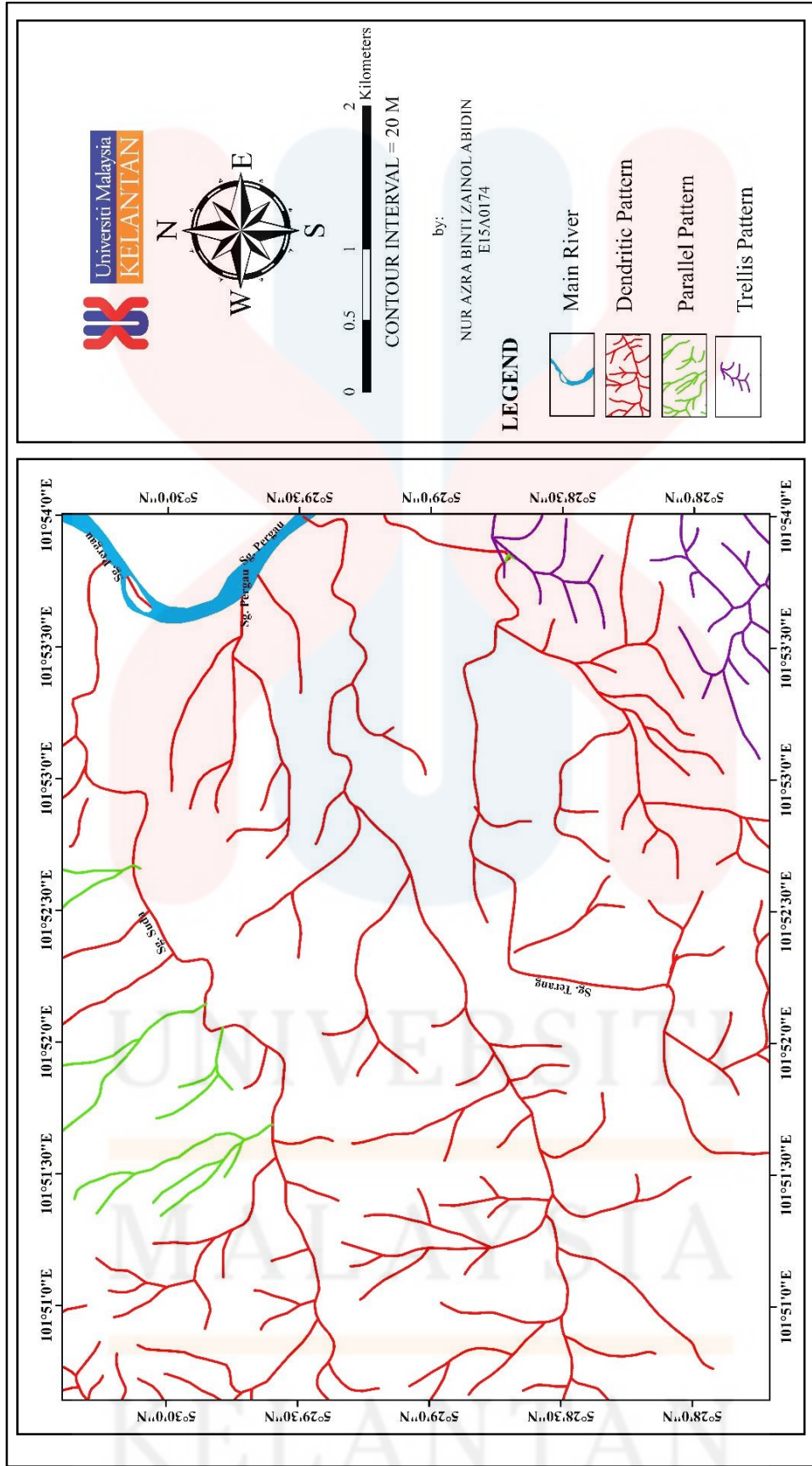


Figure 4.7. Drainage map of study area.

4.2.5 Mass Movement

Mass movement or mass wasting is the common active process occurring around the world. There also some mass movement observed in the study area. The landscape of an area can be modified or changed due to the mass movement event. Typically, it is a downslope movement of materials under influence of gravity. This phenomenon also can be linked to the weathering process.

In the study area, the mass movement commonly found at hill slope along the road directed to TNB Pergau Hydroelectric power station. Along the road there are few types of mass movement are observed such as landslide and rock fall. As shown in Figure 4.8, a landslide found in rubber plantation near to Sungai Suda. The slope face of the landslide is facing south direction. From the observation, the mass movement in the study area occurred on steep slopes.



Figure 4.8. Mass wasting nearby Sungai Suda area.

4.3 Lithostratigraphy

Lithostratigraphy is the study of strata which defined with basically physical contrast in rock type. Classification of lithostratigraphy is based on their petrography, mineralogy, and the relationship with adjacent units, both vertical and horizontal. Several types of rocks were found in the study area in which are slate, microgranite, and porphyritic granite. Geological map of the study area includes the lithology, structural geology and stratigraphy column as shown in Figure 4.9. Age of the lithologies is stated by referring to previous studies related to Stong complex and Gua Musang formation.

Each lithology is further discussed started with the oldest age rock unit to the youngest rock unit. These rock units are described partly based on nature figure and hand specimen. Few hand specimens have undergone petrographic analysis for further rock classification and nomenclature.

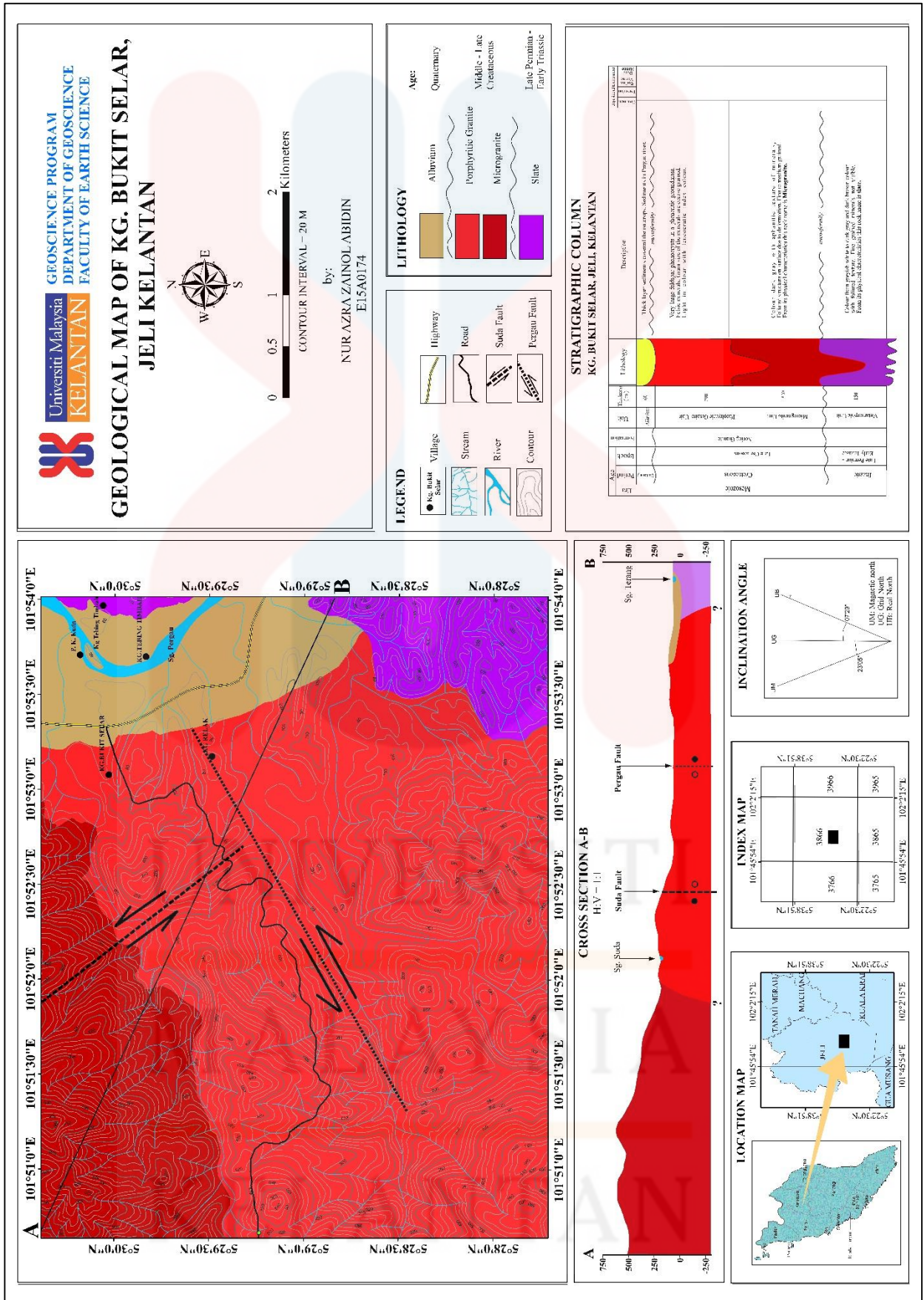


Figure 4.9. Geological Map of study area.

4.3.1 Stratigraphic Position

The vertical location of rock units in the study area are described on stratigraphic column shown in Figure 4.10. The stratigraphic column shows the sequence of lithologies from the oldest unit (at the bottom) to the youngest rock unit (on top). Stratigraphic column is constructed based on the correlation of the rock units. According to the stratigraphic column shown in Figure 4.10, the slate unit is the oldest rock unit with a Triassic period.

There is an unconformity between slate unit and microgranite unit because there was no evidence of lithology or structure related to Jurassic period found in the study area. During Late Cretaceous, microgranite of Kenerong Leucogranite started to intrude and emplaced the country rock and followed by porphyritic granite of Noring granite. It is believed that the Noring granite intrudes the earlier Kenerong leucogranite. The youngest lithology in the study area is alluvium in Quaternary.

As shown in the stratigraphic column, the thickness of each lithology unit is measured based on the elevation on geological map in Figure 4.9. All rock units are measured from 0 m elevation. The slate unit in which the country rock in the study area is 150 m thick. Microgranite unit has a thickness from 250 m to 320 m. Porphyritic granite the thickest lithology in the study area (540 m).

STRATIGRAPHIC COLUMN KG. BUKIT SELAR, JELI, KELANTAN

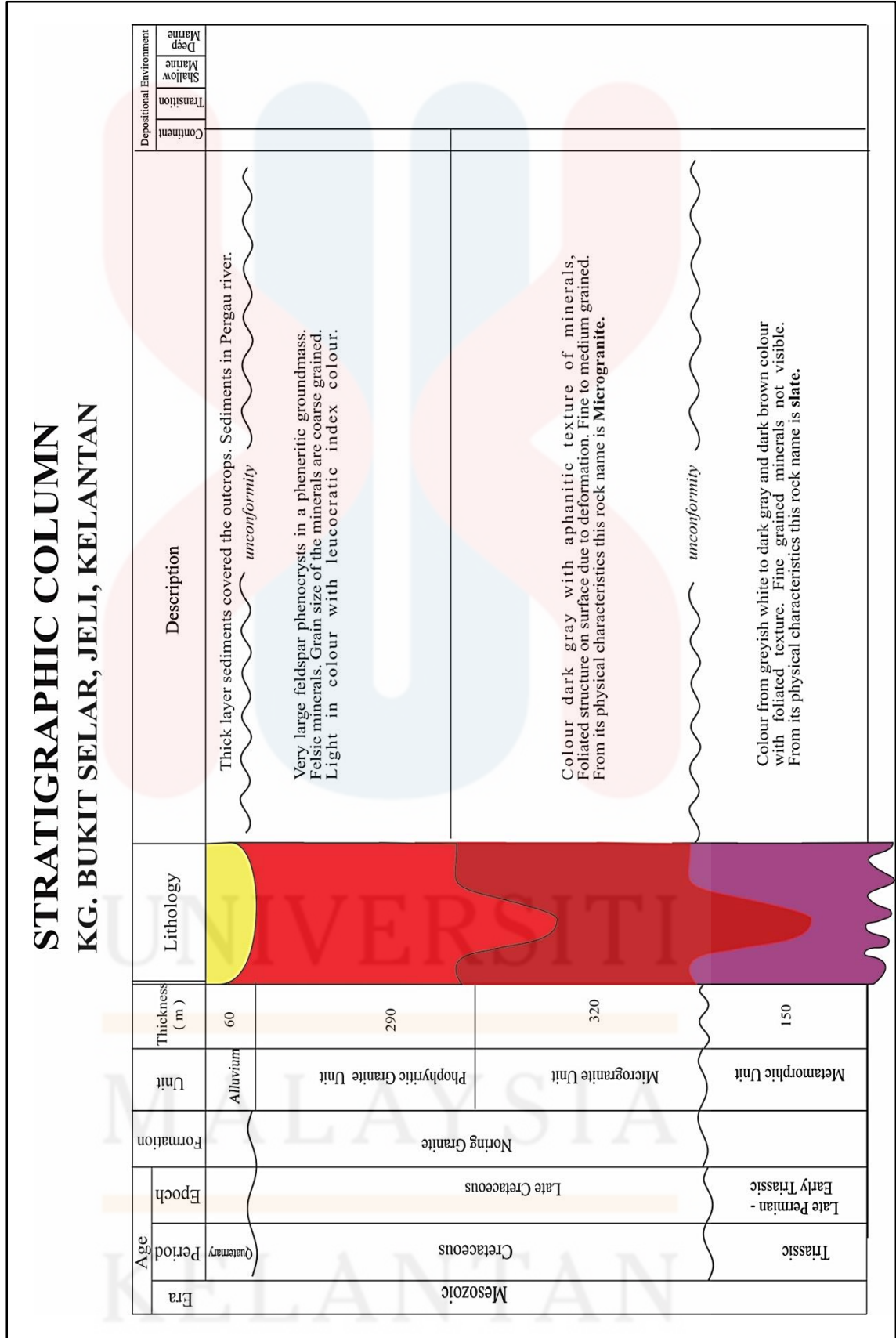


Figure 4.10. Stratigraphy column of study area.

4.3.2 Unit Explanation

a. Slate

The slate unit basically only cover approximately 5% of the total study area. Based on geological map in Figure 4.9, the outcrop (Figure 4.11) is located at N 05° 29' 29.5", E 101° 54' 01.0". It was a highly weathered outcrop located at plantation area. The slate unit is the country rock in the study area.

Slate has a fine-grained particle size and classified as low-grade metamorphic rock. It has foliated texture. Parent rock of slate is shale which mainly composed of clay or volcanic ash through low-grade regional metamorphism. Due to the inability to absorb water slate can be distinguished from shale. Slate is much more durable compared to shale because it has undergone metamorphism. It has slaty cleavage texture which results in platy foliations which have the ability to be split into thin sheets.

The hand specimen found in the study area is shown in Figure 4.12. It appears in a light brown to greyish brown colour alternately. Slate usually composed of quartz, mica, chlorite, biotite, and clay. Due to the fine-grained particle size, the minerals cannot be seen by naked eyes. This slate is brittle and easily break into pieces when touch because it is highly weathered. Slate is formed during Lower Permian in the basins between convergent plate boundaries. No petrography thin section has been done because the slate is highly weathered. Hence, the overall description of this slate is based on field observation.



Figure 4.11. Slate outcrop in the study area.
(Coordinate: N 05° 29' 29.5" E 101° 54' 01.0")



Figure 4.12. Hand specimen of slate.

KELANTAN

b. Microgranite

Microgranite unit basically covered 30% of the total extent of the study area. Based on the Figure 4.13, the microgranite outcrop is located next to Sungai Suda area with coordinate N 05° 30' 8.8", E 101° 52' 34.2". This lithology is exposed to hydrology which next Sungai Suda in the forest area. However, the outcrop does not have direct contact with running water. There are bushes covers on the microgranite outcrop. Thus, the outcrop has the effect of biological weathering.

Microgranite is a fine to medium-grained intrusive igneous rock. In the study area, the texture of the microgranite unit is fine-grained which contains interlocking and randomly oriented minerals. It is pale grey in colour (Figure 4.14). Mostly feldspar and quartz are buildups the rock unit. It also contains small specs of mafic minerals. The minerals are slightly smaller than common granite which proved that the magma cooled more quickly. This microgranite unit usually occurs in smaller intrusions than granite and the magma contains numerous quartz.

From outcrop observation (Figure 4.13), the foliated structure appears on the microgranite body. However, the hand specimen did not show any foliation. It is the grain size is aphanitic texture has no sign of foliation. Hence, it is classified as microgranite. Presence of foliation on the microgranite body is because the regional area experienced deformation at least three times. Thus, a complex network of small intrusive and vein systems are observed on the rock body. This microgranite unit served as an intrusion in the study area where it is distributed at the North-West part of the study area. Also classified as an acid intrusive rock that formed during Cretaceous.



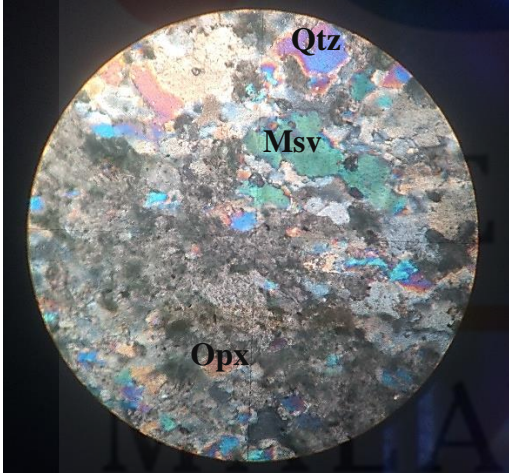
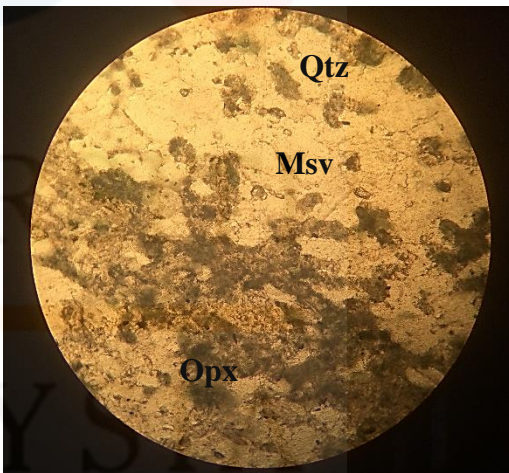
Figure 4.13. Microgranite outcrop found in Suda river area.



Figure 4.14. Hand specimen of microgranite.

KELANTAN

Table 4.3. Petrographic description of microgranite.

Reference No. : MG1	
Location : N 05° 30' 8.8", E 101° 52' 34.2"	
Name of Rock : Grey Microgranite	
Rock Type : Igneous Rock	
Microscopic : Holocrystalline, Inequigranular	
Description of Mineralogy	
Composition of Mineral	Description (Magnification 10X)
i. Orthopyroxene (Opx)	Colourless in PPL and yellowish-green colour in XPL; Moderate relief; Subhedral; No cleavage; No twinning; 24° extinction angle.
ii. Orthoclase	Colourless in PPL and white to grey in XPL; Low relief; Subhedral; First order birefringence; Carlsbad twinning; 29° extinction angle.
iii. Quartz (Qtz)	Colourless in PPL; Low relief; Anhedral; No cleavage; First order birefringence; 46° extinction angle.
iv. Muscovite (Msv)	No pleochroism; Colourless in PPL and light brown colour in XPL; Moderate relief; One-direction cleavage; Subhedral; Second order birefringence; 56° extinction angle.
Photo	
	
XPL of Microgranite with 10X magnification.	PPL of Microgranite with 10X magnification.

KELANTAN

c. **Porphyritic Granite**

Porphyritic granite covered most part of the study area. Approximately 55% of the total extent of the study area is covered by porphyritic granite. As shown in Figure 4.15, outcrops of porphyritic granite are found at coordinate N 05° 30' 0.3" E 101° 52' 44.0" (marked as checkpoint PG1) and N 05° 28' 44.6" E 101° 52' 38.7" (marked as checkpoint PG2). Both outcrops are exposed to hydrology as they have direct contact with running water and have undergone physical weathering.

Porphyritic granite is granite which experienced a very slow cooling process which resulted in the growing of well develop phenocryst crystals (Figure 4.16). This rock unit has enough time to be emplaced on the earth surface and coarse crystalline structure is well developed. Typically, porphyritic granite formed from interlocking felsic minerals; feldspar, quartz, plagioclase, and other minerals in lesser percentage. Groundmass of porphyritic granite also thoroughly develop and can be seen with naked eyes. Typical minerals that build up the groundmass are biotite, hornblende, muscovite, and other minerals.

From the hand specimen from checkpoint PG2, it can be clearly noticed that the grain size is coarse-grained. The size of feldspar phenocryst is ranging from 1.5 cm to 3.0 cm and the groundmass is a phaneritic texture with dominant biotite minerals. The outcrop is classified as fresh outcrop. Hence, detail petrography is conducted to further study its mineralogy and nomenclature. These rock bodies served as acid intrusion which intruded cut across the earlier microgranite unit. It is the youngest rock unit in the prospect area which formed during the Late Cretaceous period.



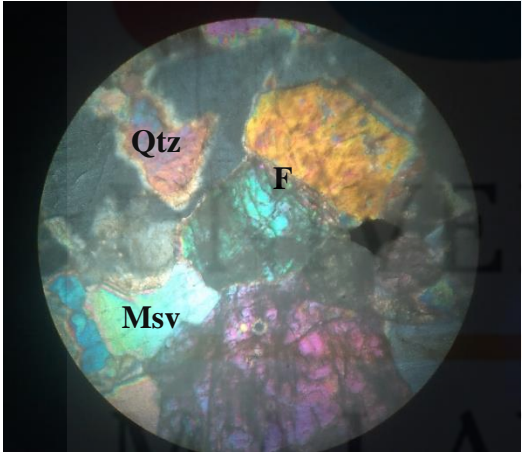
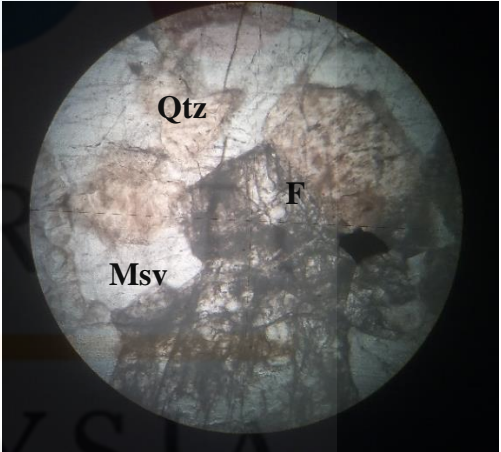
Figure 4.15. Porphyritic granite outcrop found at Sungai Suda.



Figure 4.16. Hand specimen of porphyritic granite.

KELANTAN

Table 4.4. Petrographic description of porphyritic granite.

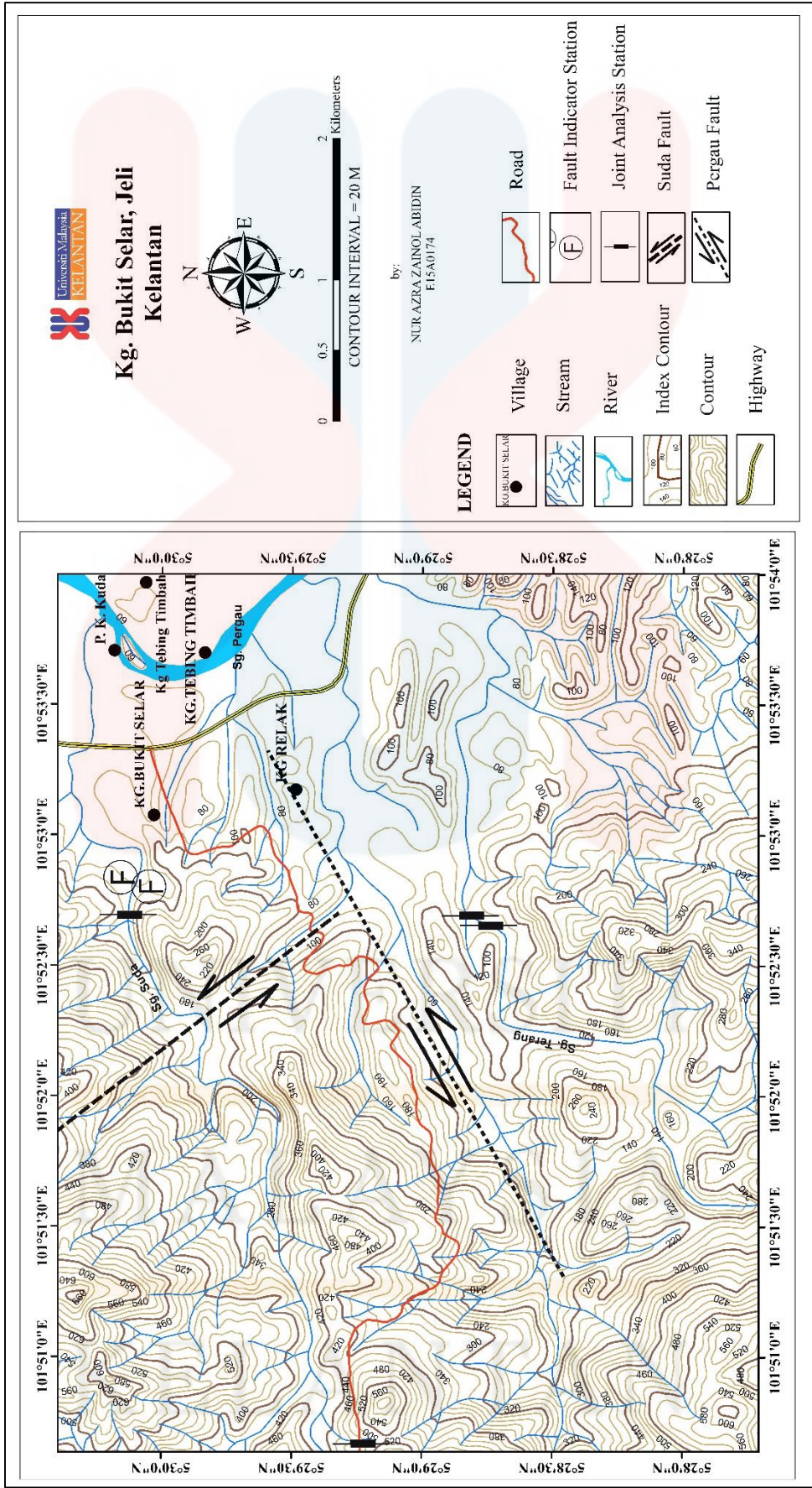
Reference No. : PG1	
Location : N 05° 28' 44.6" E 101° 52' 38.7"	
Name of Rock : Porphyritic Granite	
Rock Type : Igneous Rock	
Microscopic : Holocrystalline, Inequigranular	
Description of Mineralogy	
Composition of Mineral	Description (Magnification 10X)
i. Plagioclase	Euhedral to subhedral; 1 to 8 mm in size; normal zoning; simple twinning.
ii. Feldspar (F)	Colourless in PPL; Low relief; Anhedral; First order birefringence; Carlsbad twinning; 43° extinction angle.
iii. Quartz (Qtz)	Colourless in PPL; Low relief; Anhedral; No cleavage; First order birefringence; 45° extinction angle.
iv. Muscovite(Msv)	No pleochroism; Light brown colour in XPL; High relief; Two cleavages; Subhedral; Second order birefringence; 52° extinction angle.
v. Biotite	Anhedral plates; pleochroic scheme (dark brown and brown); crystals are weakly aligned resulting in poor foliation in the rocks.
Photo	
	
XPL of porphyritic granite with magnification 10X.	PPL of porphyritic granite with magnification 10X.

KELANTAN

4.4 Structural Geology

Structural geology is a branch of geology which study the three-dimensional distribution of the rock units, their surfaces, and the interior compositions with respect to their deformational episodes, past geological environments and events which caused the deformation. This study is done in order to interpret the stress field observed in the field as strains and geometries. The past geological events can be known based on the understanding the orientation of the stress field. Structural geology analysis involved lineament, fold and fault, and joint analysis. There are several geological structures found in the study area as shown in the structural map in Figure 4.17.

Based on structure map shown in Figure 4.16, both faults are predicted faults. Suda fault is a dextral strike-slip fault based on the offset on Sungai Suda. The dextral fault is trending to NNW-SSE direction. It is named as Suda fault due to the fault indications found along Sungai Suda and also the river offset. Meanwhile, Pergau fault is a sinistral strike-slip trending to ENE-WSW direction. The indication of this sinistral fault is based on the Sungai Pergau offset. Thus, it is named as Pergau fault on the structure map.



4.4.1 Lineament Analysis

Expression of linear or curvature underlying geological structure is known as lineament. Formation of lineament is usually influenced by the structures regional area; ridge, fault-aligned valley, a continuous series of fault or fold-aligned hills, and inconsistency of boundaries between stratigraphic formations. The lineament analysis is conducted by referring to the terrain map of the study area. There are two types of lineaments; positive lineament and negative lineament. Positive lineament represents ridge and range while negative lineament represents valleys, rivers, and faults.

Figure 4.18 shows the lineament map of the study area. Lineament analysis of study area is done by measuring the bearing of the lineaments plotted on the map. Then, the rose diagram represents the bearing of the lineaments which the maximum stress and minimum stress forces can be determined. The rose diagram shows the distribution of lineaments (Figure 4.19).

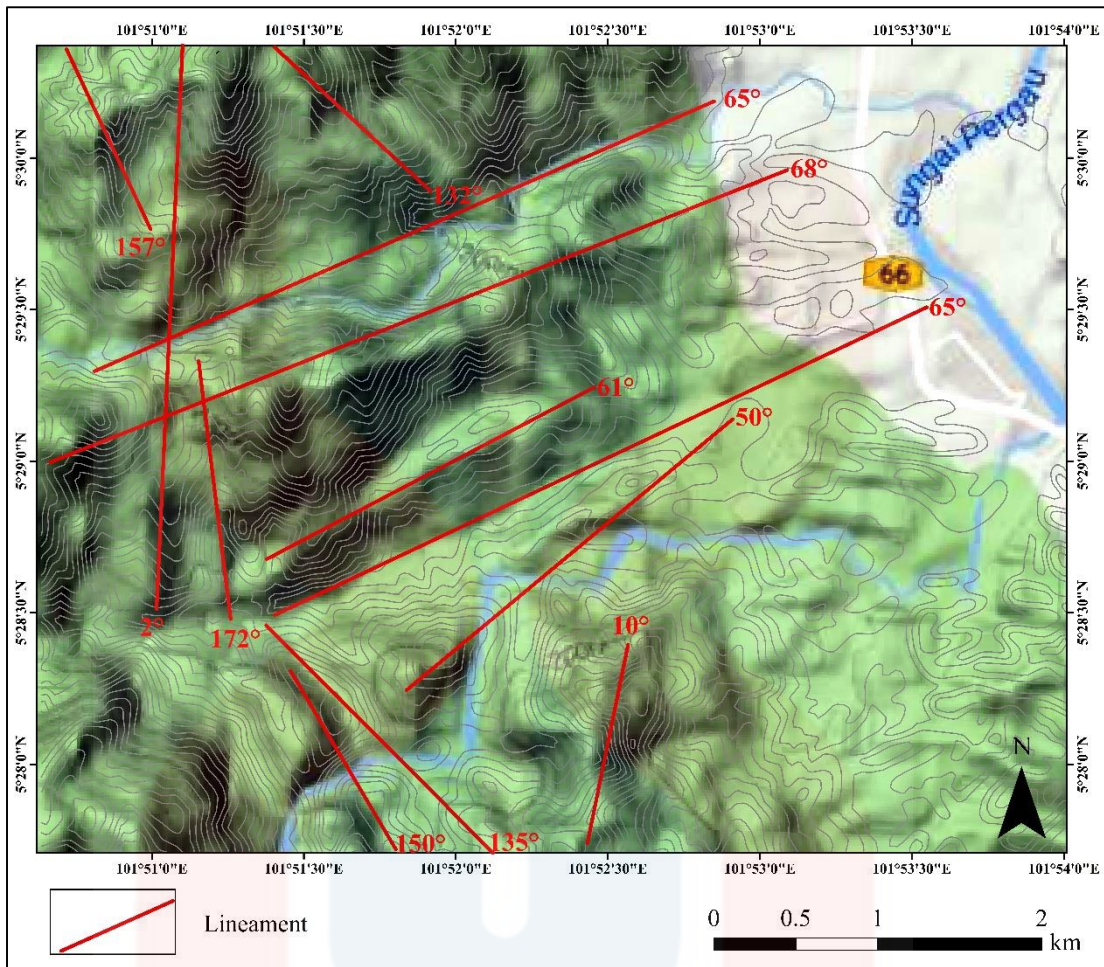


Figure 4.18. Lineament map of study area.

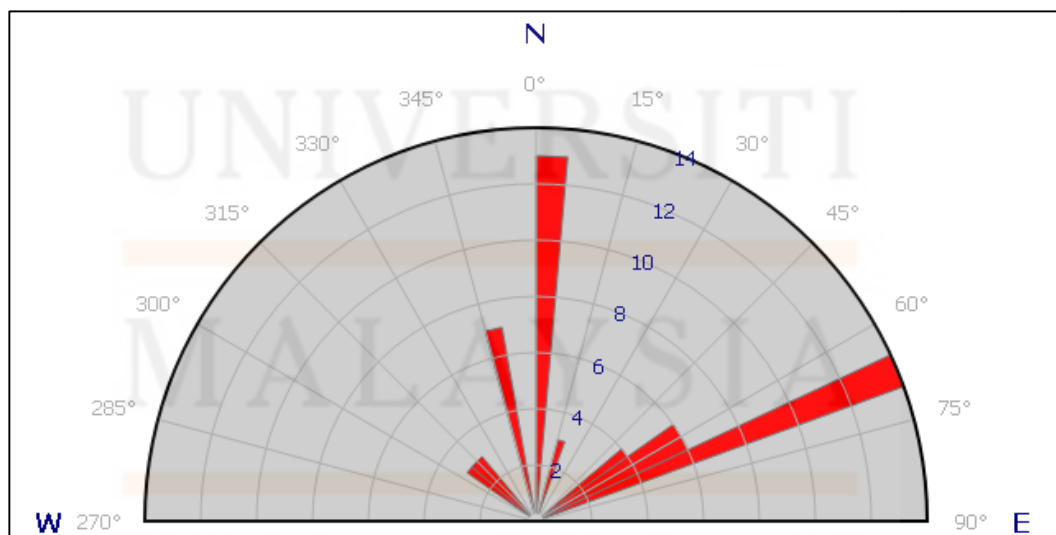


Figure 4.19. Rose diagram of lineaments.

4.4.2 Joint Analysis

Joint is the approximately parallel planar cracks on rock surface which normally due to the brittle characteristic of rock body. It extends in a various direction and easily can be found on all type of rocks. Joint is divided into two types; shear joint and extensional joint. Shear joint typically has no displacement and the extensional joint has significant displacement. However, weathering and erosion process may cause the opening to become bigger for both shear and extensional joint. When water enters the joint surface, it will lead to enlargement of the cracks. For extensional joint, it is possible to fill or infill with material. Common filling materials are quartz, calcite or any solidified magma.

From field observation, numerous joint systems are observed and being analysed. The field data joint system is analysed based on the rose diagram pattern. From the joint analysis, the shear direction which discontinuities can be known. Two joint analyses are done at different location in the study area. These locations are marked as checkpoint J1 and J2.

Figure 4.20 showed the rose diagram of joint analysis at checkpoint J1. The conjugate shear joint is shown in Figure 4.21. From the rose diagram in Figure 4.19, major shear force is interpreted at direction 350°NW . Meanwhile, the rose diagram in Figure 4.23 shows the major force acted on J2 area at direction 250°SW . The conjugate shear joint is shown in Figure 4.24.

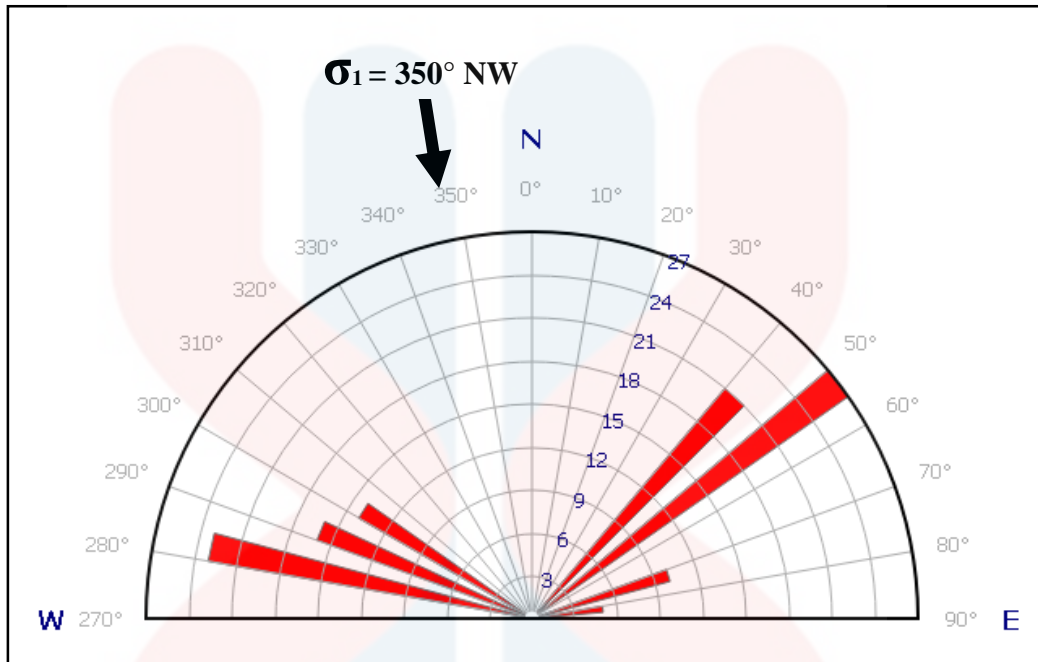


Figure 4.20. Rose Diagram for joint analysis at checkpoint J1.

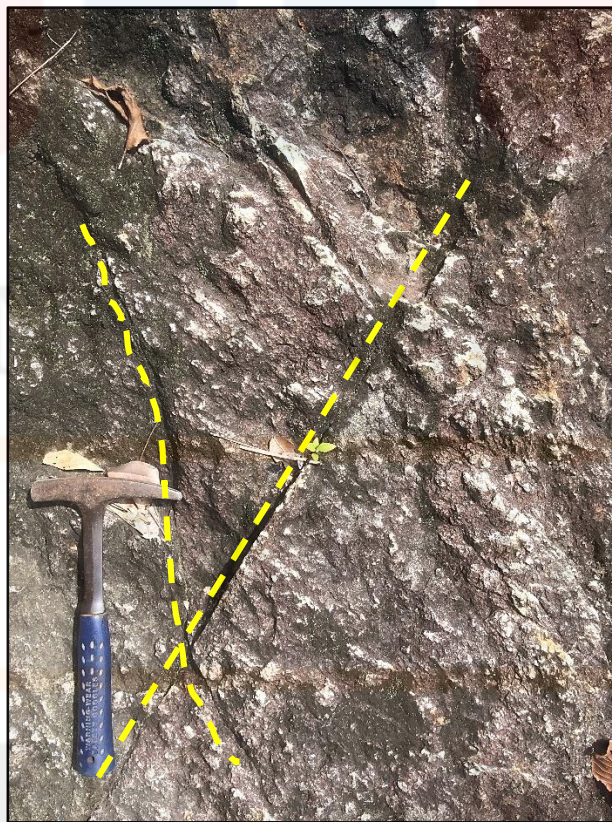


Figure 4.21. Conjugate joint structure (yellow dashed lines) of granite body at Sungai Suda.

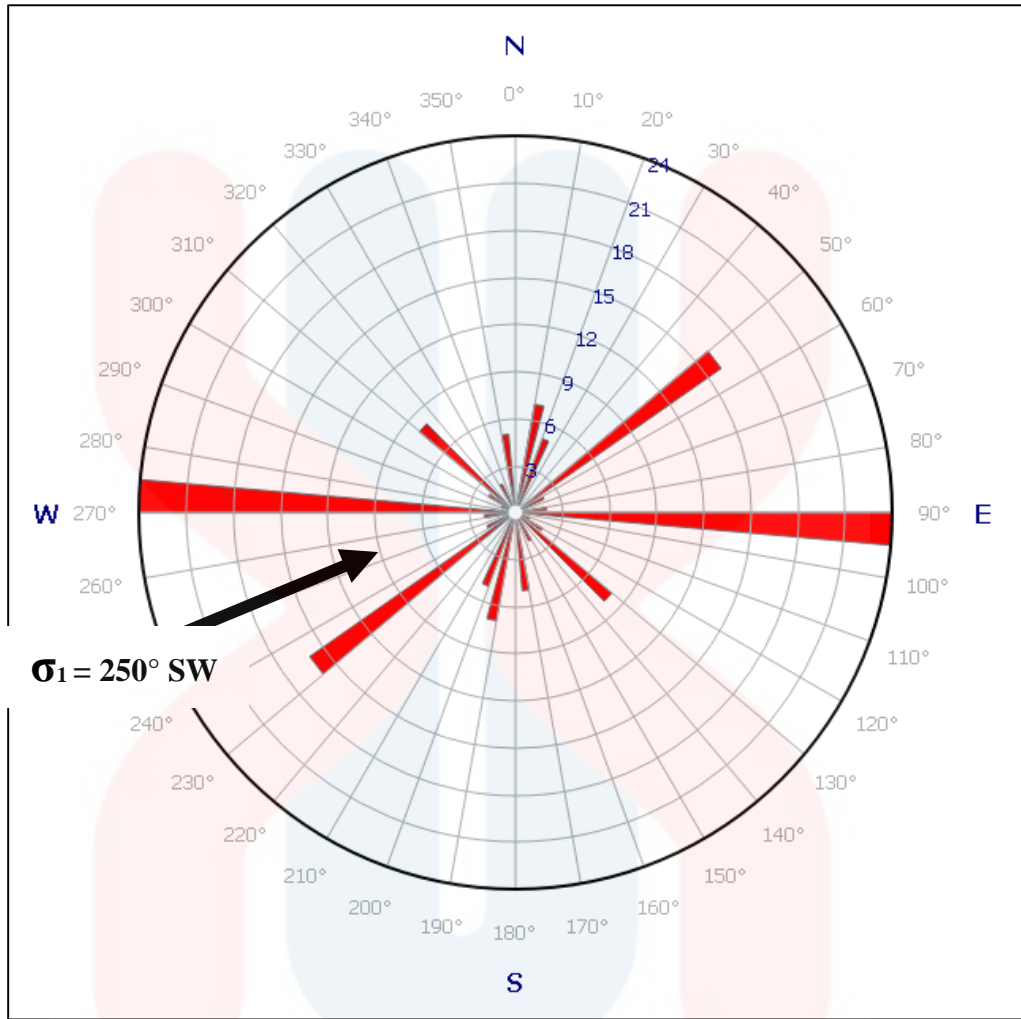


Figure 4.22. Rose Diagram for joint analysis at checkpoint J2.



Figure 4.23. Conjugate joint structure (yellow dashed lines) of granite body at Sungai Terang.

4.4.3 Fault

A fault is a planar structure formed due deformation of the rock. A fault has a significant displacement as the result of rock mass deformation. Generally, there are three types of faults, strike-slip, normal, and thrust faults. Each type of faults is a result from different direction of forces acting on the rock mass.

a) Reverse fault

Figure 4.24 showed the reverse fault which found at Sungai Suda. Based on the observation, the hanging wall moves upward and the footwall is moved downward. The maximum force, σ_1 exerted on vertical direction and the minimum force σ_3 is acting on the horizontal direction.

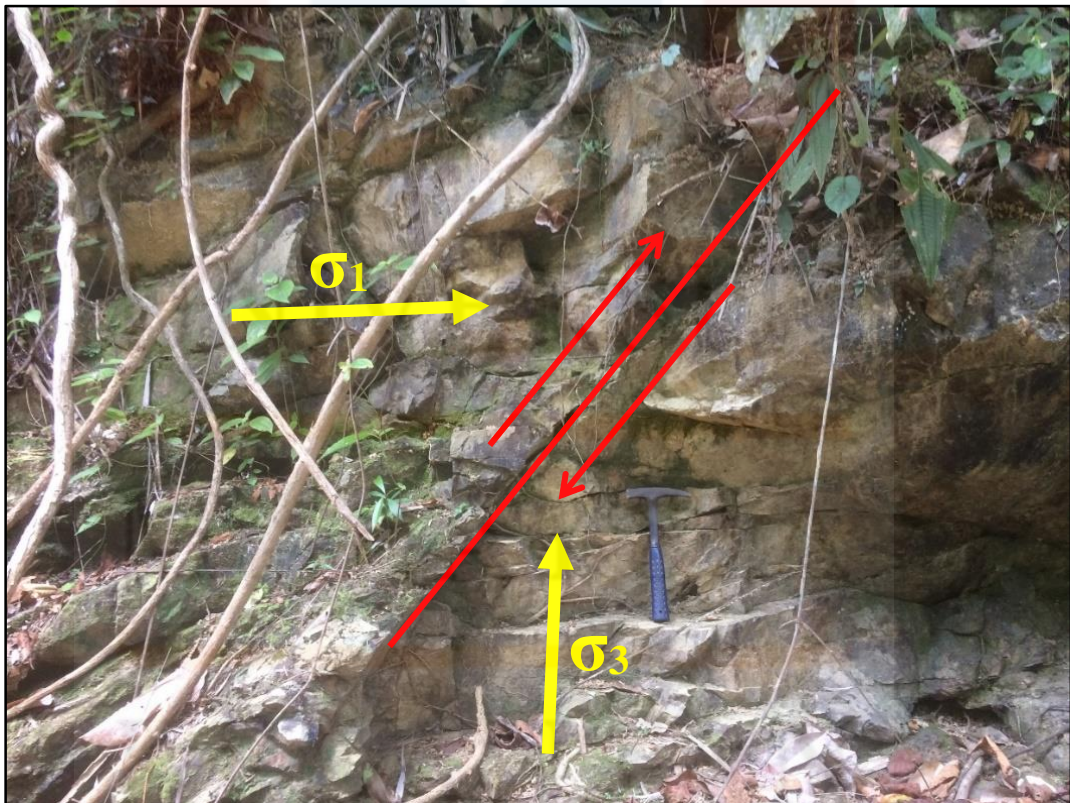


Figure 4.24. A reverse fault of the microgranite unit at Sungai Suda.

b) Minor faults

From the previous study by Ibrahim Abdullah and Jatmika Setiawan, the rock had undergone at least four phases of deformation through the metamorphism and granite intrusion. The area has undergone deformation with compression in the NE direction which linked with the formation of conjugate strike-slip faults and other minor structures. Foliation and minor faults formation can be relating to the stress system of sinistral transpressive deformation and emplacement of the granite body. From the field observation, there are few minor faults found along Sungai Suda. The minor faults are observed in the microgranite unit. Due to the deformation, folding has structure has formed on the microgranite body as shown in Figure 4.25 (a) and (b).

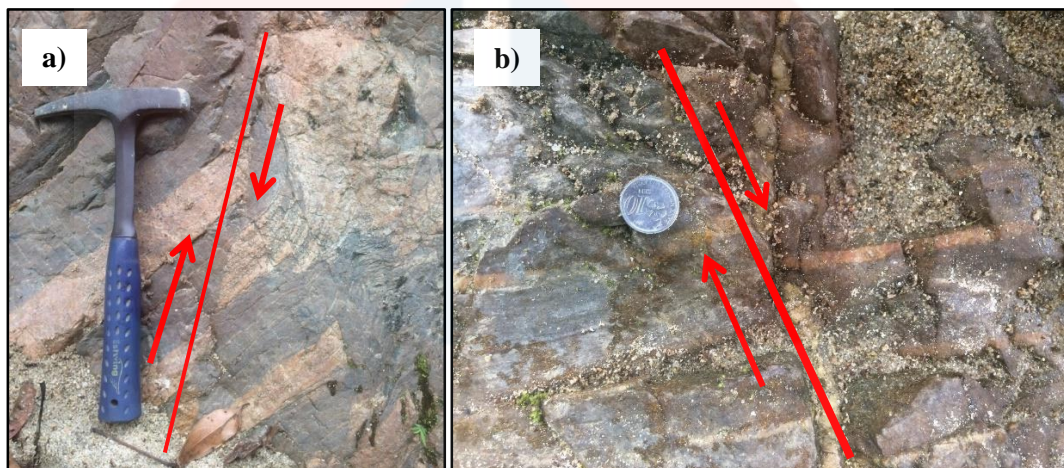


Figure 4.25. a) Minor fault on the microgranite unit in Sungai Suda. b) Minor structures on the microgranite unit at Sungai Suda.

4.4.4 Vein

The vein is a mineral mass of a tabular form which deposited along the fracture on rock mass. Vein form when the fracture is filling with crystallised mineral. Vein can presence as a small-scale or large-scale structure. Based on the field observation, there are quite numerous veins found in the study area. Most of the veins found are quartz veins. The quartz filled the fracture of microgranite and porphyritic granite which shown in Figure 4.26 (a) and (b).

Quartz veins on microgranite body mostly in thin and foliated form as shown in Figure 4.26 (a). It is foliated due to the deformation experienced by the rock body. Based on the previous study, there are at least three times of deformation occurred which resulted in the complex structure on the microgranite body. However, the quartz veins on the porphyritic granite body in Sungai Terang are mostly wide and long in size. The wide of the quartz veins are ranging from 3 cm up to 15 cm (Figure 4.26 (b)).

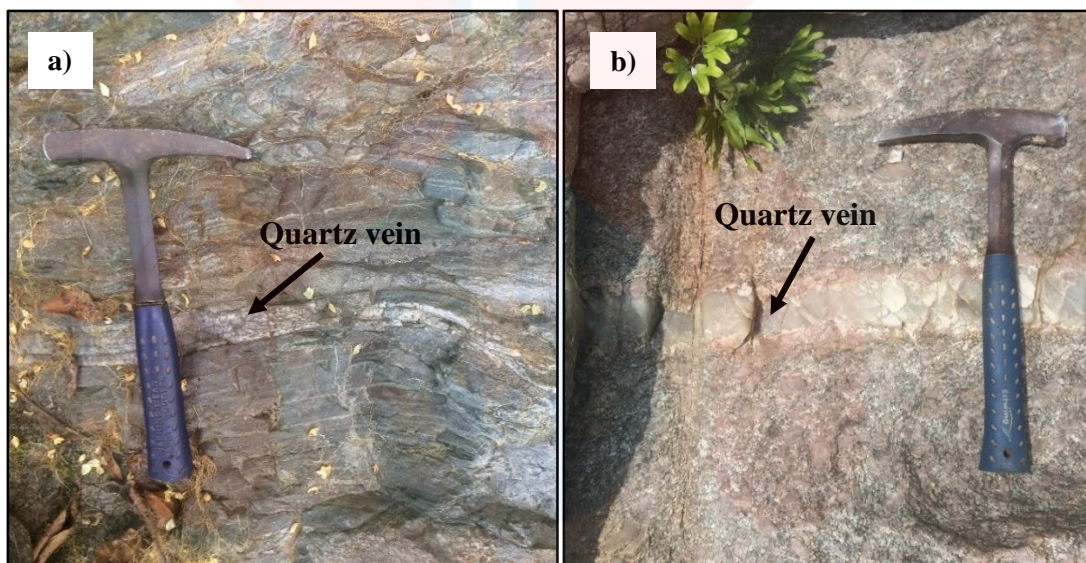


Figure 4.26. a) Quartz vein on porphyritic granite at Sungai Terang. b) Quartz vein on porphyritic granite at Sungai Suda.

4.5 Historical Geology

In Kelantan, the study area is part of Noring Granite formation of Stong Complex. Stong Complex consists of three granites; Noring granite, Kenerong granite and Berangkat granodiorite (Daanen, n.d.). During Permian and Triassic, the Complex has been intruded. Migmatisation also occurred to the sediments near the Stong Complex however it is considered as insignificant due to the size of the pluton. The felsic composition of Noring granite and Kenerong granite are respectively similar. It is suggested that Stong Complex be Cretaceous or Upper Cretaceous age. Low-grade metamorphic rock is located next to the Stong Complex but it does not show signs of contact metamorphism.

Dynamic topography response is a mechanism of the tectonic evolution of Stong Complex. It started with the temporary termination of subduction along the Sunda Margin. Dynamic topographic low supports the suspension of subduction removed forces which resulting in regional uplift and unearthing. Thus, Middle to Late Cretaceous sinistral transpression is a result of Stong Complex's tectonic evolution. Deformation is the further process of emplacement of Stong Complex.

The central zone extending from West Malaya north is mainly composed of S-type granites batholith and include migmatites. There are also subordinate hornblende-biotite granites with I-type affinities. Both S-type and I-type granites are apparently same age ranges. I-type subduction-related granites in the Western province are more felsic with increasing crustal influence and the large-scale batholiths of biotite granite in western and central provinces.

The original country rocks, metasediment are considered to be Permo-Carboniferous to Early Triassic. This metasediment is originated from the Gua Musang formation. By now, the country rocks formed the metasedimentary enclaves. Unearthing of Stong Complex after being situated in the deeper crust has resulted to lack of contact metamorphism between Stong Complex and the adjacent Triassic mete-sediments. Another evidence of Stong Complex originated at deeper crust is the formation contains high-grade garnets. The historical geology of each lithology in study area is shown in stratigraphic column in Figure 4.10.

CHAPTER 5

SLOPE INVESTIGATION BY USING ELECTRICAL RESISTIVITY SURVEY

5.1 Introduction

In Malaysia, the most geohazard occurs is landslide or slope failure. Slope failure is a natural event that a slope collapses abruptly due to weakened self-retainability of the earth. The value of factor of safety is less than 1 which caused the slope unstable. Common slope failure triggering mechanisms are intense rainfall, water-level change, seepage water flow, earthquake shaking and human activity. Subsurface factors of slope failure are water content, geometry, and type of lithology. This phenomenon can be monitor by using Electrical Resistivity Imaging (ERI) method which measured the subsurface factors of slope failure.

Electrical Resistivity Imaging (ERI) is one of geophysical methods used to determine the subsurface resistivity distribution through measuring the ground surface. Basically, the resistivity is measured in Ωm , which is the mathematical inverse of conductivity. The cross-sectional 2D plot of ERI profiles represents the subsurface geometry, lithology, water content and any anomalies. This ERI method can provide the distribution of subsurface soil and rock resistivity of slope failure. The measurement of ERI is conducted along the ground surface in order to determine the subsurface resistivity distribution. This method is suitable for slope failure investigation as it can be determining the subsurface factors which caused the slope failure. The result of ERI method is used to estimate the thickness of sliding materials,

delineate the geometry of slope failure, approximate the volume body investigated and highlight the areas with high water content.

5.2 2D Electrical Resistivity Imaging Survey Study

The electrical resistivity imaging (ERI) survey includes measuring a series of constant separation traverse with increase of electrodes spacing with each successive traverse. The depth of penetration increases with the increase of electrode spacing. The vertical contoured section is constructed based on the apparent resistivity measured at various depths. The vertical contoured section is representing the variation of resistivity both laterally and vertically. Various subsurface features can be characterized by 2D ERI survey such as geology of the subsurface lithological, structural, and hydrological condition.

5.3 Survey lines location

This research entitled Geology and Slope Investigation using Resistivity Method in Kg. Bukit Selar basically focused on slope investigation by using ERI method. There are five lines has been conducted on two slopes in the study area. As shown in Figure 5.1, the survey lines are placed on slope along the road direct to TNB Pergau Hydroelectric in Gunung Basor area. The location of Survey Line 1, Survey Line 2, Survey Line 3, Survey Line 4, and Survey Line 5 is plotted on Google Earth as shown in Figure 5.2.

The lines is proposed due the previous slope failure phenomenon occurred in the area. Two landslides has been choose in order to investigate the triggering factors of the slope failure. Basically, four lines is placed on the main slope (Slope 1) because the mass wasting size is big and considered as the main landslide in the area. Two pole-dipole arrays lines for vertical direction and three Schlumberger aays lines for horizontal direction on the slope surface.

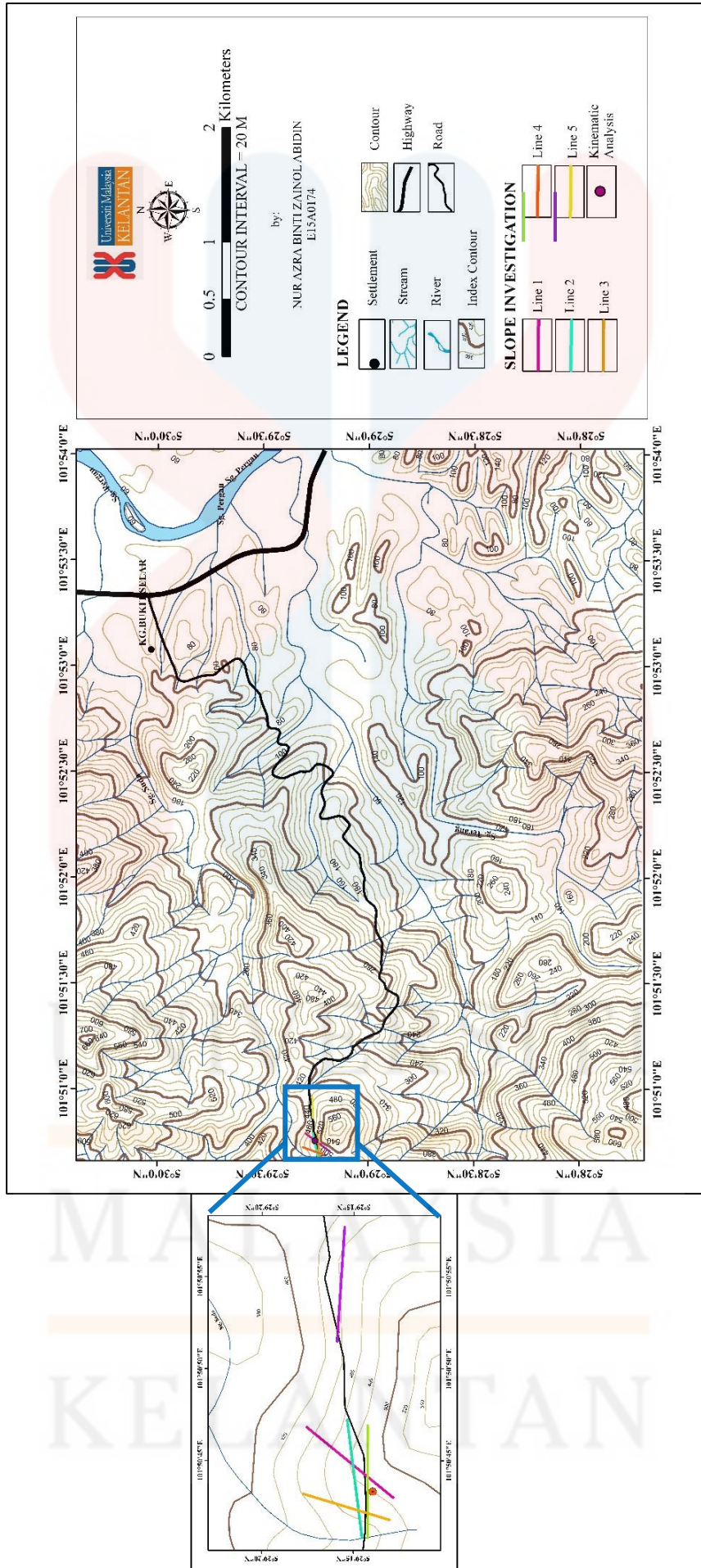




Figure 5.2. Location of survey lines. (Source: Google Earth)

5.4 Electrical resistivity imaging of slope investigation

Slope at coordinate N 05°29'15" and E 101°50'45.4" is chosen for slope investigation in this research. It is a large scale and the main landslide in the study area. This mass wasting is classified as rock fall. The width of the slope is approximately 200 m and the height is almost 100 m. The rock type is porphyritic granite and it is slightly weathered. Figure 5.3 shows the slope that has been choose for ERI survey.

The slope is chosen for ERI study because it is a main slope failure which caused destruction in the area. There are some mitigation controls have been constructed at the slope area such as rock fall barrier and a drainage system. Both method have shown that the slope is failure due to seepage problem and the type of mass wasting is rock fall.



Figure 5.3. Slope failure in study area.

5.4.1 Survey Line 1

Survey Line 1 is 200 m in length in vertical direction on the slope surface. Pole-dipole protocol is used for this line with 5 m electrode spacing. The total electrodes used is 41 electrodes which the first electrode start at coordinate of N 05°29'12.8" E 101°50'43.5" and last electrodes at coordinate N 05°29'17.5" E 101°50'46.8". The center of the electrodes is at coordinate N 05°29'15.1" E 101°50'45.4" in which the ABEM Terrameter LS is placed. The survey line is directed from SSW to NNE. Appendix shown the elevations of all electrodes. The weather is hot sunny during ERI test. Site set-up is shown in Figure 5.4 (a), Figure 5.4(b), and Figure 5.5.

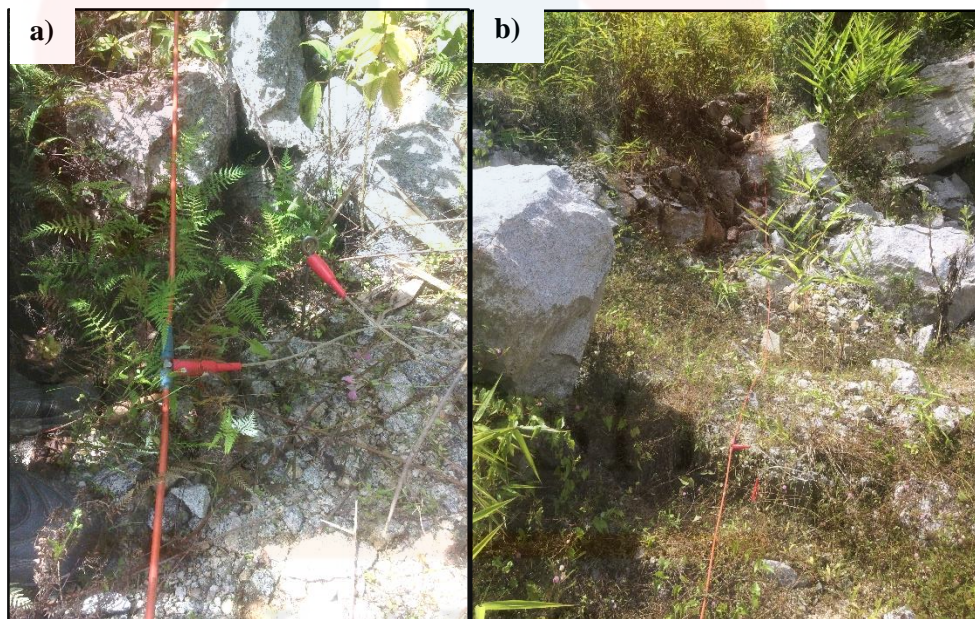


Figure 5.4. a) Set-up for an electrode. b) Set-up for spread Survey Line 1.



Figure 5.5. Set-up for center of spread Survey Line 1.

The ERI survey spread Line 1 with a length of 200 m in the SSW - NNE direction as shown in Figure 5.2. Based on the observation of the inverted pseudosection, the resistivity values are ranging from 1 Ωm to more than 3000 Ωm . From the Figure 5.6, the color ranges from dark blue to purple. The highest resistivity values zone is at 700 Ωm until more than 3000 Ωm in the bottom part which can be interpreted as the fractured granite bedrock region. This zones are located at spread 0 m to 62.5 m and 120 m to 155 m. It is interpreted as fractured rock due to the lower chargeability value (1 msec to 2 msec) in which shows the presence of water content in the zones. By comparing resistivity method and induced polarization method, existence of water can be predicted and detected the water is existing in dense rock.

Lowest resistivity zone in this pseudosection has resistivity values ranges from 1 Ωm to more than 20 Ωm . The color of the region is blue to light blue. Low resistivity values zone indicates that presence of water content or highly conductive materials. This shows the existing of weak zone for this slope at the bottom part of the slope. It is located almost 20 m underground at the center spread Line 1. By referring to Figure

5.6, there is a seepage zone can be seen clearly at approximately 87.5 m spread on Survey Line 1. There is low resistivity zone at the bottom part of the pseudosection which show the source of seepage flow from the subsurface dense rock according to IP values ranging from 10 msec to 20 msec.

The uppermost zone shows the thin layer of loose to dense residual soil with moist to dry condition. Several rotated blocks, cracks, and headscarps can be seen at the upper part of pseudosection. The zone is approximately 10 m deep from the ground surface. Vertical electrical contrast in the thin layer of top part of the slope shows the sliding plane of the slope failure (Figure 5.6). There is a fault can be seen due to the discontinuity of rock at spread 70 m and 97 m from first electrode).

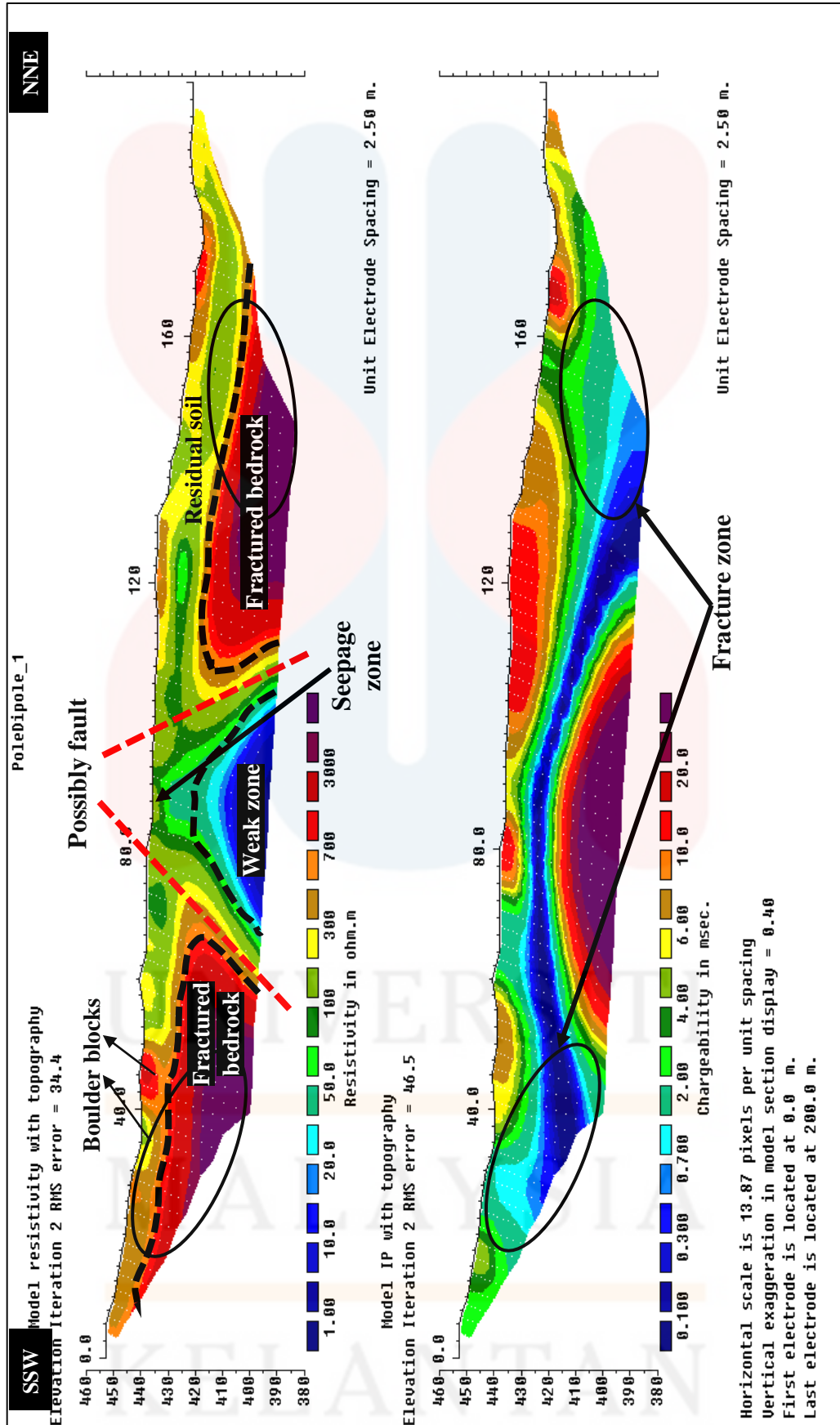


Figure 5.6. Inverse resistivity and IP pseudosection the topography of Survey Line 1.

5.4.2 Survey Line 2

Survey Line 2 is 200 m in length in horizontal direction on the slope surface. Schlumberger protocol is used for this line with 5 m electrode spacing. The total electrodes used is 41 electrodes which the first electrode start at coordinate of N 05°29'14.5" E 101°50'40.8" and last electrodes at coordinate N 05°29'15.3" E 101°50'47.2". The center of the electrodes is at coordinate N 05°29'15.2" E 101°50'44.0" in which the ABEM Terrameter LS is placed. The survey line is directed from W to E. Appendix shown the elevations of all electrodes. The weather is hot sunny during ERI test. Site set-up is shown in Figure 5.7(a), Figure 5.7(b), and Figure 5.8.

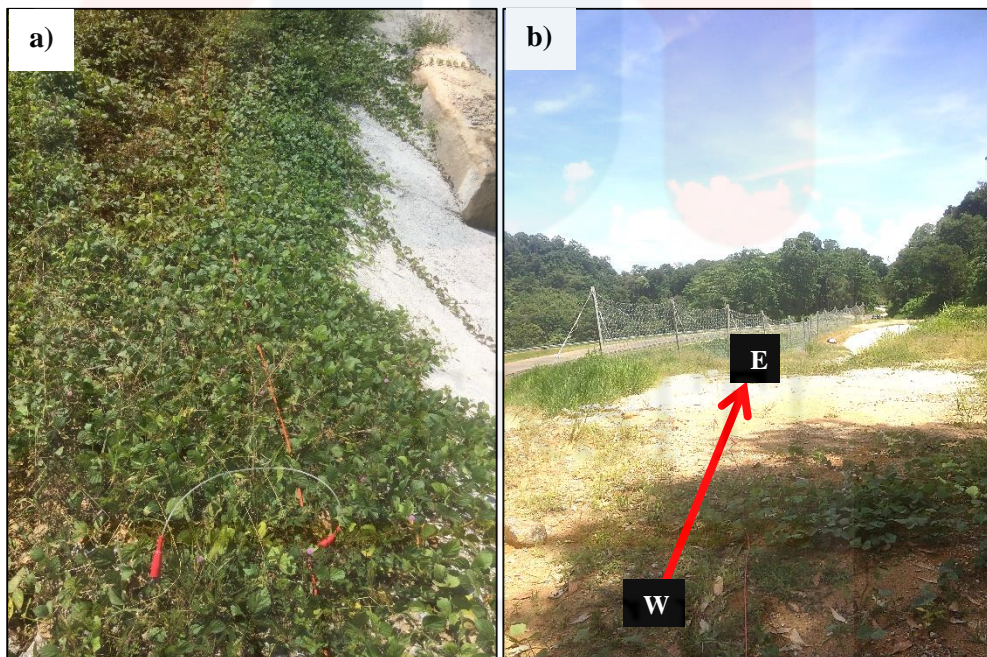


Figure 5.7. a) Set-up for an electrode. b) Set-up for spread Survey Line 2 in W-E direction.

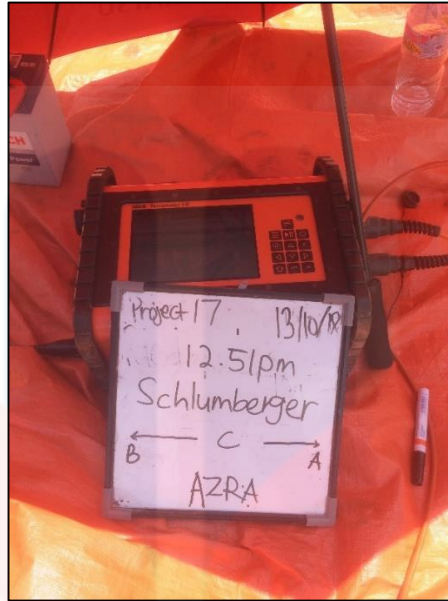


Figure 5.8. Set-up for center of spread Survey Line 2.

The ERI survey spread Line 2 with a length of 200 m in the W-E direction as shown in Figure 5.2. Based on the inverted pseudosection, the resistivity values are ranging from 1 Ωm to more than 700 Ωm . From the Figure 5.9, the color ranges from dark blue to red. The lowest resistivity values area around 1 Ωm to 20 Ωm in the bottom part in which resides most of the pseudosection can be interpreted as the water content region. This zone is located at elevation between 415 m to 440 m. For slope failure this region can be interpreted as groundwater source of seepage.

Meanwhile, the top part of pseudosection which has high resistivity values start from 300 Ωm to more than 700 Ωm , is interpreted as the boulder blocks of porphyritic granite rock due to rock fall. The zone between 5 m to 10 m deep from the ground surface. Top zone also can be interpreted as the region with loose to dense residual soil with moist to dry condition as the layer is thin layer with 5 m to 10 m thick. By comparing resistivity value and IP value, existence of water can be detected is existing in fractured zone.

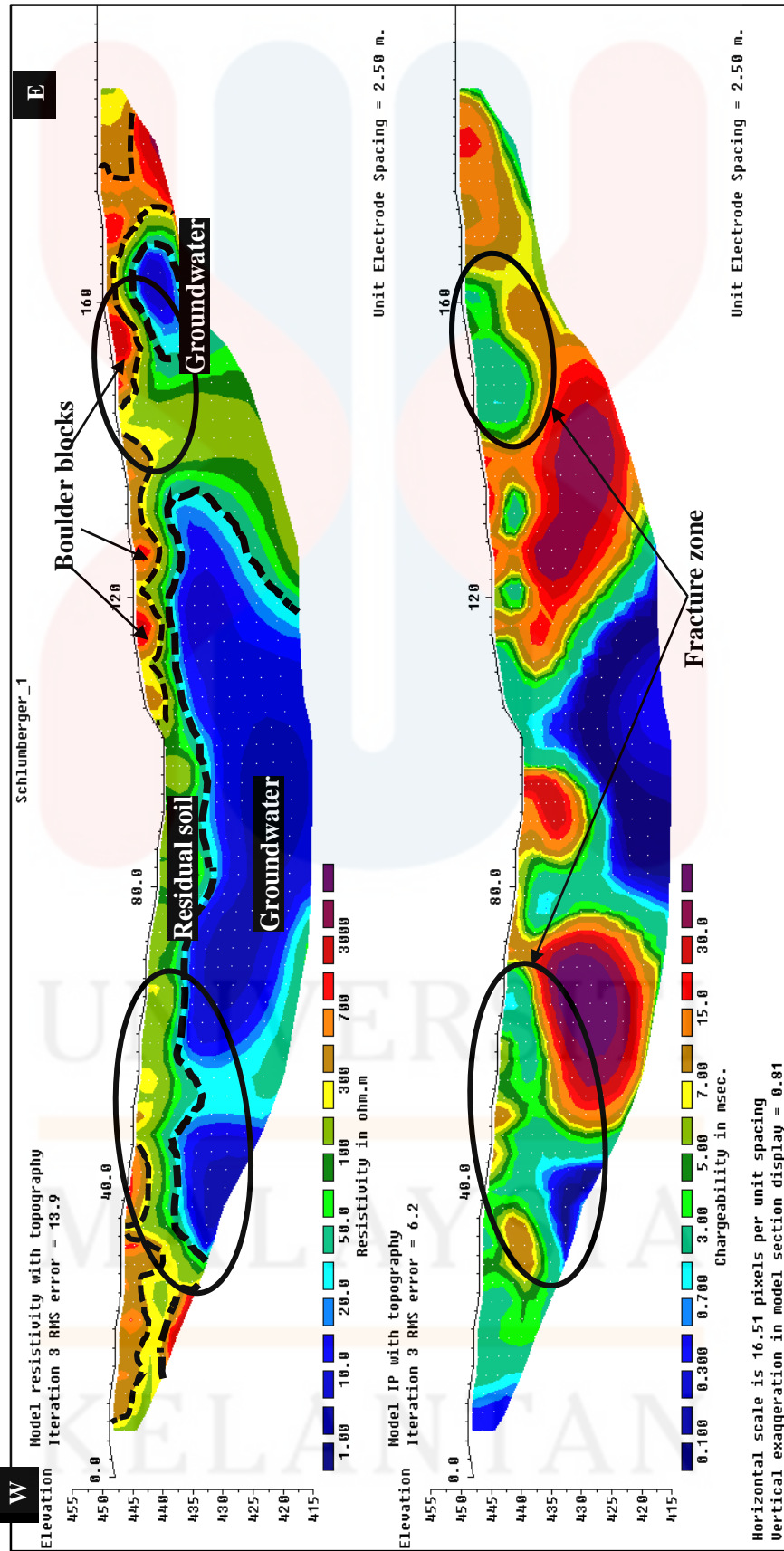


Figure 5.9. Inverse resistivity and IP pseudosection the topography of Survey Line 2..

4.4.3 Survey Line 3

Survey Line 3 is 200 m in length in horizontal direction on the slope surface. Schlumberger protocol is used for this line with 5 m electrode spacing. The total electrodes used is 41 electrodes which the first electrode start at coordinate of N 05°29'14.2" E 101°50'40.8" and last electrodes at coordinate N 05°29'15.1" E 101°50'46.9". The center of the electrodes is at coordinate N 05°29'14.1" E 101°50'43.8" in which the ABEM Terrameter LS is placed. Appendix shown the elevations of all electrodes. The weather is hot sunny during ERI test.

The ERI survey spread Line 3 with a length of 200 m in the W-E direction as shown in Figure 5.2. Based on the observation of the inverted pseudosection, the resistivity values are ranging from 10 Ωm to more than 3000 Ωm . From the Figure 5.10, the color ranges from blue to purple. The highest resistivity values area at 700 Ωm to more than 3000 Ωm in the bottom part which can be interpreted as the granite bedrock region. This zone is located at elevation between 400 m to 410 m.

Lowest resistivity zone in this pseudosection has resistivity values ranges from 10 Ωm to more than 20 Ωm . The color of the region is blue to light blue at elevation 435 m to 475 m. Low resistivity values zone indicates that presence of water content or highly conductive materials. This shows the existing of weak zone for this slope. By referring to Figure 5.14, there is an overflow seepage zone can be seen clearly at approximately 10 m spread on Survey Line 3.

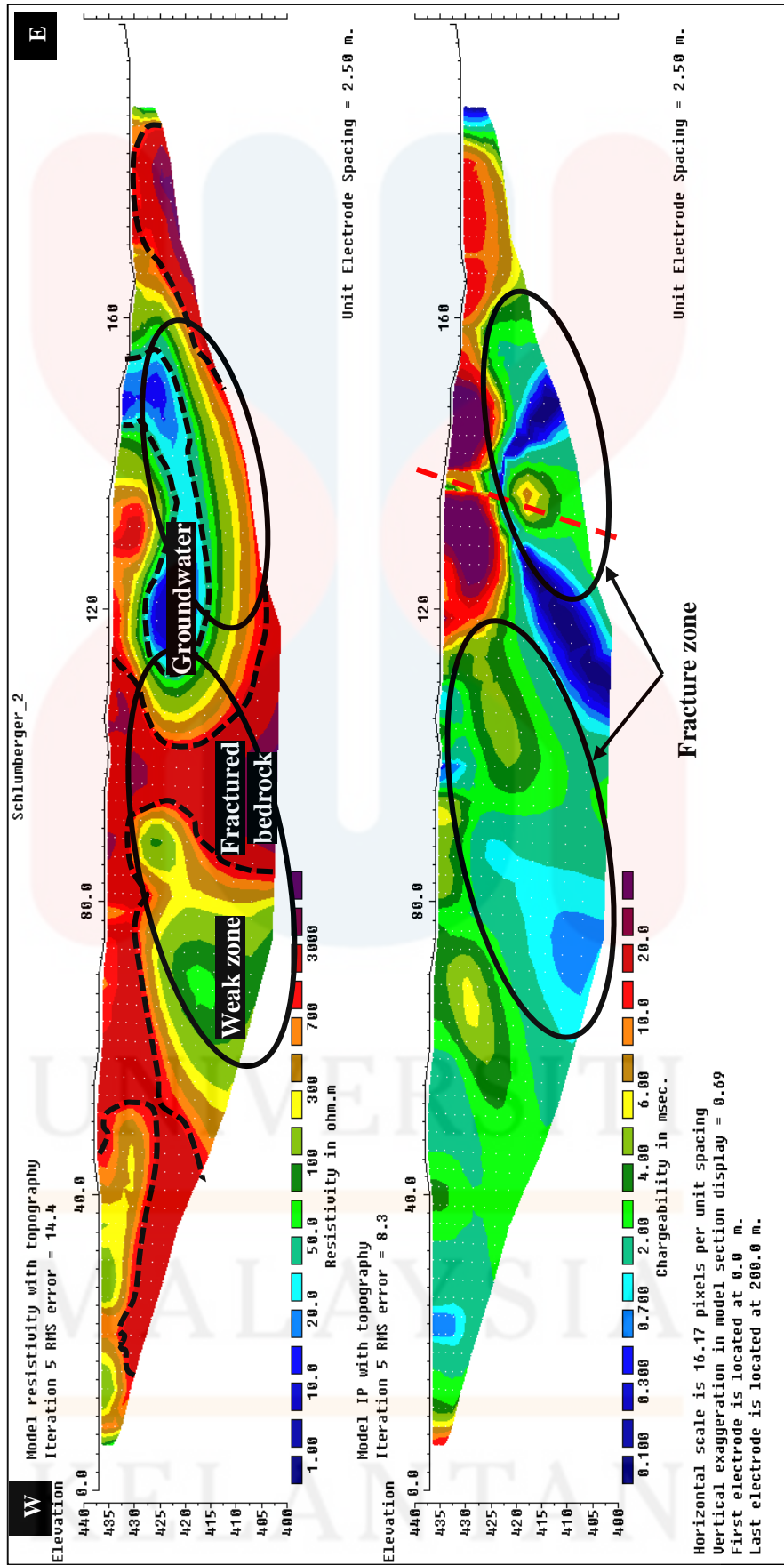


Figure 5.10. Inverse resistivity and IP pseudosection the topography of Survey Line 3.

5.4.4 Survey Line 4

Survey Line 5 is 200 m in length in vertical direction on the slope surface. Pole-dipole protocol is used for this line with 5 m electrode spacing. The total electrodes used is 41 electrodes which the first electrode start at coordinate of N 05°29'13.1" E 101°50'41.8" and last electrodes at coordinate N 05°29'17.7" E 101°50'43.2". The center of the electrodes is at coordinate N 05°29'14.6" E 101°50'43.4" in which the ABEM Terrameter LS is placed. Appendix shown the elevations of all electrodes. The weather is hot sunny during ERI test. Site set-up is shown in Figure 5.11(a), Figure 5.11(b), Figure 5.12(a), and Figure 5.12(b).

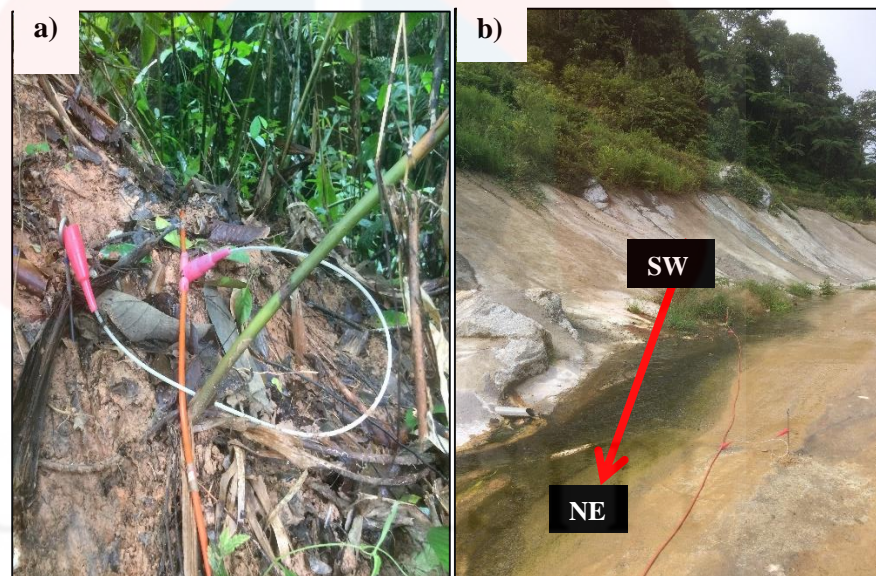


Figure 5.11. a) Set-up for an electrode. b) Set-up for spread Survey Line 4 in SW-NE direction.

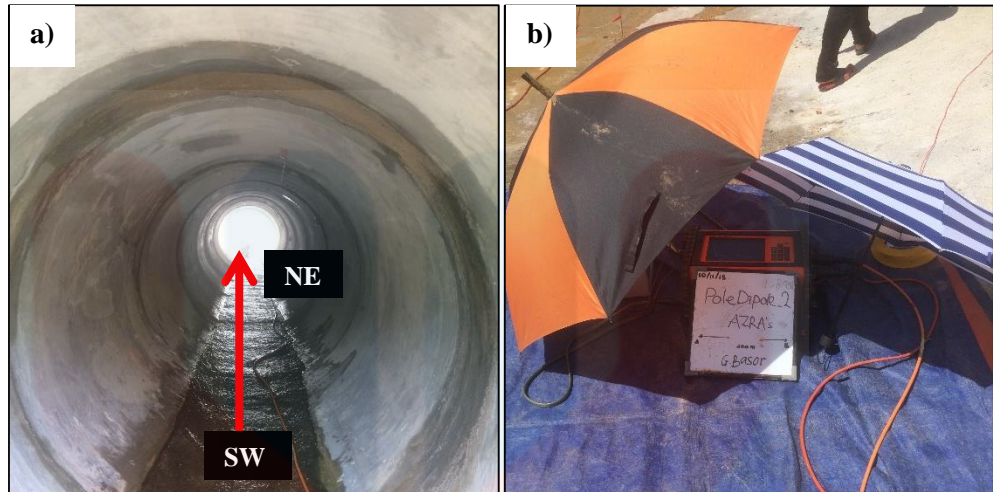


Figure 5.12. a) Set-up for spread Survey Line 4 in SW-NE direction. b) Set-up for center of spread Survey Line 4.

The ERI survey spread Line 4 with a length of 200 m in the SW – NE direction as shown in Figure 5.2. Based on the observation of the inverted pseudosection, the resistivity values are ranging from 1 Ωm to more than 3000 Ωm . From the Figure 5.13, the color ranges from dark blue to purple. The highest resistivity values zone is at 1000 Ωm until more than 3000 Ωm in the bottom part which can be interpreted as the granite bedrock region. This zone is located at elevation between 370 m to 420 m.

Lowest resistivity zone in this pseudosection has resistivity values ranges from 1 Ωm to more than 20 Ωm . The color of the region is blue to light blue. Low resistivity values zone indicates that presence of water content or highly conductive materials. This shows the existing of weak zone for this slope at almost 10 m deep from ground surface. By referring to Figure 5.13, there is a seepage zone can be seen clearly at approximately 3 m spread on Survey Line 4. There is low resistivity zone at the bottom part of the pseudosection which show the source of seepage flow from the subsurface.

The uppermost zone shows the thin layer of loose to dense residual soil with moist to dry condition at spread 70 m to 200 m from first electrode point. Several

rotated blocks, cracks, and headscarps can be seen at the upper part of pseudosection. Vertical electrical contrast in the thin layer of top part of the slope shows the sliding plane (white lines) of the slope failure (Figure 5.13). There is a fault can be seen due to the discontinuity of rock at elevation 430 m (spread 157 m from first electrode).

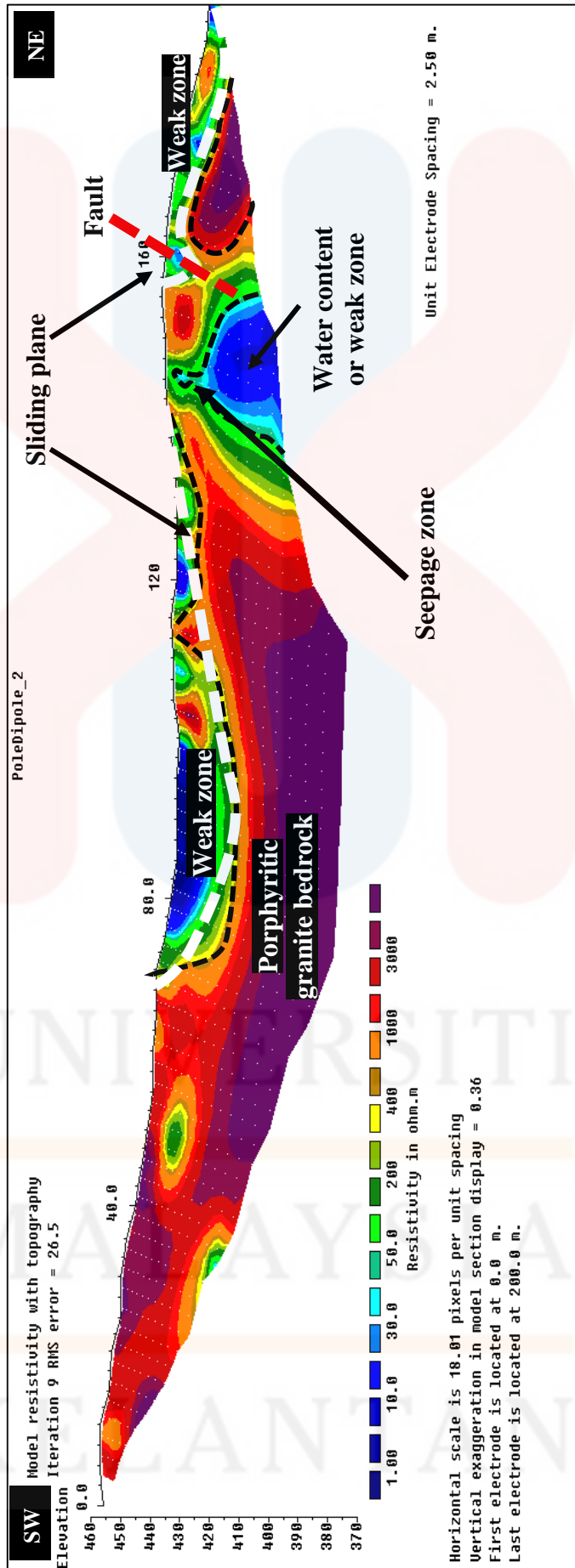


Figure 5.13. Inverse resistivity pseudosection the topography of Survey Line 4.

5.4.5 Survey Line 5

Survey Line 5 is 200 m in length in horizontal direction on the slope surface. Schlumberger protocol is used for this line with 5 m electrode spacing. The total electrodes used is 41 electrodes which the first electrode start at coordinate of N 05°29'15.5" E 101°50'57.7" and last electrodes at coordinate N 05°29'15.9" E 101°50'51.9". The center of the electrodes is at coordinate N 05°29'16.3" E 101°50'54.3" in which the ABEM Terrameter LS is placed. Appendix shown the elevations of all electrodes. The weather is hot sunny during ERI test.

The ERI survey spread Line 5 with a length of 200 m in the E-W direction as shown in Figure 5.2. Based on the observation of the inverted pseudosection, the resistivity values are ranging from 50 Ωm to more than 3000 Ωm . From the Figure 5.18, the color ranges from light green to purple. The highest resistivity values area at 700 Ωm to more than 3000 Ωm which most of the part can be interpreted as the fractured granite bedrock region. The fractured zone is circle on both resistivity and IP pseudosections. The IP values is 1 msec to 2 msec. By comparing resistivity value and IP value, existence of water can be detected is existing in fractured zone. The highest resistivity value (more than 3000 Ωm) covered at bottom part of the profile at elevation 410 m to 420 m and some are at elevation 430 m to 440 m.

Lowest resistivity zone in this pseudosection has resistivity values ranges from 50 Ωm to more than 300 Ωm . The color of the region is light green to yellow with thickness of 10 m to 15 m. Low resistivity values zone indicates the existing of weak zone for this horizontal spread line between Slope 1 and Slope 2. By referring to Figure 5.14, there are several seepages formed on the rock body.

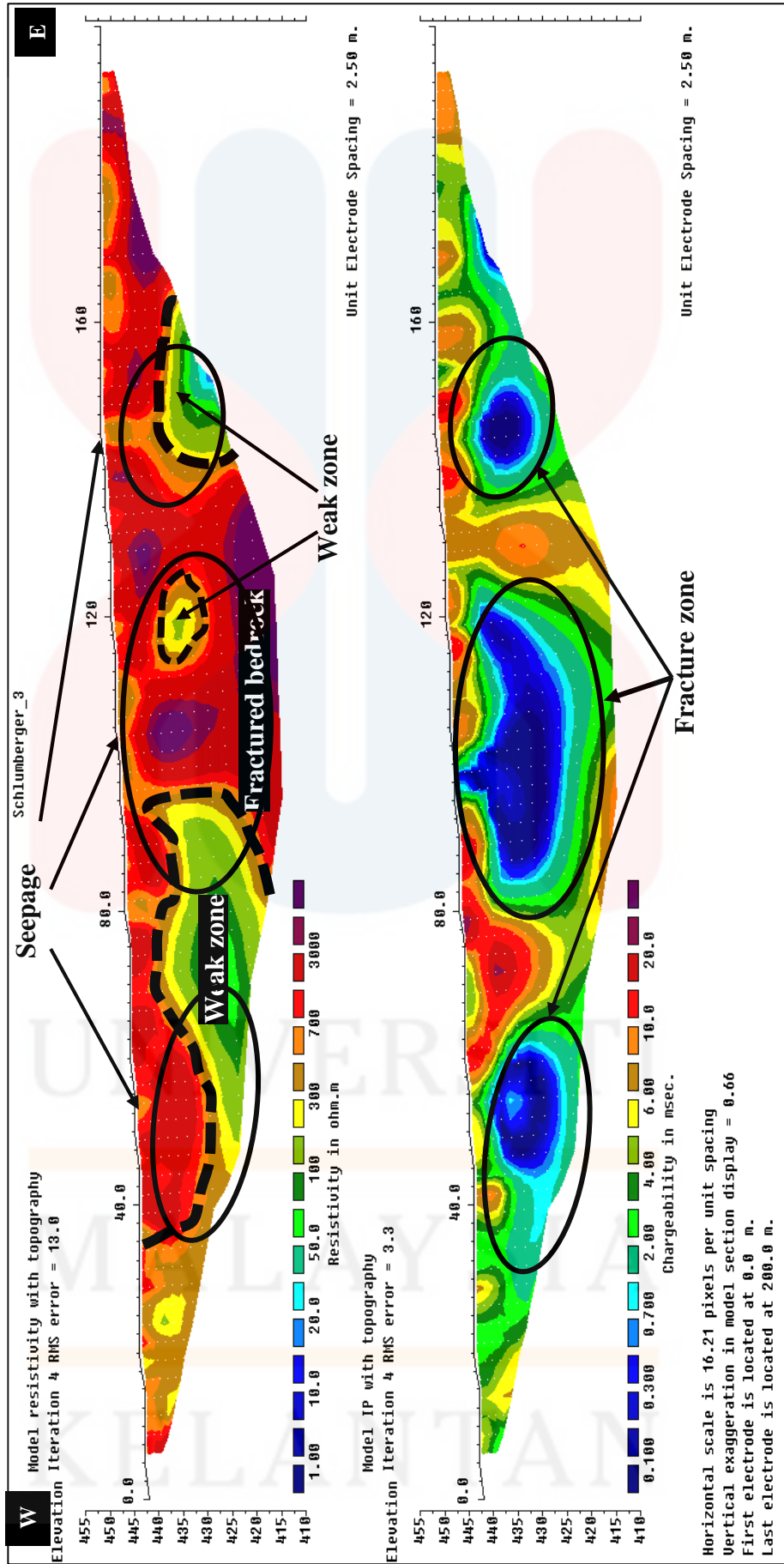


Figure 5.14 Inverse resistivity and IP pseudosection the topography of Survey Line 5.

5.5 Kinematic Analysis of slope failure (Slope 1)

Kinematic analysis is a preliminary method that study the potential of rock slope failure by analysing the orientation of discontinuity data. this method uses stereonet to represent discontinuity data as planes and lines and plotted the great circle of slope geometry to identify any possibility of failure form the discontinuity data. in this research, kinematic analysis was used as a supporting data to evaluating the rock slope failure that was done by using ERI method.

The first step in kinematic analysis was projected the discontinuity data (Figure 5.15). Discontinuity data was taken on a large granite rock slope that was consist of trend, plunge, persistence and spacing of joint that formed on rock body. Stereographic projection of the discontinuity data was done by plotting the trend and plunge of all joint in an Equal Area (Schmidt) Net.

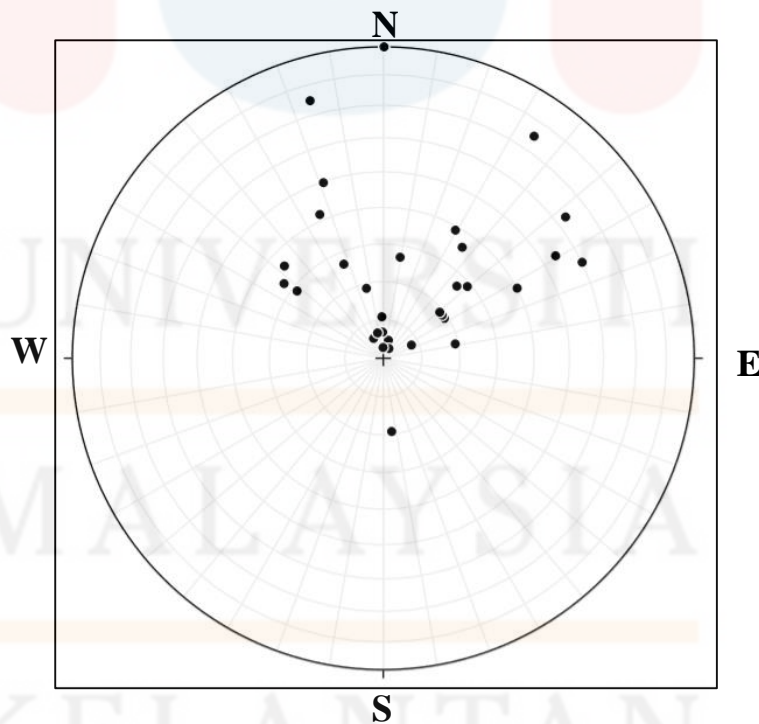


Figure 5.15. Stereographic projection of joint in Slope 1.

The trends and plunges data of joints were projected in form of lines (points) in the stereonet. To effectively measure the influence of discontinuity towards rock slope failure, the abundance of the discontinuity data was divided into joint sets, which a set of joint that were closely spaced by plotting a density contour on the stereonet. The density contour was plotted on a concentrated stereonet data indicates a joint sets using the contour (Figure 5.16). In this research, there were four joint sets from the contouring on the stereonet.

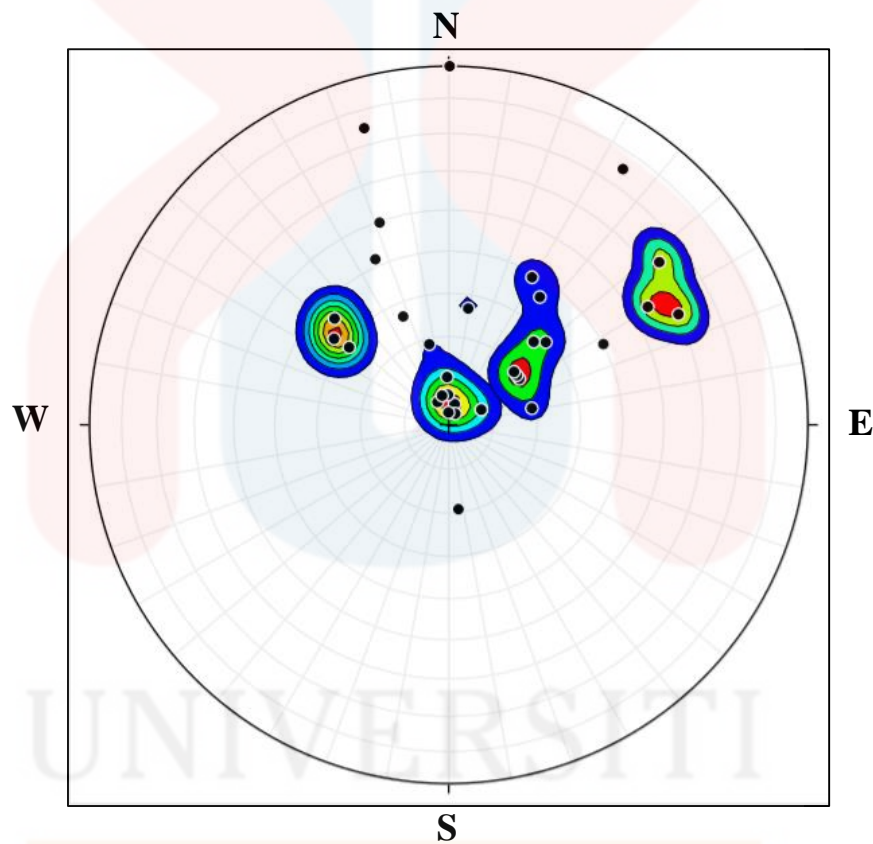


Figure 5.16. Contour of closely spaced joint data were plotted on the stereonet.

After the contour was plotted, best fit plane of each contour were plotted as a representative for each joint set (Figure 5.17). The best fit planes then were used to for kinematic analysis of rock slope and identify the type of failure and direction of failure of slope 1.

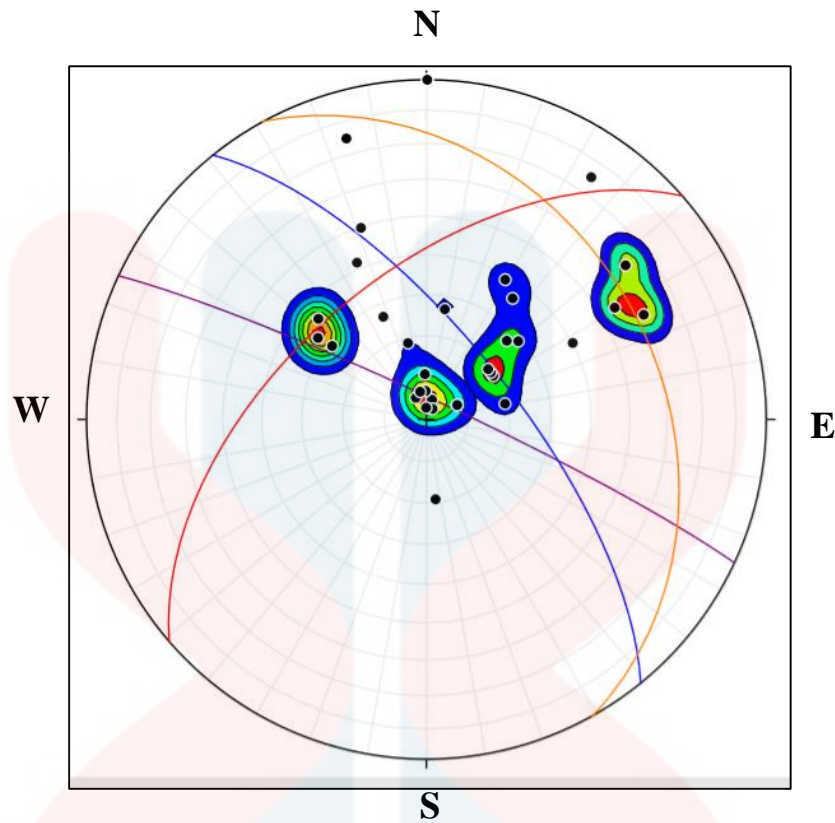


Figure 5.17. Best fit plane for each joint set were plotted on the stereonet.

From the field study, the geometry of slope such as slope angle and direction of slope face was measured. The data showed that the slope angle was 48° with the slope face was facing NNE direction. The slope geometry data was plotted as a dashed great circle in the stereonet as the slope geometry was essential for kinematic analysis of the rock slope as shown in Figure 5.18.

MALAYSIA
KELANTAN

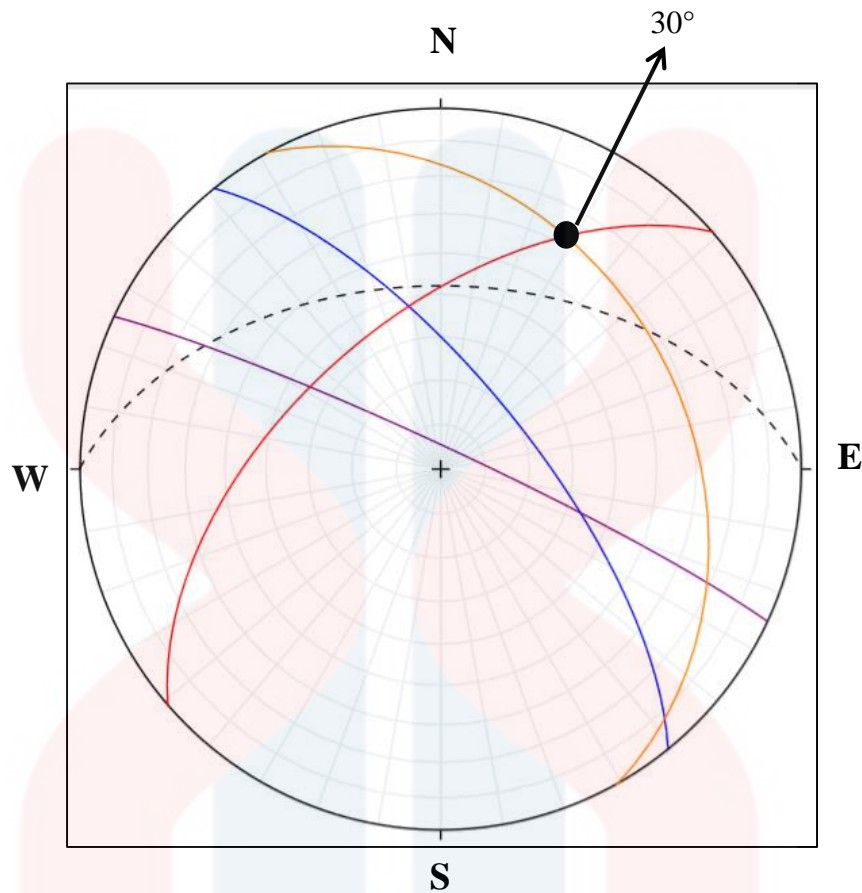


Figure 5.18. The slope geometry was plotted as a dashed plane in the stereonet.

From Figure 5.18, there were possibility of wedge failure occur between the intersection of joint set 3 (red line) and 4 (orange line). Other joint sets showed no possibility of rock slope failure since the joint set plunge was more inclined that the slope angle where the “daylight” not occur from the joint data. Daylight envelopes are used primarily in slope stability analysis work. It is kinematically feasible for any poles that plot within a daylight envelope to slide.

From the intersection of joint set 3 and 4, wedge failure may occur due to the intersection angle was lower than the slope angle and “daylight” would occur. From the kinematic analysis the direction of failure may occur at 30° (northeast).

5.6 Discussion

From the study of all five survey lines in the study area, it can be concluded that the main triggering factor of the landslide occurrence in the study area is due to the existing overflow seepage. The pseudosections show that the slope is composed of weak materials in which fractured rock. Basically, the bedrock is saturated with water. Low resistivity and chargeability values indicate the region is saturated with water. Relation between high resistivity values with low chargeability values showed that the bedrock is a fractured rock which contained water. It is also classified as a weak zone of slope.

Result from Survey Line 5 shows that, the triggering factor for both Slope 1 and Slope 2 is water content even though the type of mass wasting is different. As mentioned above, Slope 1 is a rock fall phenomenon while Slope 2 is a landslide. Along the road, there are several other slope failures observed. It can be concluded that the main factor of all landslides is subsurface water content which disturbs the factor of safety of the slopes.

Kinematic analysis is conducted to study the type and direction of slope failure for Slope 1. As analysed, the slope failure is a large scale hazard it is necessary to study the type, direction of slope failure, structural geology and weathering of the area.

CHAPTER 6

CONCLUSION AND RECOMMENDATION

6.1 Conclusion

This chapter concluded all the results obtained from this research for both geological mapping of study area and slope investigation using resistivity method. Geological mapping of study area provided the lithology, structures, geomorphology, and historical geology spread in study area. This 30 km² of study area composed of slate as the country rock, and porphyritic granite and microgranite as the granite intrusion. Major lithology in the study area is porphyritic granite which covered almost 50% of the total area of study area. This lithology served as acid intrusion in the study area. Porphyritic granite is the youngest lithology of the study area. Microgranite spread on the NW part of the study area. It is grey microgranite which moderately deformed due to the three phase of deformation occurred on the rock body. Both porphyritic granite and microgranite are lithology unit for Noring Granite member in Stong Complex. There are two regional fault were identified. Both faults are strike-slip fault in which named as Suda fault and Pergau fault.

For slope investigation part, two slope has been chosen for this research. Slope 1 is rock fall and Slope 2 is landslide. The slope failures due to seepage problem were successfully being investigated using ERI method. Based on the pseudosections, all the lines show the seepage zone was detected at the bottom part (Survey Line 1) and uppermost part (Survey Line 4) at the centre of resistivity line 1 and 4. The geometry and electrical resistivity The findings has proved that this approach is suitable and

reliable for slope investigation as the triggering factors such as weak zone, water content, seepage, faulting, and tension cracks. This ERI method is a new approach for slope failure assessment especially for slope seepage assessment since this method can reduce time, cost, and destruction on the slope failure especially by its 2D surface technique of investigation.

6.2 Recommendation

As this thesis discussed much about geology of granite lithology and slope investigation using ERI method, it can be used as guideline for the students to study about granite unit and slope investigation. For geology of the study area, it is recommended to conduct more detail geochemistry of granite in the study area. As mentioned in Chapter 4 this rock unit covered more than half part of the study area. It is recommended to conduct soil characteristics in the study area.

For slope investigation, it is recommended that more thorough study should be conducted in which include both geophysical method and engineering method. The area has high potential for slope area because the slope geometry and seepage problem. Due to the high potential of groundwater, it is good to study about the groundwater in the study area.

REFERENCES

- Aizebeokhai, A. P. (2010). 2D and 3D geoelectrical resistivity imaging: Theory and field design. *Scientific Research and Essays*, 3594.
- Alain Tabbagh, M. D. (2000). Soil resistivity: a non-invasive tool to map soil structure horizonation. *Elsevier Science*, 395.
- Bakhshipour, Z., Huat, B. B., Ibrahim, S., Asadi, A., & Kura, N. U. (2013). Application of Geophysical Techniques for 3D Geohazard Mapping to Delineate Cavities and Potential Sinkholes in the Northern Part of Kuala Lumpur, Malaysia. *The Scientific World Journal*.
- Bárta, J., Dostál, D., Beneš, V., & Tesař, M. (2005). Application of geophysical methods in the study of landslide movements, taking into account geological conditions in the sudety mountains. *Acta geodyn. Geomater* , 121-129.
- Bell, R., Kruse, J.-E., Gracia, A., Glade, T., & Hordt, A. (2006). Subsurface Investigation of Landslides Using Geophysical Method-Geoelectrical applications in Swabian Albs (Germany). *Subsurface investigation of landslides*, 201-208.
- Briney, A. (2017, 3 17). *Mass Wasting and Landslide*. Retrieved from ThoughtCo: www.thoughtco.com/mass-wasting-and-landslides-1434984
- Commitee, T. M.-T. (2014). *Litho- and Biostratigraphy Correlations of Chert Bed in Various Rock Units Along the Malaysia-Thailand Border*. Mineral and Geoscience Department Malaysia.
- Cook, J., McGown, A., Hurley, G., & Choy, L. E. (1998). The role of engineering geology in the hazard zonation of a Malaysian highway. In *Geohazard in Engineering Geology* (pp. 221-229). The Geological Society.
- Cruden, D. M., & Varnes, D. J. (1996). Landslide types and processes. In A. K. Tuener, & R. L. Schuster, *Landslides investigation and mitigation* (pp. 36-37). Transportation Research Board.
- Gasim, M. B., Toriman, M. E., & Juahir, H. (2015). Phenomenon of Slope Failure Occurrences along Gerik-Jeli Highway, Malaysia. *Journal of Applied Sciences*, 545-551.
- Gelisli, K., & Ersoy, H. (2017). Landslide investigation with the use of geophysical methods: a case study in northeastern turkey. *Advances in Biology & Earth Sciences*, 52-64.
- H. Sahbi, D. J. (1997). Theoretical Study of Slope Effects in Resistivity Surveys and Application. *European Association of Geoscientist and Engineers*, 795-796.
- Herman, R. (2001). An introduction to electrical resistivity in geophysics. 944.

- Hu, Z., Shan, W., & Jiang, H. (2014). Based on the Drilling and High-density Resistivity Method to Research Landslide in the Permafrost Regions. In S. W., G. Y., W. F., M. H., & S. A., *Landslides in Cold Regions in the Context of Climate Change* (pp. 163-175). environmental Science and Engineering. Springer, Cham.
- Hutchison, C. S. (1989). *Geological Evolution of South-East Asia*. Malaysia: Geological Society of Malaysia.
- Hutchison, C. S. (2014). Tectonic Evolution of South East Asia. *Bulletin of Geological Society of Malaysia*, 9.
- James S. Monroe Reed Wicander, R. W. H. (2007). Mass wasting. In *Physical Geology: Exploring the Earth, 6th Edition* (pp. 424–455). Cengage Learning, 2006.
- John, M. (2003). Resistivity method. In *Field geophysics* (Third, pp. 97–113). England: John Wiley & Sons Ltd.
- K., R. J. (2004). Failures at slope-cut in sedimentary bedrocks of Peninsular Malaysia. *Geol. Soc. Malaysia Bulletin* 49, 25-19.
- Kamal Roslan Mohamed, N. A. (2016). The Gua Musang Group: A newly proposed stratigraphic unit for the Permo-Triassic sequence of Northern Central Belt, Peninsula Malaysia. *Bulletin of Geological Society of Malaysia* , 133.
- Lateh, H., Tay, L. T., Khan, Y. A., Kamil, A. A., & Azizat, N. (2013). Prediction of landslide using Rainfall Intensity-Duration Threshold along EastWest. *Caspian Journal of Applied Sciences Research*, 124-133.
- Lawrence R. Walker, A. B. (2013). *Landslide Ecology*. United Kingdom: Cambridge University Press.
- Leman, M. S. (1995). Permian ammonoids from Kuala Betis area, Kelantan, and Their Paleographic Significance. *Geological Society of Malaysia Bulletin* 38, 153-158.
- Lim, T., Rahardjo, H., Chang, M., & Fredlund, D. (1996). Effect of rainfall in matric suctions in a residual soil slope. *Can. Geotech. J*, 618-628.
- M.M. Nordiana, I. A. (2016). Slope failures evaluation and landslides investigation using 2-D Resistivity Method. *NRIAG Journal of Astronomy and Geophysics*, 1.
- Mohd Hazreek Bin Zainal Abidin, R. B. (2012). Integral Analysis Of Geoelectrical (Resistivity) And Geotechnical (Spt) Data In Slope Stability Assessment. *Academic Journal of Science*, 305-306.
- Muhammad Barzzani Gasim, Mohd Ekhwan Toriman, H. J. (2015). Phenomenon of slope failure occurrences along Gerik-Jeli Highway, Malaysia. *Journal of Applied Sciences*, 15(3), 545–551.

- Palacky, G. (1988). Resistivity characteristics of Geologic Target. In J. D. Misac N. Nabighian, *Electromagnetic Methods in Applied Geophysics: Theory* (p. 55). New York: Society of Exploration Geophysics.
- Palaskar, S. M. (2016). Slope Stability Study. *2nd International Conference on "Latest Innovation in Science, Engineering, and Management"*, 295.
- Paul J. Gibson, D. M. G. (2013). Electrical Geophysical Techniques. In *Environmental applications of geophysical surveying techniques* (Second, pp. 159–212). Nova Science Publishers, Inc.
- Peng, L. C. (2009). Paleozoic Stratigraphy. In D. T. C.S Hutchison, *Geology of Peninsula Malaysia* (pp. 80-81). Malaysia: Geological Society of Malaysia.
- Peter Doyle, M. R. (2001). *The Key to Earth History, An introduction to stratigraphy*. USA: Wiley Publication.
- Phillip Kearey, M. B. (2002). *An Introduction to Geophysical Exploration*. Victoria, Australia: Blackwell Science Ltd.
- Reynolds, J. M. (2011). *An Introduction to Apply and Environmental Geophysics*. USA: Wiley-Blackwell.
- Samsudin, A. R. (1990). Geofizik, Konsep dan Penggunaan. Malaysia: Dewan Bahasa dan Pustaka.
- Shuib, M. K., Taib, S. H., & Abdullah, M. (2006). Discontinuity Controlled Cut-Slope Failures on Weathered Low-Grade Metamorphic Rocks along the East-West Highway, Grik to Jeli. In *Geological Society of Malaysia Bulletin* (pp. 43-53).
- Siti Aishah Ismail, S. I. (2009). Application of Electrical Resistivity Imaging Technique in Slope Stability Study in Banding Island, Perak. *2009 International Conference for Technical Postgraduates (TECHPOS)*.
- Syed B. Syed Osman, F. I. (2014). Possible Assessment on Sustainability of Slopes By Using Electrical Resistivity: Comparison of Field and Laboratory Result. *Energy, Environment, Biology and Biomedicine*, 69.
- T.T Khoo, B. T. (1983). Geological Evolution of Peninsula Malaysia. *Workshop on Stratigraphy Correlation of Thailand and Malaysia*, 253-254.
- W., L. (2007). Resistivity. In L. W, *Fundamentals of Geophysics* (p. 393). New York.
- W.M Telford, L. G. (1990). *Applied Geophysics, Second Edition*. USA: Cambridge Univesity Press.
- Yilmaz, S. (2011). A case study of the application of electrical resistivity imaging for investigation of a landslide along the highway. *International Journal of the Physical Sciences*, 6(24), 5843. <https://doi.org/10.5897/IJPS11.564>

Appendix I

Geological mapping data

Joint readings for location J1.

Bearing	Frequency
220°	21
230°	26
250°	10
260°	5
280°	25
290°	16
300°	11

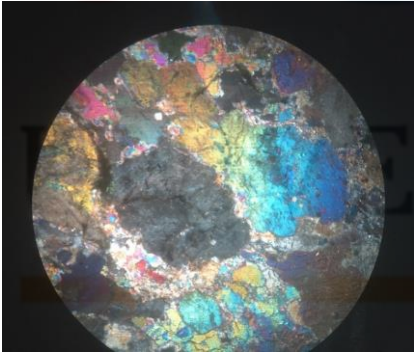
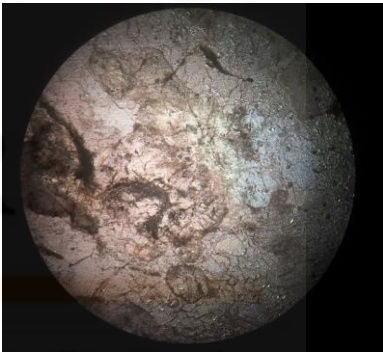
Joint readings for location J2.

Bearing	Frequency
200°	7
210°	12
220°	16
230°	3
280°	9
290°	4
310°	1

Joint readings for location J3.

Bearing	Frequency
190°	7
200°	3
230°	16
240°	2
260°	3
270°	24
290°	1
300°	2
310°	8
330°	2
350°	5

Petrographic description of pink granite.

Reference No. :	
Location :	
Name of Rock : Pink Granite	
Rock Type : Igneous Rock	
Microscopic : Holocrystalline; Hyperdiomorphic; Inequigranular.	
Description of Mineralogy	
Composition of Mineral	Description (Magnification 10X)
Pyroxene	Colourless in PPL and light brown in XPL; Medium relief; Subhedral; First order birefringence; No twinning; 57° extinction angle.
Quartz	Colourless in PPL; Low relief; Subhedral; No cleavage; First order birefringence; 62° extinction angle.
Hornblende	Colourless in PPL and Reddish-brown in XPL; Medium relief; No cleavage; Subhedral; Carlsbad twinning; 30° extinction angle.
Muscovite	High pleochroism; Colourless in PPL; Low relief; Subhedral; Two-direction cleavage; 45° extinction angle.
Biotite	Anhedral plates; pleochroic scheme (dark brown and brown); crystals are weakly aligned resulting in poor foliation in the rocks.
Photo	
	
XPL of monzonite with magnification 10X.	PPL of monzonite with magnification 10X.

KELANTAN

Appendix II

Data for Slope Investigation by using ERI method

Data for Survey Line 1 (Pole-Dipole configuration)

Electrode	Elevation	Electrode	Elevation	Electrode	Elevation
SA01	453	SA15	438	SA30	429
SA02	451	SA16	438	SA31	426
SA03	450	SA17	438	SA32	425
SA04	448	SA18	436	SA33	423
SA05	446	SA19	436	SA34	422
SA06	445	SA20	436	SA35	420
SA07	445	SA21/22	435	SA36	420
SA08	438	SA23	435	SA37	417
SA09	438	SA24	434	SA38	418
SA10	441	SA25	434	SA39	421
SA11	439	SA26	435	SA40	422
SA12	439	SA27	434	SA41	421
SA13	441	SA28	434	SA42	421
SA14	438	SA29	430		

Data for Survey Line 2 (Schlumberger configuration)

Electrode	Elevation	Electrode	Elevation	Electrode	Elevation
SB01	448	SB15	443	SB30	447
SB02	449	SB16	442	SB31	448
SB03	449	SB17	441	SB32	448
SB04	448	SB18	441	SB33	449
SB05	448	SB19	440	SB34	450
SB06	447	SB20	440	SB35	450
SB07	447	SB21/22	440	SB36	450
SB08	447	SB23	443	SB37	451
SB09	446	SB24	444	SB38	451
SB10	445	SB25	445	SB39	451
SB11	445	SB26	445	SB40	451
SB12	444	SB27	445	SB41	451
SB13	444	SB28	446	SB42	451
SB14	443	SB29	446		

Data for Survey Line 3 (Schlumberger configuration)

Electrode	Elevation	Electrode	Elevation	Electrode	Elevation
SC01	437	SC15	437	SC30	434
SC02	437	SC16	436	SC31	433
SC03	437	SC17	436	SC32	433
SC04	437	SC18	436	SC33	431
SC05	437	SC19	436	SC34	431
SC06	437	SC20	436	SC35	430
SC07	437	SC21/22	435	SC36	431
SC08	437	SC23	436	SC37	431
SC09	437	SC24	435	SC38	431
SC10	438	SC25	435	SC39	431
SC11	438	SC26	435	SC40	431
SC12	438	SC27	435	SC41	431
SC13	437	SC28	435	SC42	432
SC14	437	SC29	435		

Data for Survey Line 4 (Pole-Dipole configuration)

Electrode	Elevation	Electrode	Elevation	Electrode	Elevation
SD01	456	SD15	438	SD30	434
SD02	457	SD16	435	SD31	435
SD03	457	SD17	433	SD32	435
SD04	454	SD18	431	SD33	436
SD05	453	SD19	431	SD34	435
SD06	450	SD20	431	SD35	434
SD07	450	SD21/22	430	SD36	432
SD08	448	SD23	432	SD37	429
SD09	445	SD24	432	SD38	427
SD10	443	SD25	433	SD39	424
SD11	441	SD26	431	SD40	421
SD12	439	SD27	431	SD41	420
SD13	439	SD28	431	SD42	420
SD14	438	SD29	432		

Data for Survey Line 5 (Schlumberger configuration)

Electrode	Elevation	Electrode	Elevation	Electrode	Elevation
SE01	442	SE15	446	SE30	451
SE02	443	SE16	446	SE31	452
SE03	443	SE17	447	SE32	452
SE04	443	SE18	447	SE33	452
SE05	444	SE19	447	SE34	452
SE06	444	SE20	448	SE35	452
SE07	444	SE21/22	448	SE36	452
SE08	444	SE23	449	SE37	452
SE09	444	SE24	449	SE38	452
SE10	444	SE25	449	SE39	452
SE11	445	SE26	450	SE40	452
SE12	445	SE27	450	SE41	452
SE13	446	SE28	450	SE42	452
SE14	446	SE29	451		



UNIVERSITI
MALAYSIA
KELANTAN

FYP FSB

Appendix III

Joint data for Kinematic Analysis

Joint reading on the right of the slope.

No.	Trend	Plunge	Spacing, cm	Length, cm
C01	64	30	150	600
C02	174	71	60	200
C03	28	51	30	100
C04	52	27	13	60
C05	52	27	60	60
C06	177	55	100	100
C07	9	61	90	300
C08	340	71	90	200
C09	333	84	90	100
C10	9	87	60	400
C11	355	87	60	400
C12	34	15	45	300
C13	13	85	-	200
C14	25	87	45	300
C15	357	79	45	300
C16	357	83	45	300
C17	346	83		200

Joint reading on the centre of the slope.

No.	Trend	Plunge	Spacing, cm	Length, cm
B01	341	40	54	300
B02	302	33	78	250
B03	307	57	40	200
B04	23	56	18	400
B05	336	48	80	400
B06	337	63	65	100
B07	313	40	93	100
B08	313	54	60	200
B09	308	61		300

Joint reading on the left side of the slope.

No.	Trend	Plunge	Spacing, cm	Length, cm
C01	64	30	150	600
C02	174	71	60	200
C03	28	51	30	100
C04	52	27	13	60
C05	52	27	60	60
C06	177	55	100	100
C07	9	61	90	300
C08	340	71	90	200
C09	333	84	90	100
C10	9	87	60	400
C11	355	87	60	400
C12	34	15	45	300
C13	13	85		200
C14	25	87	45	300
C15	357	79	45	300
C16	357	83	45	300
C17	346	83		200